

The Diabetic Foot

Lead Guest Editor: Ilias Migdalis

Guest Editors: Leszek Czupryniak, Nebojsa Lalic, David Leslie, Nikolaos Papanas,
and Paul Valensi





The Diabetic Foot

Journal of Diabetes Research

The Diabetic Foot

Lead Guest Editor: Ilias Migdalis

Guest Editors: Leszek Czupryniak, David Leslie,
and Nikolaos Papanas



Copyright © 2017 Hindawi. All rights reserved.

This is a special issue published in “Journal of Diabetes Research.” All articles are open access articles distributed under the Creative Commons Attribution License, which permits unrestricted use, distribution, and reproduction in any medium, provided the original work is properly cited.

Editorial Board

Steven F. Abcouwer, USA
Reza Abdi, USA
Abdelaziz Amrani, Canada
Fabrizio Barbetti, Italy
Simona Bo, Italy
Monica Bullo, Spain
Stefania Camastra, Italy
Norman Cameron, UK
Ilaria Campesi, Italy
Riccardo Candido, Italy
Brunella Capaldo, Italy
Sergiu Catrina, Sweden
Subrata Chakrabarti, Canada
Munmun Chattopadhyay, USA
Eusebio Chiefari, Italy
Secundino Cigarran, Spain
Kim Connelly, Canada
Laurent Crenier, Belgium
Christophe De Block, Belgium
Khalid M. Elased, USA
Ulf J. Eriksson, Sweden
Paolo Fiorina, USA
Andrea Flex, Italy
Daniela Foti, Italy
Georgia Fousteri, Italy
Maria Pia Francescato, Italy

Pedro M. Geraldès, Canada
Thomas J. Hawke, Canada
Ole Kristian Hejlesen, Denmark
Daisuke Koya, Japan
Frida Leonetti, Italy
Afshan Malik, UK
Roberto Mallone, France
Raffaele Marfella, Italy
Carlos Martínez Salgado, Spain
Lucy Marzban, Canada
Raffaella Mastrocola, Italy
David Meyre, Canada
Maria G. Montez, USA
Jiro Nakamura, Japan
Pratibha V. Nerurkar, USA
Monika A. Niewczas, USA
Francisco Javier Nóvoa, Spain
Craig S. Nunemaker, USA
Hiroshi Okamoto, Japan
Ike S. Okosun, USA
Fernando Ovalle, USA
Jun Panee, USA
Cesare Patrone, Sweden
Subramaniam Pennathur, USA
Bernard Portha, France
Ed Randell, Canada

Jordi Lluís Reverter, Spain
Ulrike Rothe, Germany
Christoph H. Saely, Austria
Ponnusamy Saravanan, UK
Toshiyasu Sasaoka, Japan
Andrea Scaramuzza, Italy
Yael Segev, Israel
Suat Simsek, Netherlands
Marco Songini, Italy
Janet H. Southerland, USA
David Strain, UK
Kiyoshi Suzuma, Japan
Patrizio Tatti, Italy
Farook Thameem, USA
Michael J. Theodorakis, UK
Peter Thule, USA
Andrea Tura, Italy
Ruben Varela-Calvino, Spain
Christian Wadsack, Austria
Kazuya Yamagata, Japan
Shi Fang Yan, USA
Mark A. Yorek, USA
Liping Yu, USA
David Zangen, Israel
Dan Ziegler, Germany

Contents

The Diabetic Foot

I. Migdalis, L. Czupryniak, N. Lalic, R. D. Leslie, N. Papanas, and P. Valensi
Volume 2017, Article ID 3585617, 2 pages

Sympathetic Denervation Accelerates Wound Contraction but Inhibits Reepithelialization and Pericyte Proliferation in Diabetic Mice

Zhifang Zheng, Yu Wan, Yishu Liu, Yu Yang, Jianbing Tang, Wenhua Huang, and Biao Cheng
Volume 2017, Article ID 7614685, 12 pages

Development of a Plantar Load Estimation Algorithm for Evaluation of Forefoot Load of Diabetic Patients during Daily Walks Using a Foot Motion Sensor

Ayano Watanabe, Hiroshi Noguchi, Makoto Oe, Hiromi Sanada, and Taketoshi Mori
Volume 2017, Article ID 5350616, 8 pages

Alcohol Consumption Is a Risk Factor for Lower Extremity Arterial Disease in Chinese Patients with T2DM

Shanshan Yang, Shuang Wang, Bo Yang, Jinliang Zheng, Yuping Cai, and Zhengguo Yang
Volume 2017, Article ID 8756978, 6 pages

Therapeutic Effects of Static Magnetic Field on Wound Healing in Diabetic Rats

Jing Zhao, Yong-guo Li, Kai-qin Deng, Peng Yun, and Ting Gong
Volume 2017, Article ID 6305370, 5 pages

Efficacy of Administration of an Angiotensin Converting Enzyme Inhibitor for Two Years on Autonomic and Peripheral Neuropathy in Patients with Diabetes Mellitus

Triantafyllos Didangelos, Konstantinos Tziomalos, Charalambos Margaritidis, Zisis Kontoninas, Ioannis Stergiou, Stefanos Tsotoulidis, Eleni Karlafti, Alexandros Mourouglakis, and Apostolos I. Hatzitolios
Volume 2017, Article ID 6719239, 6 pages

NLRP3 Inflammasome Expression and Signaling in Human Diabetic Wounds and in High Glucose Induced Macrophages

Xiaotian Zhang, Jiezhai Dai, Li Li, Hua Chen, and Yimin Chai
Volume 2017, Article ID 5281358, 7 pages

Investigation of the Effects and Mechanisms of Mai Tong Formula on Lower Limb Macroangiopathy in a Spontaneous Diabetic Rat Model

Guangming Gong, Haipo Yuan, Ya Liu, and Luguang Qi
Volume 2016, Article ID 8076796, 8 pages

Sweet Bones: The Pathogenesis of Bone Alteration in Diabetes

Mohammed Al-Hariri
Volume 2016, Article ID 6969040, 5 pages

Editorial

The Diabetic Foot

I. Migdalis,¹ L. Czupryniak,² N. Lalic,³ R. D. Leslie,⁴ N. Papanas,⁵ and P. Valensi⁶

¹Second Medical Department and Diabetes Centre, NIMTS Hospital, 12 Monis Petraki, 11521 Athens, Greece

²Department of Diabetology and Internal Medicine, Warsaw Medical University, Warsaw, Poland

³Clinic for Endocrinology, Diabetes and Metabolic Diseases, CCS, Faculty of Medicine, University of Belgrade, Belgrade, Serbia

⁴Department of Diabetes, Saint Bartholomew's Hospital, University of London and Blizard Institute, EC1A 7BE, London, UK

⁵Diabetic Foot Clinic-Diabetes Centre, Second Department of Internal Medicine, Democritus University of Thrace, 68100 Alexandroupolis, Greece

⁶Department of Endocrinology, Diabetology and Nutrition, Jean Verdier Hospital, AP-HP, Paris Nord University, CRNH-IdF, CINFO, 93140 Bondy, France

Correspondence should be addressed to I. Migdalis; ilianmig@otenet.gr

Received 20 July 2017; Accepted 25 July 2017; Published 10 October 2017

Copyright © 2017 I. Migdalis et al. This is an open access article distributed under the Creative Commons Attribution License, which permits unrestricted use, distribution, and reproduction in any medium, provided the original work is properly cited.

Diabetic foot ulcers remain a serious medical problem, which is extremely difficult to heal and exhibits a high recurrence rate [1]. Thus, it is continuously receiving increased scientific attention, in an effort to improve outcomes [2–4]. There is ongoing progress in peripheral arterial disease [1], neuropathy [1, 5], off-loading [1, 2], infection [1, 2], and wound healing [1, 2]. The present special issue is devoted to new research in the field of diabetic foot.

S. Yang et al. in their paper entitled “Alcohol Consumption Is a Risk Factor for Lower Extremity Arterial Disease in Chinese Patients with T2DM” reported that alcohol consumption was a significant independent risk factor for peripheral arterial disease in hospitalized Chinese patients with type 2 diabetes, and this finding has obvious practical implications.

In their experimental paper “Investigation of the Effects and Mechanisms of Mai Tong Formula on Lower Limb Macroangiopathy in a Spontaneous Diabetic Rat Model,” G. Gong et al. examined a new Chinese herbal formula, which has recently been used to treat peripheral arterial disease in diabetes. In the spontaneous diabetic rat model, they found that this formula reduced fasting blood glucose, triglycerides, total cholesterol, interleukin-6, and vascular endothelial growth factor, while it increased serum insulin. Histology and ultrasonography provided evidence that

treatment also reduced endothelial dysfunction and injury. More experience is anticipated.

T. Didangelos et al. in their article “Efficacy of Administration of an Angiotensin Converting Enzyme Inhibitor for Two Years on Autonomic and Peripheral Neuropathy in Patients with Diabetes Mellitus” examined the effect of a 2-year quinapril treatment on diabetic cardiovascular autonomic neuropathy and peripheral neuropathy. They documented improvement in cardiovascular autonomic neuropathy, mainly parameters of parasympathetic dysfunction, and this may merit further clinical utilization.

Z. Zheng et al. in their article “Sympathetic Denervation Accelerates Wound Contraction but Inhibits Reepithelialization and Pericyte Proliferation in Diabetic Mice” turned their attention to the impact of sympathetic denervation using intraperitoneal 6-hydroxydopamine administration on inflammation, angiogenesis, and wound healing in diabetic mice. They found that treatment decreased epidermal growth factor, hindering reepithelialization, and it impaired pericyte proliferation. However, it enhanced wound contraction by reducing interleukin-1 β and mast cells.

A. Watanabe et al. in their paper entitled “Development of a Plantar Load Estimation Algorithm for Evaluation of Forefoot Load of Diabetic Patients during Daily Walks Using a Foot Motion Sensor” used a motion sensor attached

to each shoe, in order to obtain forefoot acceleration and angular velocity data. This promising modality identified excessive forefoot loading during 3-hour daily walks of 2 diabetic patients. It may now be further employed to ascertain differences between walking on level ground and on slopes/stairs.

J. Zhao et al. in their manuscript entitled “Therapeutic Effects of Static Magnetic Field on Wound Healing in Diabetic Rats” looked at the effects of static magnetic field on incisional wound healing in streptozotocin-induced diabetic rats. In comparison with sham magnetic treatment, static magnetic field accelerated healing and increased tissue strength. More experience in humans would be welcome.

X. Zhang et al. in their paper “NLRP3 Inflammasome Expression and Signaling in Human Diabetic Wounds and in High Glucose Induced Macrophages” included patients with type 2 diabetes and chronic foot wounds. They demonstrated higher expression of the NLRP3 inflammasome, caspase-1, and interleukin-1 β in comparison with wounds in nondiabetic patients. The higher expression was confirmed at both mRNA and protein level. These findings should be interpreted in the context of increased inflammation in diabetic foot ulcerations.

Finally, M. Al-Hariri in the review article entitled “Sweet Bones: The Pathogenesis of Bone Alteration in Diabetes” outlined bone changes in diabetes. These mainly relate to deficits in mineralization, decreased osteoid surface, osteoblast activity, accumulation of advanced glycation end products, and oxidative stress, as well as increased urinary excretion of calcium and magnesium. Certainly, bone pathology in diabetes deserves further attention, but we should also take into consideration the effects of some antidiabetic agents [6].

There are considerable new research data in miscellaneous issues pertaining to the diabetic foot. New investigations need to be carefully interpreted, so that they can mature into useful clinical implications. This process is vital for improved management of the diabetic foot [1, 3].

I. Migdalis
L. Czupryniak
N. Lalic
R. D. Leslie
N. Papanas
P. Valensi

References

- [1] D. G. Armstrong, A. J. M. Boulton, and S. Bus, “Diabetic foot ulcers and their recurrence,” *The New England Journal of Medicine*, vol. 376, no. 24, pp. 2367–2375, 2017.
- [2] N. Papanas and R. Mani, “Advances in infections and wound healing for the diabetic foot,” *The International Journal of Lower Extremity Wounds*, vol. 12, no. 2, pp. 83–86, 2013.
- [3] J. M. Forbes and A. K. Fotheringham, “Vascular complications in diabetes: old messages, new thoughts,” *Diabetologia*, vol. 60, no. 11, pp. 2129–2138, 2017.
- [4] C. A. Manu, O. G. Mustafa, M. Bates et al., “Transformation of the multidisciplinary diabetic foot clinic into a multidisciplinary diabetic foot day unit,” *The International Journal of Lower Extremity Wounds*, vol. 13, no. 3, pp. 173–179, 2014.
- [5] N. Papanas and D. Ziegler, “Emerging drugs for diabetic peripheral neuropathy and neuropathic pain,” *Expert Opinion on Emerging Drugs*, vol. 21, no. 4, pp. 393–407, 2016.
- [6] S. E. Inzucchi, R. M. Bergenstal, J. B. Buse et al., “Management of hyperglycaemia in type 2 diabetes, 2015: a patient-centred approach. Update to a position statement of the American Diabetes Association and the European Association for the Study of Diabetes,” *Diabetologia*, vol. 58, no. 3, pp. 429–442, 2015.

Research Article

Sympathetic Denervation Accelerates Wound Contraction but Inhibits Reepithelialization and Pericyte Proliferation in Diabetic Mice

Zhifang Zheng,^{1,2,3} Yu Wan,^{1,2} Yishu Liu,^{2,4} Yu Yang,^{1,2} Jianbing Tang,² Wenhua Huang,^{1,3} and Biao Cheng^{1,2,3,4,5,6}

¹The Graduate School of Southern Medical University, Guangzhou, China

²Department of Plastic Surgery, Guangzhou General Hospital of Guangzhou Military Command, Guangzhou, China

³Department of Anatomy, School of Basic Medicine Sciences, Southern Medical University, Guangzhou, China

⁴The Graduate School of Third Military Medical University, Chongqing, China

⁵Center of Wound Treatment, Guangzhou General Hospital of Guangzhou Military Command, Guangzhou, China

⁶The Key Laboratory of Trauma Treatment & Tissue Repair of Tropical Area, PLA, Guangzhou, China

Correspondence should be addressed to Biao Cheng; chengbiaocheng@163.com

Received 28 February 2017; Accepted 28 June 2017; Published 24 September 2017

Academic Editor: Ilias Migdalis

Copyright © 2017 Zhifang Zheng et al. This is an open access article distributed under the Creative Commons Attribution License, which permits unrestricted use, distribution, and reproduction in any medium, provided the original work is properly cited.

Previous studies focused on the effects of sympathetic denervation with 6-hydroxydopamine (6-OHDA) on nondiabetic wounds, but the effects of 6-OHDA on diabetic wounds have not been previously reported. In this study, treated mice received intraperitoneal 6-OHDA, and control mice received intraperitoneal injections of normal saline. Full-thickness wounds were established on the backs of mice. The wounds were sectioned (four mice per group) for analysis at 2, 5, 7, 10, 14, 17, and 21 days after injury. The wound areas in the control group were larger than those in the treatment group. Histological scores for epidermal and dermal regeneration were reduced in the 6-OHDA-treated group on day 21. The mast cells (MCs) in each field decreased after sympathectomy on days 17 and 21. The expression levels of norepinephrine, epidermal growth factor (EGF), interleukin-1 beta, NG2 proteoglycan, and desmin in the treatment group were less than those in the control group. In conclusion, 6-OHDA delays reepithelialization during wound healing in diabetic mice by decreasing EGF, but increases wound contraction by reducing IL-1 β levels and the number of MCs. Besides, 6-OHDA led to reduced pericyte proliferation in diabetic wounds, which might explain the vascular dysfunction after sympathetic nerve loss in diabetic wounds.

1. Introduction

Diabetic foot ulcers (DFUs) are a common cause of hospitalization in diabetic patients [1]. Approximately 10–15% of diabetic patients develop foot ulcers, and 15% of DFU patients require amputation [2]. In contrast to nondiabetic wounds, diabetic wounds are characterized by prolonged inflammation, delayed wound closure [3], and impaired

angiogenesis [4]. The neuroimmune axis and successful angiogenesis are essential for DFU healing [5, 6]. Although great progress has been made in the treatment of DFUs, they remain difficult to fully cure. Thus, there is a continuing need to understand the mechanisms behind DFUs and to explore new treatments.

Sympathetic efferents are important for the healing of DFUs. Sympathetic nerve damage is an important feature

of diabetic neuropathy [7] and impairs vasomotor control and increases skin capillary permeability in diabetic patients [8]. Lumbar sympathectomy is a revascularization technique used in diabetic patients with ischemic feet [9]. However, the findings of Kokobelian et al. suggest that sympathectomy is ineffective for DFUs [10]. Therefore, the role of sympathetic nerve failure in the wound healing of DFUs remains controversial.

6-Hydroxydopamine (6-OHDA) is a specific sympathetic neurotoxin that selectively destroys peripheral sympathetic nerve termini. Nerve regeneration after chemical sympathectomy with 6-OHDA requires at least 1 month [11], which allows for continued wound observation after sympathetic denervation. Previous studies have shown the effects of 6-OHDA on nondiabetic wounds. Kim et al. [12] reported that 6-OHDA reduces inflammation and significantly delays epidermal wound healing in linear skin incisions in rats. Saburo et al. [13] suggested that 6-OHDA may decrease collagen metabolism and reduce the number of capillaries during the wound healing of animal burns. Souza et al. [14] found that intraperitoneal administration of 6-OHDA in 1% ascorbic acid accelerated wound contraction during cutaneous wound healing in rats. However, the effects of 6-OHDA on diabetic wounds have not been reported.

The wound-healing process includes an inflammatory change and proliferation phase, which includes fibroplasia, angiogenesis, and reepithelialization [15]. Angiogenesis during wound healing depends upon dynamic interactions between endothelial cells, angiogenic cytokines, and the extracellular matrix (ECM) [16]. NG2 proteoglycan and desmin are pericyte markers in mice [17]. To explore the role of sympathetic denervation in the healing of DFUs, wound reepithelialization, wound contraction, collagen fibers, mast cell (MC) distribution, and the protein levels of norepinephrine (NE), epidermal growth factor (EGF), interleukin-1 beta (IL-1 β), NG2 proteoglycan, desmin, and MMP-9 were observed in cutaneous wound healing after chemical sympathectomy with 6-OHDA in diabetic (db/db) mice.

2. Materials and Methods

2.1. Animals and Materials. Spontaneously diabetic female mice ($n = 56$, BKS.Cg-Dock7m^{+/+}Leprdb/JNju, aged 6 weeks) were purchased from Nanjing Biomedical Institute, Nanjing University, Nanjing, China. Their diabetes was generated by a homozygous mutation in the leptin receptor gene, producing recognizable phenotypes characteristic of obesity and diabetes. The diabetic mice were maintained on a normal-fat and normal-sugar diet, and their blood sugar levels increased from 4 to 8 weeks of age. The fasting random glucose levels from the tail vein in the diabetic mice were measured in both 6-OHDA-treated and control groups during the experimental phase. 6-OHDA and ascorbic acid were purchased from Sigma-Aldrich (St. Louis, MO, USA). Primary antibodies for EGF, IL-1 β , NG2 proteoglycan, desmin, and MMP-9 were purchased from Abcam (Cambridge, UK), and a primary antibody for NE was purchased from Lifespan (Cambridge, UK).

2.2. Chemical Sympathectomy. The mice were housed for 1 week before use. The animals were maintained at 22–24°C under a 12/12 h light/dark cycle with free access to standard laboratory food and water. Animal experiments were conducted according to institutional guidelines and were approved by the animal care committee. The mice were divided randomly into 6-OHDA-treated and control groups. The treatment mice received intraperitoneal injections of 100 mg/kg 6-OHDA in 0.9% NaCl plus 10⁻⁷ M ascorbic acid on days -7 and -5 and 200 mg/kg 6-OHDA on day -3. Control mice received intraperitoneal injections of 0.9% NaCl plus 10⁻⁷ M ascorbic acid [11, 18].

2.3. In Vivo Wound Closure. The mice were anesthetized with 0.6% pentobarbital sodium (40 mg/kg), and skin punches were used to generate two rounds of full-thickness dermal wounds (0.6 cm in diameter, at a distance of at least 1.0 cm) on both sides of the dorsal trunk. After the wounding procedure, the animals were housed individually in separate cages. The wounds were imaged using a digital camera at 2, 5, 7, 10, 14, 17, and 21 days after injury. The wound sizes were measured using Image-Pro Plus software (ver. 6.0; Media Cybernetics Corp., Silver Springs, MD, USA) and calculated against the original area (on day 0), which was set at 100%. The wounds, including the tissue 2 mm around the edge of the wound, were sectioned under anesthesia (four mice per group) for analyses at each time point.

2.4. Hematoxylin-Eosin (H&E) Staining. Samples were harvested and fixed in 10% neutral formalin, dehydrated in a graded series of ethanol, and embedded in paraffin for routine H&E staining. All slides were examined by a pathologist with no prior knowledge of the treatment. The histological scores for epidermal and dermal regeneration used in this study were evaluated as previously described [19].

2.5. Masson's Trichrome Staining. Specimens were fixed in formalin and embedded in paraffin wax using routine laboratory techniques. Serial 5 μ m sections were cut and stained with Masson's trichrome to detect collagen fibers in the wounds. Deparaffinized sections were incubated with hematoxylin for 10 min, 0.5% hydrochloric acid/alcohol for 3 s, and 0.6% ammonia for 30 s. After washing in tap water for 1 min, sections were stained with Ponceau SP liquid for 1 h and then washed in tap water for 1 min. After 5 min in phosphomolybdic acid solution, sections were stained in water-soluble aniline blue for 5 min and then incubated in 1% acetic acid for 1 min. After routine alcohol- and xylene-based dehydration, the sections were fixed in 10% neutral buffered formalin for light microscopy. A pathologist who was blinded to the research design examined all sections and described any pathological changes.

Additionally, Image-Pro Plus (ver. 6.0) was used to scan and quantify the collagen deposition areas. The ratio of the fibrotic areas to the whole area was calculated as a relative objective index to assess the level of collagen fibers [20]. The results are presented as the mean of 10 different fields in each section.

TABLE 1: The glucose levels in both 6-OHDA-treated and control groups during this experimental phase.

	2 d	5 d	7 d	Days 10 d	14 d	17 d	21 d
Groups							
Control	19.95 ± 0.74	20.83 ± 1.86	20.78 ± 3.72	20.30 ± 0.66	21.86 ± 3.96	21.95 ± 3.10	21.90 ± 3.73
6-OHDA treated	20.15 ± 0.66	19.65 ± 1.01	20.08 ± 1.40	21.90 ± 2.89	20.36 ± 0.81	20.15 ± 0.66	21.10 ± 2.80
<i>p</i> value	0.700	0.309	0.737	0.322	0.493	0.333	0.743

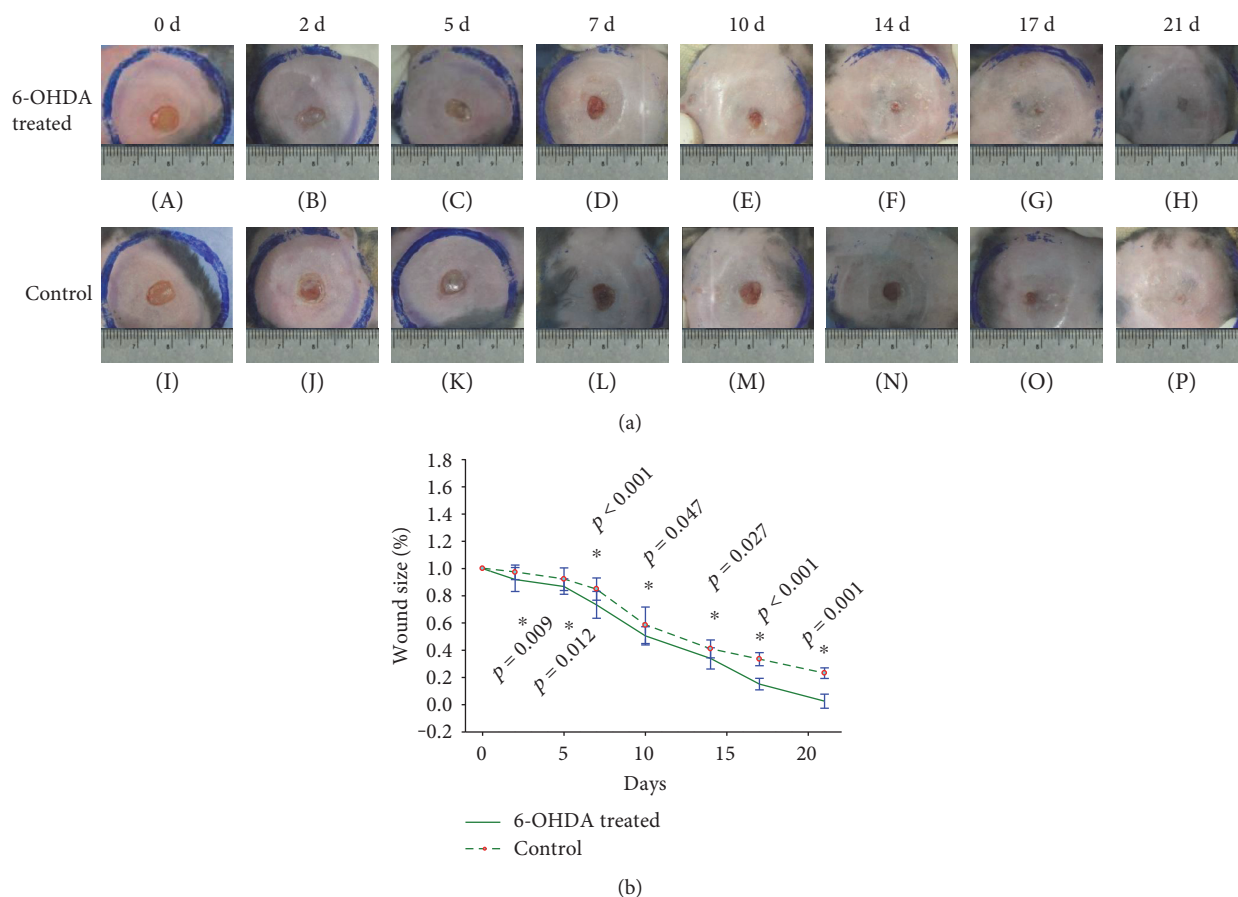


FIGURE 1: Wound size in 6-OHDA-treated and control groups after the establishment of full-thickness wounds in diabetic mice. (a) Wound size at different time points in the 6-OHDA-treated group (A–H) and the control group (I–P). (b) Significant differences in wound size in the 6-OHDA-treated group and the control group after the establishment of full-thickness wounds in diabetic mice. * $p < 0.05$, 6-OHDA-treated versus control.

2.6. Toluidine Blue Staining. Toluidine blue staining was used to assess the presence of MCs. Paraffin wax sections were deparaffinized and hydrated. Sections were stained with 1% toluidine blue for 10 min. The sections were washed under running water for 2 min and then differentiated with 95% and 100% alcohol. The sections were warmed and cleared in xylene and mounted with neutral resin. The number of MCs in the wound area (between the bilateral edges of the wound, 10 fields for each sample) was estimated by blinded pathologists.

2.7. Immunohistochemistry. Paraffin wax sections (5 μm) were deparaffinized, washed three times in PBS for 5 min,

and blocked with 5% serum for 30 min. The slides were subsequently incubated with primary antibodies against EGF (1 : 100), IL-1 β (1 : 200), NG2 proteoglycan (1 : 100), desmin (1 : 200), or MMP-9(1 : 200) at 4°C overnight. After rinsing three times with PBS, the slides were incubated with horseradish peroxidase-labelled secondary antibodies at 37°C for 20–30 min and developed with 3,3'-diaminobenzidine tetrahydrochloride solution.

2.8. Western Blots. Skin tissue was homogenized in 500 μL of cell lysate and transferred to a 1.5 mL microcentrifuge tube. The samples were lysed for 30 min and then centrifuged (14,000 $\times g$, 10 min, 4°C), and the supernatant was collected.

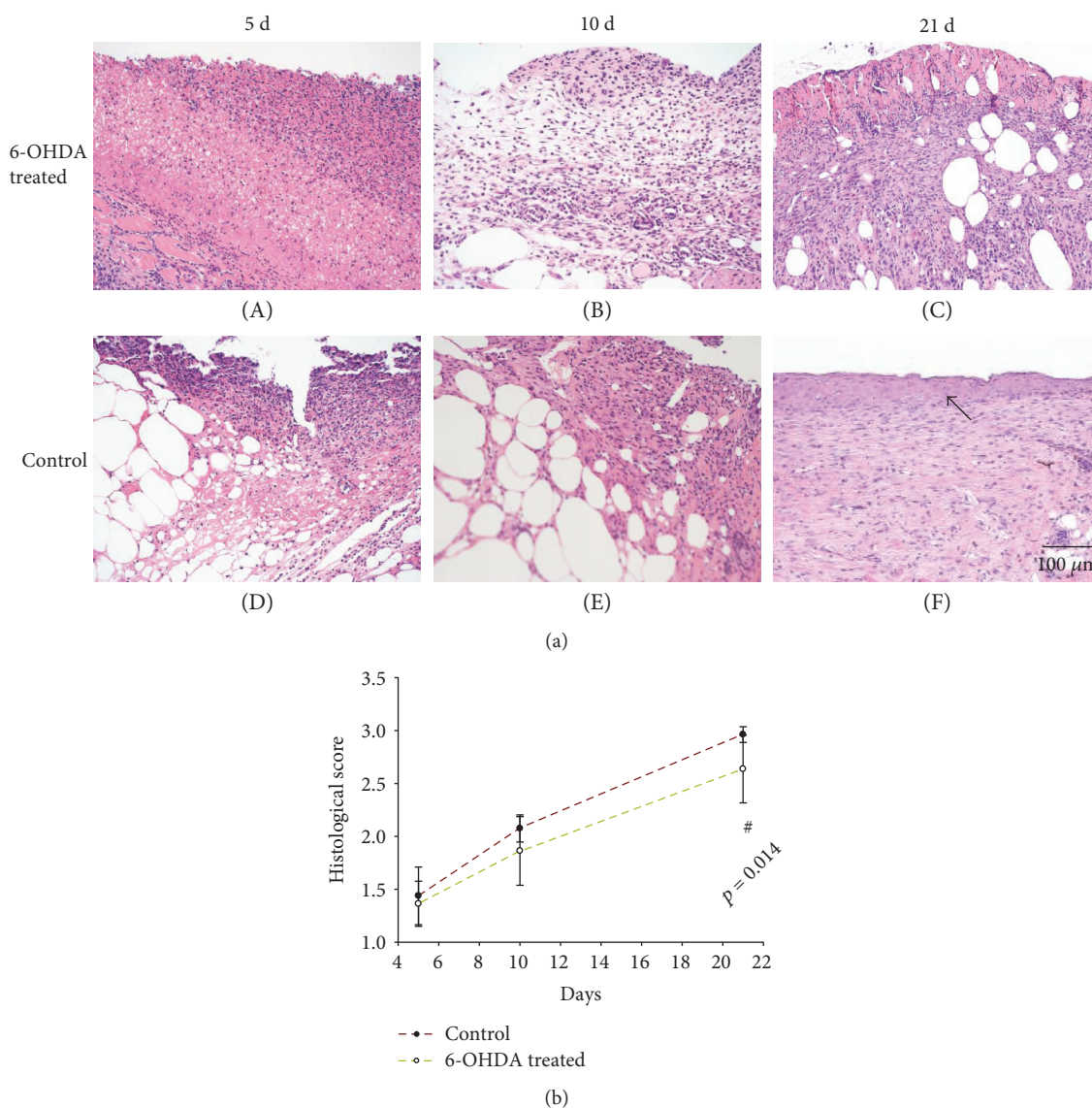


FIGURE 2: (a) H&E staining; the arrow indicates wound reepithelialization in the treatment and control groups (the bar corresponds to 100 μm). (b) The histological scores of epidermal and dermal regeneration in the 6-OHDA-treated and control groups. $^{\#}p < 0.05$, 6-OHDA-treated versus control.

Protein concentrations were determined using the BSA method, and the skin lysates were denatured at 95°C for 5 min in sample buffer. Then, 50 μg of total protein was resolved by 10% SDS-PAGE and transferred to PVDF membranes. Membranes were blocked with 5% skim milk for 1 h at room temperature and incubated with primary antibodies against EGF (1:2000), NE (1:1500), IL-1β (1:1000), desmin (1:800), NG2 proteoglycan (1:2000), or MMP-9 (1:1000) overnight at 4°C. The membranes were then washed and incubated for 1 h at room temperature with an anti-rabbit or anti-mouse secondary antibody (1:10,000). After washing, the membranes were incubated with detection reagent (Immobilon Western Chemiluminescent HRP Substrate, Millipore Corp., Billerica, MA, USA). Band intensities were quantified using Image-Pro Plus (ver. 6.0). Protein levels were calculated relative to the sample's GAPDH level.

2.9. Statistical Analyses. The data of the size of wound belongs to the repeated measurement data, so we used the nonequidistant repeated measure variance analysis with the SPSS software (ver. 21; IBM). For the data of HE staining and Western blot (which belongs to the quantitative data), we found that the data in every group was homogeneity of variance after homogeneity test of variance. Then, we analyzed the data with independent-samples *t*-test. *p* values < 0.05 were considered to indicate statistical significance.

3. Results

3.1. The Glucose Levels in Both Groups. The glucose levels in the control group were not different from those in the experimental group on days 2 ($p = 0.700$), 5 ($p = 0.309$), 7 ($p = 0.737$), 10 ($p = 0.322$), 14 ($p = 0.493$), 17 ($p = 0.333$), and 21 ($p = 0.743$) (Table 1).

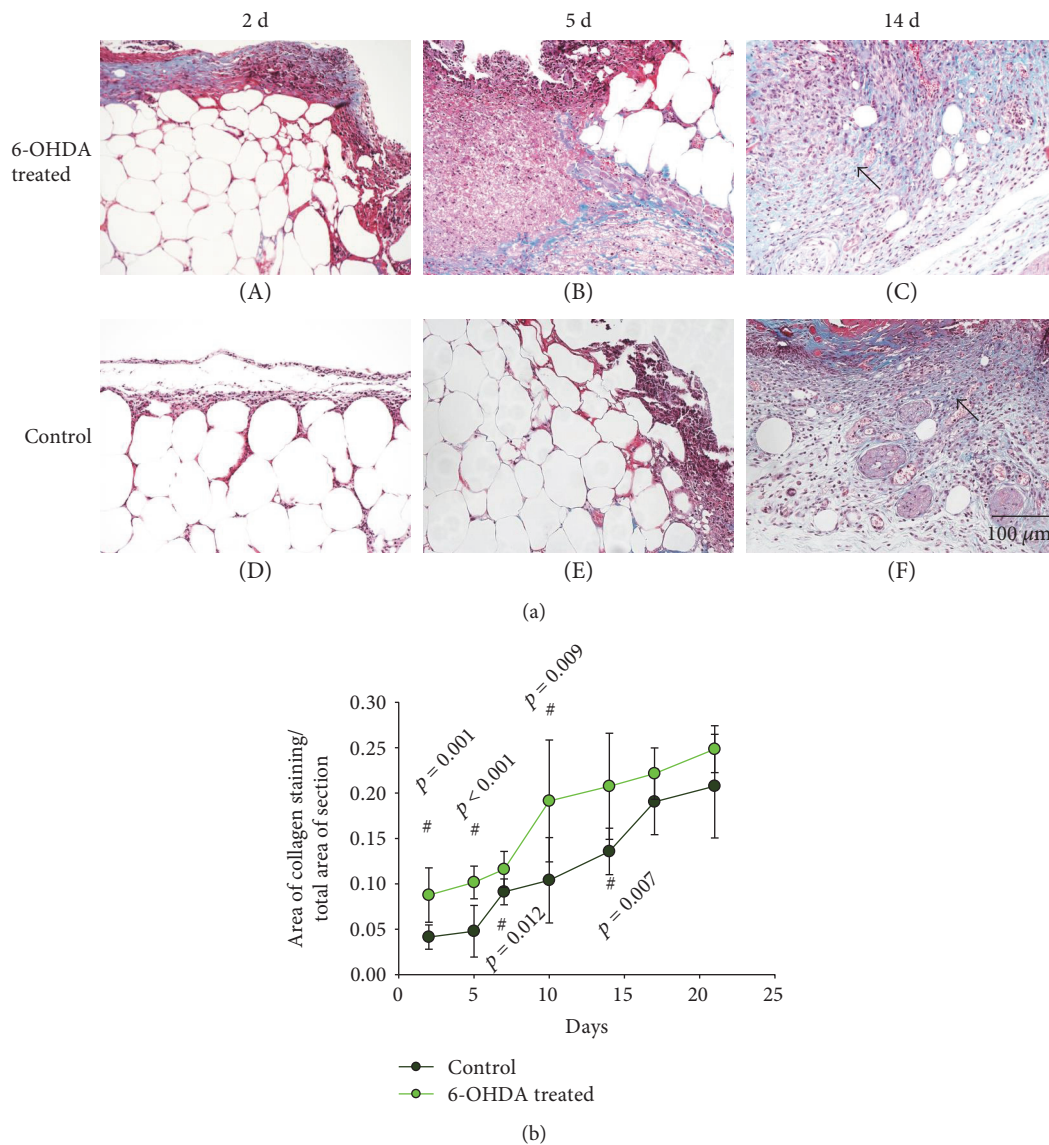


FIGURE 3: (a) Histological analyses of Masson staining in dorsal skin after full-thickness wounds at different time points in the 6-OHDA-treated group (A–C) and the control group (D–F). The bar corresponds to 100 μm. (b) The ratio of fibrotic area to the whole area in diabetic wounds. # $p < 0.05$, 6-OHDA-treated versus control.

3.2. Wound Areas in the Diabetic Mice. All mice survived until they were sacrificed. Wound areas in the control group were larger than those in the experimental group on days 2 ($p = 0.009$), 5 ($p = 0.012$), 7 ($p < 0.001$), 10 ($p = 0.047$), 14 ($p = 0.027$), 17 ($p < 0.001$), and 21 ($p = 0.001$) (Figures 1(a) and 1(b)).

3.3. Histological Observation of Wounds through H&E Staining. Skin structure in diabetic mice was shown in Figure S1 available online at <https://doi.org/10.1155/2017/7614685>, which had continuous epidermal structure and hair follicles. Many inflammatory cells were observed in the wounds during the early stage of healing. Throughout the entire wound-healing process, collagen fibers increased steadily, and the wound surface was gradually covered by

epidermal cells (Figure 2(a)). The histological scores for epidermal and dermal regeneration in the 6-OHDA-treated group were lower than those in the control group on days 5 ($p = 0.550$), 10 ($p = 0.107$), and 21 ($p = 0.014$) (Figure 2(b)).

3.4. Histological Observation of Wounds through Masson's Trichrome Staining. There are many blue-stained collagen fibers in the extracellular matrix of the skin in diabetic mice (Figure S2). On day 2, the skin wounds showed obvious inflammatory responses. During the healing process, epithelial cells proliferated and migrated to the wound bed, and the number of collagen fibers increased in the wounds and wound edges (Figure 3(a)). The ratio of the fibrotic area to the whole area was higher in the treatment group than in the control group on days 2 ($p = 0.001$), 5 ($p < 0.001$), 7

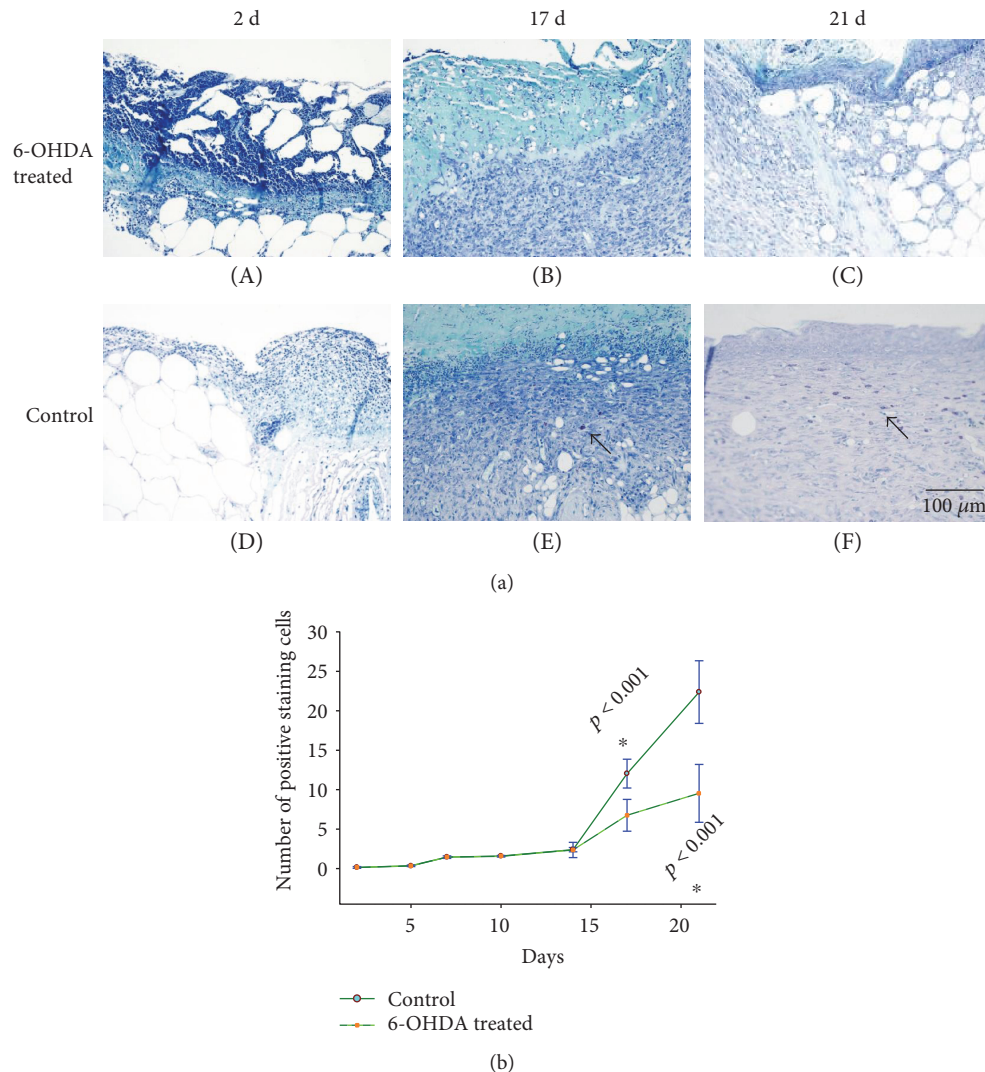


FIGURE 4: (a) Histological analyses of dorsal skin stained with toluidine blue after full-thickness wounds at different time points in the 6-OHDA-treated group (A–C) and the control group (D–F). Arrows indicate positive staining within MCs. The bar corresponds to 100 μm. (b) The number of MCs in each field in the 6-OHDA-treated and control groups. * $p < 0.05$, 6-OHDA-treated versus control.

($p = 0.012$), 10 ($p = 0.009$), 14 ($p = 0.007$), 17 ($p = 0.076$), and 21 ($p = 0.087$) (Figure 3(b)).

3.5. MC Staining. There were some purple cells (MCs) in the skin of diabetic mice without wound (Figure S3). Few MCs were observed in the skin wounds by toluidine blue staining on days 2, 5, 7, or 10. MCs were localized primarily in healthy skin tissue and the wound edges. MCs became more apparent during the healing of the diabetic wounds (Figure 4(a)). Fewer MCs were observed in each field in the treatment group than in the control group on days 2 ($p = 0.642$), 5 ($p = 0.513$), 7 ($p = 1.000$), 10 ($p = 0.549$), 14 ($p = 0.917$), 17 ($p < 0.001$), and 21 ($p < 0.001$) (Figure 4(b)).

3.6. Expression of Proteins in Wounds. The expressions of EGF, IL-1 β , desmin, NG2 proteoglycan, and MMP-9 in the skin of diabetic mice are indicated in Figures 4, 5, 6, 7, and 8. Immunohistochemistry results for EGF, IL-1 β , desmin,

NG2 proteoglycan, and MMP-9 are shown in Figures 5, 6, 7, 8, and 9. EGF was found in normal epithelial cells (Figure 5). IL-1 β is a member of the IL-1 cytokine family and is produced by activated macrophages as a proprotein to induce various acute-phase reactions [21] (Figure 6). Desmin filaments exist in smooth muscle cells [22] (Figure 7). NG2 proteoglycan was invariably expressed by the mural cell component of mouse neovascular structures [23] (Figure 8). MMP-9 (Figure 9) is a matrix metalloproteinase and was widely distributed in various tissues and body fluids.

Protein levels detected by Western blot are shown in Figure 10(a). EGF was reduced in the treatment group on days 2 ($p < 0.001$), 5 ($p = 0.001$), 7 ($p < 0.001$), 10 ($p = 0.001$), 14 ($p = 0.224$), 17 ($p < 0.001$), and 21 ($p < 0.001$) (Figure 10(b)). The levels of IL-1 β in the treatment group were lower on days 2 ($p = 0.048$), 5 ($p = 0.001$), 7 ($p = 0.139$), 10 ($p = 0.408$), 14 ($p = 0.008$), 17 ($p < 0.001$), and 21 ($p = 0.116$) after

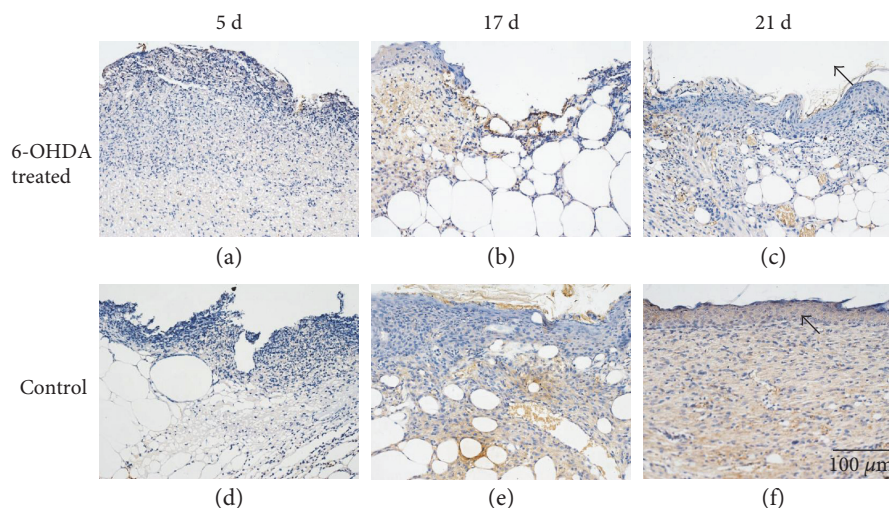


FIGURE 5: EGF immunohistochemistry. EGF is expressed in normal epithelial cells and fibroblasts. Arrows indicate positive staining within epithelial cells. The bar corresponds to 100 μm .

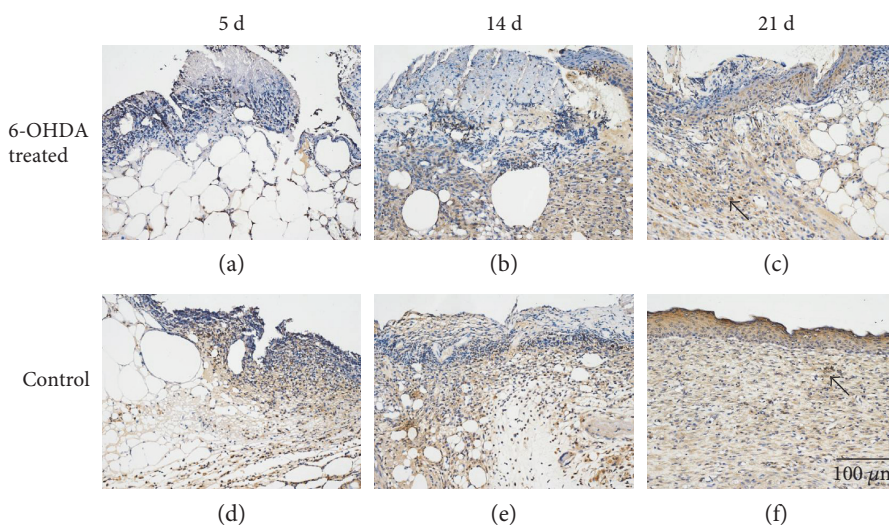


FIGURE 6: IL-1 β immunohistochemistry. IL-1 β is widely expressed on fibroblasts, macrophages, and epidermal cells. Arrows indicate positive staining within fibroblasts. The bar corresponds to 100 μm .

injury (Figure 10(c)) compared with those in the control group. Desmin expression in the treatment group was significantly less than that in the control group on days 2 ($p < 0.001$), 5 ($p < 0.001$), 7 ($p < 0.001$), 10 ($p < 0.001$), 14 ($p = 0.442$), 17 ($p = 0.698$), and 21 ($p = 0.869$) (Figure 10(d)). The expression of NG2 proteoglycan in the 6-OHDA-treated group was lower than that in the control group on days 2 ($p < 0.001$), 5 ($p < 0.001$), 7 ($p < 0.001$), 10 ($p = 0.001$), 14 ($p < 0.001$), 17 ($p < 0.001$), and 21 ($p < 0.001$) (Figure 10(e)). MMP-9 expression in the experimental group exceeded that of the control group on days 2 ($p < 0.001$), 5 ($p < 0.001$), and 7 ($p = 0.115$). However, MMP-9 expression in the control group increased and surpassed that of the treatment group on days 10 ($p = 0.056$), 14 ($p < 0.001$), 17 ($p = 0.777$), and 21 ($p < 0.001$) (Figure 10(f)). NE levels decreased significantly after

sympathectomy on days 2 ($p < 0.001$), 5 ($p < 0.001$), 7 ($p < 0.001$), 10 ($p = 0.004$), 14 ($p = 0.009$), 17 ($p < 0.001$), and 21 ($p = 0.025$) (Figure 10(g)).

4. Discussion

Wound healing requires successive phases of inflammation, cell proliferation, cell migration, angiogenesis, and reepithelialization [5]. Sympathetic denervation, prolonged inflammatory responses, and impaired angiogenesis are often present in patients with DFUs. The relationship between these three features in the diabetic foot is not completely clear. Sympathetic nerve activity may correlate with reepithelialization, neurogenic inflammation [12], collagen metabolism, and angiogenesis [6]. The role of sympathetic nerve failure in DFUs remains controversial.

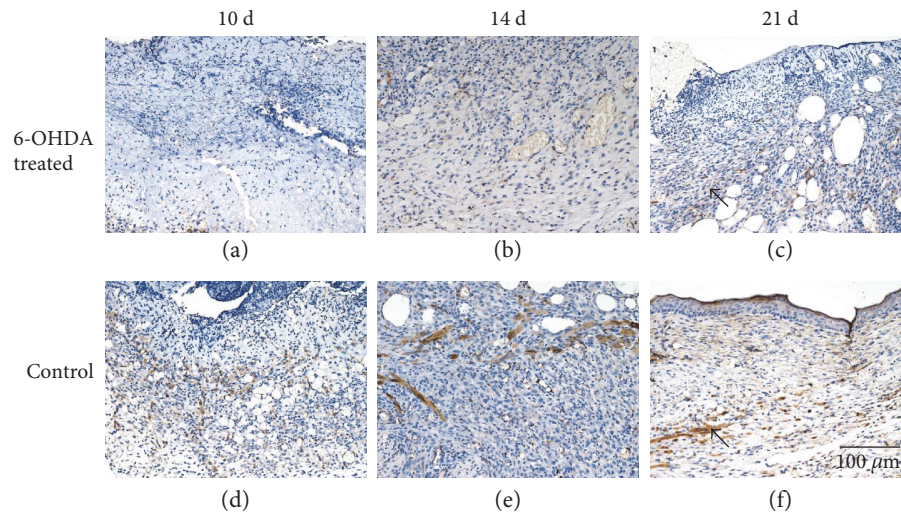


FIGURE 7: Immunohistochemical staining of desmin in the wounds of diabetic mice. Desmin is expressed by pericytes. The bar corresponds to 100 μm .

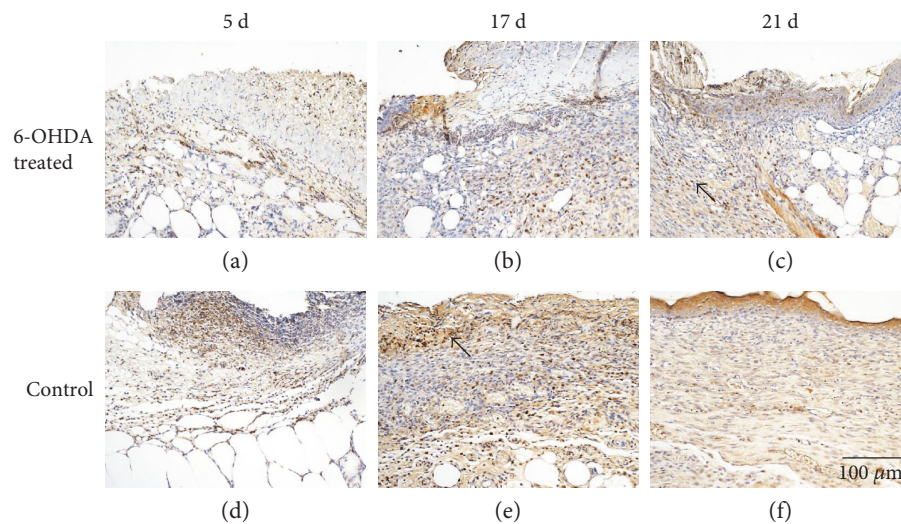


FIGURE 8: Immunohistochemical staining of NG2 proteoglycan in the wounds of diabetic mice. NG2 proteoglycan is expressed by the mural cell component of mouse neovascular structures. The bar corresponds to 100 μm .

Sympathetic nerves are located near pericytes in the microvessels [6]. It has not been reported how sympathetic denervation affects inflammation and angiogenesis in DFUs.

6-OHDA can reduce NE concentrations [24] and can be used to create animal models of sympathetic denervation, which was also shown in our study (Figure 10(g)). We show here that chemical sympathectomy with 6-OHDA accelerates wound contraction in diabetic wounds (Figures 1(a) and 1(b)). There were more collagen fibers in the 6-OHDA-treated group than in the control group (Figures 3(a) and 3(b)). This result differs from the report of Kokobelian et al. [10], who concluded that sympathectomy was ineffective for the treatment of DFUs.

Epithelialization is an important aspect of the healing process. We found that the reepithelialization rate in

wounds was reduced after sympathectomy (Figures 2(a) and 2(b)), suggesting that the delayed reepithelialization in DFUs [25] may be due to sympathetic nerve failure. Previous studies also showed that chemical sympathectomy with 6-OHDA can delay reepithelialization in cutaneous wounds [12, 14]. EGF plays an essential role in wound healing by stimulating epidermal and dermal regeneration [26]. EGF was found to be decreased in diabetic wounds after sympathectomy (Figures 5 and 10). Thus, 6-OHDA may delay reepithelialization in diabetic wounds by reducing their EGF levels.

MCs participate in the inflammatory process of wound healing and in obesity and diabetes [27]. The number of degranulated MCs was found to be increased in the unwounded forearm and foot skin of diabetic patients and in the unwounded dorsal skin of diabetic mice [28]. MCs

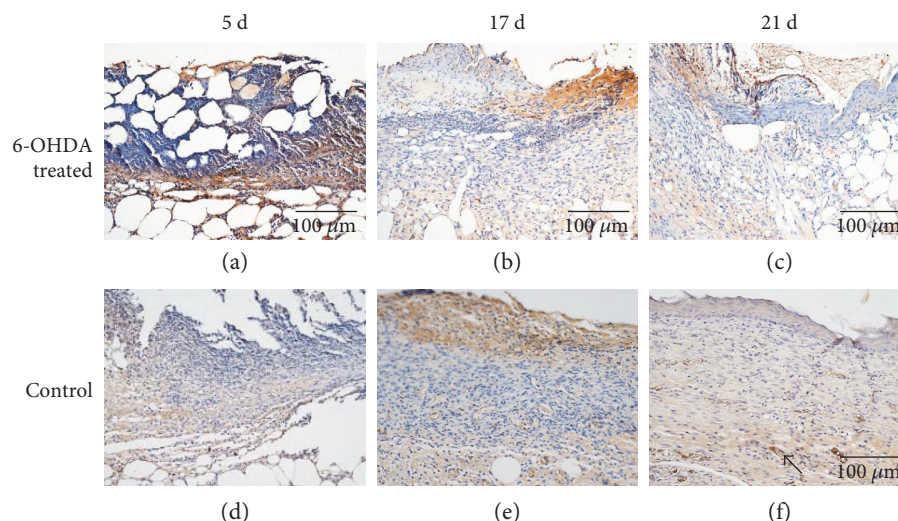


FIGURE 9: Immunohistochemical staining of MMP-9 in the wounds of diabetic mice. MMP-9 is widely distributed in various tissues and bodily fluids. The bar corresponds to 100 μm .

recruit inflammatory cells directly and indirectly [27] and act as transducers between peripheral nerves and local inflammatory events [29]. We found few MCs in inflamed skin wounds (Figure 4(a)), but MCs began to increase rapidly during the remodeling phase. This finding is consistent with a report by Nishikori et al. [30]. Additionally, in our experiment, MCs were significantly decreased after sympathectomy (Figure 4(b)). Similarly, Souza et al. [14] demonstrated that chemical sympathectomy led to reduced MC migration during cutaneous wound healing in rats. This finding suggests that a reduction in MCs may promote diabetic wound healing in 6-OHDA-treated animals.

IL-1 β is upregulated during the inflammatory phase of diabetic wounds [31]. Inhibiting the IL-1 β pathway in the wounds of diabetic mice led to an increase in the levels of wound growth factors and improved wound healing [32]. We found that 6-OHDA reduced the levels of IL-1 β in diabetic wounds (Figures 6 and 10). Kim et al. [12] showed that 6-OHDA significantly reduced neurogenic inflammation in animal skin incisions. This finding suggests that sympathetic denervation can inhibit the prolonged inflammatory response induced by IL-1 β and MCs in diabetic wounds.

The process of angiogenesis includes endothelial cell activation, the degradation of the vascular basement membrane, and vascular sprouting [33]. Angiogenesis depends upon the balance of pericytes and endothelial cells. Pericytes embedded within the basement membrane of capillaries and postcapillary venules play an important role in endothelial cell proliferation, migration, and stabilization [34]. An imbalance of pericytes and endothelial cells will impair the development of functional capillaries in DFUs [35]. Few studies have evaluated the effect of sympathetic denervation on angiogenesis in DFUs.

In this experiment, lower expression levels of desmin and NG2 proteoglycan were observed in the 6-OHDA-treated group (Figures 7, 8, and 10). Previous studies demonstrated that surgical sympathectomy may cause a reduction in pericyte markers (platelet-derived growth factor-BB (PDGF-

BB) and NG2 proteoglycan) in rat retinas [36]. Thus, pericyte proliferation in diabetic wounds may be inhibited by sympathectomy. Pericytes are derived from hematopoietic stem cells [37]. The number of hematopoietic stem and progenitor cells (HSPC) mobilized by granulocyte colony-stimulating factor was dramatically reduced in 6-OHDA-lesioned mice [38]. Adrenergic receptors were found to be present in endothelial cells and pericytes [6]. Therefore, reduced levels of pericytes in 6-OHDA-treated diabetic mice may be due to abrogated HSPC migration.

Pericytes are crucial for the survival of endothelial cells and may control endothelial cell proliferation [39]. Pericyte-derived NG2 promotes endothelial cell migration and morphogenesis during the early stages of neovascularization [40]. The number of endothelial cells and pericytes was significantly reduced in the retina of NG2-knockout mice [41]. This finding suggests that a reduction in pericytes after sympathectomy may lead to a decrease in endothelial cells.

MMP-9 is involved in the dynamic remodeling of the ECM, which is essential for all stages of angiogenesis [33]. An increased ratio of serum MMP-9 has been observed in DFU patients [42]. In our study, MMP-9 expression in the treatment group was significantly higher than in the control group on days 2 and 5. With the effect of sympathetic denervation gradually diminishing, MMP-9 expression increased in the control group and surpassed the treatment group on days 10, 14, 17, and 21. Thus, increased MMP-9 expression in diabetic wounds may result in part from sympathetic denervation.

Previous studies found that inflammatory factors, such as MCs and IL-1 β , were upregulated in the skin and wounds of diabetic patients. Excessive inflammatory responses are harmful in diabetic wounds; thus, the control of inflammation by 6-OHDA can promote wound contraction. The level of angiogenesis in wounds often correlates with the inflammatory response, largely because inflammatory cells produce an abundance of proangiogenic mediators [43]. In this study, the selective reduction of inflammation and

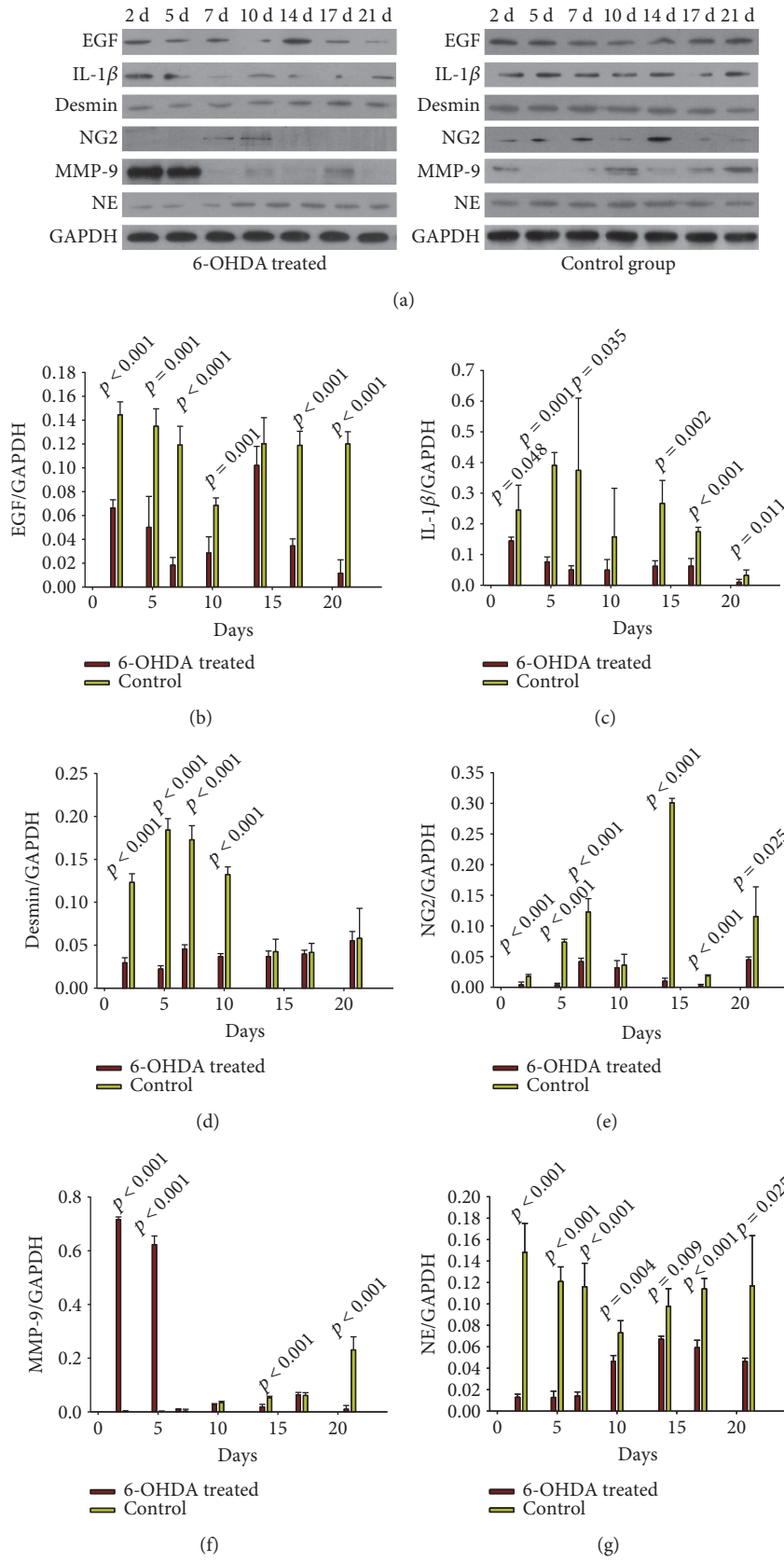


FIGURE 10: (a) Western blot results. (b)–(g) Relative protein expression levels of EGF, IL-1 β , desmin, NG2, MMP-9, and NE in the wounds of diabetic mice. Protein expression levels were calculated relative to GAPDH from the same sample. The values shown are the mean \pm standard deviations, $n = 4$ specimens per group at each time point. $p < 0.05$, 6-OHDA treated versus control (one-way analysis of variance (ANOVA)).

angiogenesis were both found after sympathectomy in diabetic wounds. The relationship between inflammation and angiogenesis is complex, and further research is required to determine which process plays the more predominant role in diabetic wound healing.

In conclusion, as Souza et al.'s report in normal rats [14], sympathetic denervation accelerates wound contraction but delays reepithelialization in diabetic mice. We further proved that 6-OHDA decreased EGF, IL-1 β levels, and the number of mast cells (MCs). Besides, the sympathetic denervation caused by 6-OHDA led to reduced pericyte proliferation in diabetic wounds, which might explain the vascular dysfunction after sympathetic nerve loss in diabetic wounds.

Conflicts of Interest

The authors declare that they have no conflict of interest.

Authors' Contributions

Zhifang Zheng was responsible for paper writing. Zhifang Zheng, Yu Wan, Yishu Liu, and Yu Yang completed the experiments. The study was designed by Biao Cheng and Jianbing Tang.

References

- [1] S. Vuorisalo, M. Venermo, and M. Lepantalo, "Treatment of diabetic foot ulcers," *The Journal of Cardiovascular Surgery*, vol. 50, pp. 275–291, 2009.
- [2] J. Ahmad, "The diabetic foot," *Diabetes & Metabolic Syndrome*, vol. 10, pp. 48–60, 2016.
- [3] T. Dinh, F. Tecilazich, A. Kafanas et al., "Mechanisms involved in the development and healing of diabetic foot ulceration," *Diabetes*, vol. 61, pp. 2937–2947, 2012.
- [4] E. Dreha, K. Stankowska, A. Kulwas, and D. Rosc, "Endothelial progenitor cells in diabetic foot syndrome," *Advances in Clinical and Experimental Medicine : Official Organ Wroclaw Medical University*, vol. 21, pp. 249–254, 2012.
- [5] L. Pradhan, C. Nabzdyk, N. D. Andersen, F. W. LoGerfo, and A. Veves, "Inflammation and neuropeptides: the connection in diabetic wound healing," *Expert Reviews in Molecular Medicine*, vol. 11, article e2, 2009.
- [6] L. Pan, J. Tang, H. Liu, and B. Cheng, "Sympathetic nerves: how do they affect angiogenesis, particularly during wound healing of soft tissues?," *Clinical Hemorheology and Microcirculation*, vol. 62, pp. 181–191, 2016.
- [7] P. J. Watkins and M. E. Edmonds, "Sympathetic nerve failure in diabetes," *Diabetologia*, vol. 25, pp. 73–77, 1983.
- [8] J. D. Lefrandt, E. Bosma, P. H. Oomen et al., "Sympathetic mediated vasomotion and skin capillary permeability in diabetic patients with peripheral neuropathy," *Diabetologia*, vol. 46, pp. 40–47, 2003.
- [9] N. A. Shor, F. Chumak Iu, V. P. Reuka, and O. A. Zhukov, "Revascularization of the lower limbs for ischemic diabetic foot with pyonecrotic tissue lesions," *Angiologija i Sosudistaia Khirurgija = Angiology and Vascular Surgery*, vol. 10, pp. 85–89, 2004.
- [10] A. R. Kokobelian and I. M. Zigmantovich, "Syndrome of diabetic foot and atherosclerosis of the lower extremity arteries," *Vestnik Khirurgii Imeni I. I. Grekova*, vol. 165, pp. 74–78, 2006.
- [11] W. Qi, J. Tian, C. Zhang et al., "Potential role of HPA axis and sympathetic nervous responses in depletion of B cells induced by H9N2 avian influenza virus infection," *PLoS One*, vol. 7, article e51029, 2012.
- [12] L. R. Kim, K. Whelpdale, M. Zurowski, and B. Pomeranz, "Sympathetic denervation impairs epidermal healing in cutaneous wounds," *Wound Repair and Regeneration : Official Publication of the Wound Healing Society [and] the European Tissue Repair Society*, vol. 6, pp. 194–201, 1998.
- [13] K. Saburo, K. Hiroshi, and M. Toshihiro, "The role of sympathetic catecholaminergic nerves in wound healing," *Burns, Including Thermal Injury*, vol. 9, pp. 135–141, 1982.
- [14] B. R. Souza, J. F. Cardoso, T. P. Amadeu, A. Desmouliere, and A. M. Costa, "Sympathetic denervation accelerates wound contraction but delays reepithelialization in rats," *Wound Repair and Regeneration : Official Publication of the Wound Healing Society [and] the European Tissue Repair Society*, vol. 13, pp. 498–505, 2005.
- [15] A. Kasuya and Y. Tokura, "Attempts to accelerate wound healing," *Journal of Dermatological Science*, vol. 76, pp. 169–172, 2014.
- [16] M. Felcht, R. Luck, A. Schering et al., "Angiopoietin-2 differentially regulates angiogenesis through TIE2 and integrin signaling," *The Journal of Clinical Investigation*, vol. 122, pp. 1991–2005, 2012.
- [17] A. P. Hall, "Review of the pericyte during angiogenesis and its role in cancer and diabetic retinopathy," *Toxicologic Pathology*, vol. 34, pp. 763–775, 2006.
- [18] K. M. Grebe, K. Takeda, H. D. Hickman et al., "Cutting edge: sympathetic nervous system increases proinflammatory cytokines and exacerbates influenza A virus pathogenesis," *Journal of Immunology*, vol. 184, pp. 540–544, 2010.
- [19] D. Altavilla, A. Saitta, D. Cucinotta et al., "Inhibition of lipid peroxidation restores impaired vascular endothelial growth factor expression and stimulates wound healing and angiogenesis in the genetically diabetic mouse," *Diabetes*, vol. 50, pp. 667–674, 2001.
- [20] B. L. Chen, J. Peng, Q. F. Li, M. Yang, Y. Wang, and W. Chen, "Exogenous bone morphogenetic protein-7 reduces hepatic fibrosis in *Schistosoma japonicum*-infected mice via transforming growth factor- β /Smad signaling," *World Journal of Gastroenterology*, vol. 19, pp. 1405–1415, 2013.
- [21] C. A. Dinarello, "Interleukin-1 and the pathogenesis of the acute-phase response," *The New England Journal of Medicine*, vol. 311, pp. 1413–1418, 1984.
- [22] D. Paulin and Z. Li, "Desmin: a major intermediate filament protein essential for the structural integrity and function of muscle," *Experimental Cell Research*, vol. 301, pp. 1–7, 2004.
- [23] U. Ozerdem, K. A. Grako, K. Dahlin-Huppe, E. Monosov, and W. B. Stallcup, "NG2 proteoglycan is expressed exclusively by mural cells during vascular morphogenesis," *Developmental Dynamics : an Official Publication of the American Association of Anatomists*, vol. 222, pp. 218–227, 2001.
- [24] S. Yamada, H. I. Yamamura, and W. R. Roeske, "Effects of chemical sympathectomy with 6-hydroxydopamine on α - and β -adrenoceptors and muscarinic cholinergic receptors in rat kidney," *European Journal of Pharmacology*, vol. 121, pp. 345–353, 1986.
- [25] K. Anderson and R. L. Hamm, "Factors that impair wound healing," *The Journal of the American College of Clinical Wound Specialists*, vol. 4, pp. 84–91, 2012.

- [26] R. J. Bodnar, "Epidermal growth factor and epidermal growth factor receptor: the Yin and Yang in the treatment of cutaneous wounds and cancer," *Advances in Wound Care*, vol. 2, pp. 24–29, 2013.
- [27] M. A. Shi and G. P. Shi, "Different roles of mast cells in obesity and diabetes: lessons from experimental animals and humans," *Frontiers in Immunology*, vol. 3, p. 7, 2012.
- [28] A. Tellechea, E. C. Leal, A. Kafanas et al., "Mast cells regulate wound healing in diabetes," *Diabetes*, vol. 65, pp. 2006–2019, 2016.
- [29] H. P. Kleij and J. Bienenstock, "Significance of conversation between mast cells and nerves," *Allergy, Asthma, and Clinical Immunology : Official Journal of the Canadian Society of Allergy and Clinical Immunology*, vol. 1, pp. 65–80, 2005.
- [30] Y. Nishikori, N. Shiota, and H. Okunishi, "The role of mast cells in cutaneous wound healing in streptozotocin-induced diabetic mice," *Archives of Dermatological Research*, vol. 306, pp. 823–835, 2014.
- [31] J. Berlanga-Acosta, C. Valdéz-Pérez, W. Savigne-Gutiérrez et al., "Pro-inflammatory cytokines as tumor necrosis factor- α and interleukin- 1β are increased in diabetic wounds with negative local and remote consequences," *Biotecnología Aplicada*, vol. 27, pp. 255–261, 2010.
- [32] R. E. Mirza, M. M. Fang, W. J. Ennis, and T. J. Koh, "Blocking interleukin-1beta induces a healing-associated wound macrophage phenotype and improves healing in type 2 diabetes," *Diabetes*, vol. 62, pp. 2579–2587, 2013.
- [33] D. R. Senger and G. E. Davis, "Angiogenesis," *Cold Spring Harbor Perspectives in Biology*, vol. 3, article a005090, 2011.
- [34] D. Ribatti, B. Nico, and E. Crivellato, "The role of pericytes in angiogenesis," *The International Journal of Developmental Biology*, vol. 55, pp. 261–268, 2011.
- [35] L. Qiao, S. L. Lu, J. Y. Dong, and F. Song, "Abnormal regulation of neo-vascularisation in deep partial thickness scalds in rats with diabetes mellitus," *Burns : Journal of the International Society for Burn Injuries*, vol. 37, pp. 1015–1022, 2011.
- [36] L. A. Wiley, G. R. Rupp, and J. J. Steinle, "Sympathetic innervation regulates basement membrane thickening and pericyte number in rat retina," *Investigative Ophthalmology & Visual Science*, vol. 46, pp. 744–748, 2005.
- [37] I. Rajantie, M. Ilmonen, A. Alminaitte, U. Ozerdem, K. Alitalo, and P. Salven, "Adult bone marrow-derived cells recruited during angiogenesis comprise precursors for periendothelial vascular mural cells," *Blood*, vol. 104, pp. 2084–2086, 2004.
- [38] Y. Katayama, M. Battista, W. M. Kao et al., "Signals from the sympathetic nervous system regulate hematopoietic stem cell egress from bone marrow," *Cell*, vol. 124, pp. 407–421, 2006.
- [39] H. P. Hammes, J. Lin, O. Renner et al., "Pericytes and the pathogenesis of diabetic retinopathy," *Diabetes*, vol. 51, pp. 3107–3112, 2002.
- [40] J. Fukushi, I. T. Makagiansar, and W. B. Stallcup, "NG2 proteoglycan promotes endothelial cell motility and angiogenesis via engagement of galectin-3 and $\alpha 3\beta 1$ integrin," *Molecular Biology of the Cell*, vol. 15, pp. 3580–3590, 2004.
- [41] U. Ozerdem and W. B. Stallcup, "Pathological angiogenesis is reduced by targeting pericytes via the NG2 proteoglycan," *Angiogenesis*, vol. 7, pp. 269–276, 2004.
- [42] Z. Li, S. Guo, F. Yao, Y. Zhang, and T. Li, "Increased ratio of serum matrix metalloproteinase-9 against TIMP-1 predicts poor wound healing in diabetic foot ulcers," *Journal of Diabetes and its Complications*, vol. 27, pp. 380–382, 2013.
- [43] L. A. DiPietro, "Angiogenesis and wound repair: when enough is enough," *Journal of Leukocyte Biology*, vol. 100, pp. 979–984, 2016.

Research Article

Development of a Plantar Load Estimation Algorithm for Evaluation of Forefoot Load of Diabetic Patients during Daily Walks Using a Foot Motion Sensor

Ayano Watanabe,¹ Hiroshi Noguchi,² Makoto Oe,³ Hiromi Sanada,¹ and Taketoshi Mori²

¹Department of Gerontology, Graduate School of Medicine, The University of Tokyo, 7-3-1 Hongo, Bunkyo-ku, Tokyo, Japan

²Department of Life Support Technology (Molten), Graduate School of Medicine, The University of Tokyo, 7-3-1 Hongo, Bunkyo-ku, Tokyo, Japan

³Department of Advanced Nursing Technology, Graduate School of Medicine, The University of Tokyo, 7-3-1 Hongo, Bunkyo-ku, Tokyo, Japan

Correspondence should be addressed to Taketoshi Mori; tmoriics-tky@umin.ac.jp

Received 6 February 2017; Accepted 25 May 2017; Published 3 August 2017

Academic Editor: Ilias Migdalis

Copyright © 2017 Ayano Watanabe et al. This is an open access article distributed under the Creative Commons Attribution License, which permits unrestricted use, distribution, and reproduction in any medium, provided the original work is properly cited.

Forefoot load (FL) contributes to callus formation, which is one of the pathways to diabetic foot ulcers (DFU). In this study, we hypothesized that excessive FL, which cannot be detected by plantar load measurements within laboratory settings, occurs in daily walks. To demonstrate this, we created a FL estimation algorithm using foot motion data. Acceleration and angular velocity data were obtained from a motion sensor attached to each shoe of the subjects. The accuracy of the estimated FL was validated by correlation with the FL measured by force sensors on the metatarsal heads, which was assessed using the Pearson correlation coefficient. The mean of correlation coefficients of all the subjects was 0.63 at a level corridor, while it showed an intersubject difference at a slope and stairs. We conducted daily walk measurements in two diabetic patients, and additionally, we verified the safety of daily walk measurement using a wearable motion sensor attached to each shoe. We found that excessive FL occurred during their daily walks for approximately three hours in total, when any adverse event was not observed. This study indicated that FL evaluation method using wearable motion sensors was one of the promising ways to prevent DFUs.

1. Introduction

Diabetic foot ulcer (DFU) is one of the serious and prevalent complications of diabetes, and they are defined as cutaneous erosions characterized by a loss of epithelium that extends into or through the dermis to deeper tissues [1]. Diabetes is known to delay wound healing, and 85% of all amputations are the result of a nonhealing DFU [2, 3]. Through many clinical cases, callus has been recognized as a pathway to DFU because tissue damage is caused under the hyperkeratotic plantar epidermis [4]. A previous study reported that 56.3% of all of DFUs were located beneath metatarsal heads (MTHs) [5]. Hyperkeratosis is caused by excessive mechanical loading, which is more likely on bony prominences of the

forefoot such as MTHs [6]. Thus, the forefoot is at particular risk of developing DFUs.

There have been few studies investigating plantar load in the daily lives of patients with diabetes, while previous measurements of plantar load during walking have been tried as a means of assessing the at-risk foot and to prevent ulceration [7, 8]. Also, some studies have carried out comparison of plantar load in diabetic patients and healthy control subjects [9, 10]. However, these measurements have been applied generally within laboratory and outpatient settings that specialize in DFU. Furthermore, plantar load measurement is typically limited to walking on a short, level walkway, despite the fact that some clinical cases have indicated development of DFUs might be related to the excessive load occurring in

daily walks. For example, diabetic patients who are still working walk more often in their daily lives than the elderly, so their feet are more exposed to the risk of DFUs caused by calluses [11]. Also, there are cases in which custom-made shoes for pressure relief sometimes fail to improve the callus of patients with diabetes who walked a lot routinely [12]. These cases indicate the necessity of plantar load evaluation in the actual daily life of patients such as locations where they walk or their activity. There is thus the possibility that greater load which was not observed in the above settings happens in the patients' daily life environment.

As it stands now, it is challenging technically to establish methods to measure plantar force directly over a long time in daily living. In laboratory settings, two types of plantar force measurement systems are mainly used: platform systems and in-shoe systems [13]. Platform systems are composed of a flat, rigid array of pressure-sensing elements arranged in a matrix configuration and embedded in the floor. Therefore, the use of platform systems is generally restricted to laboratories. In-shoe force measurement systems are flexible and inserted in the shoe. The in-shoe systems are used in various studies of gait but several cables connecting force sensors and a data logger disturb activities in daily living. In addition, soft force sensors are not strong enough to bear continuous load for a long time, whereas rigid force sensors have risk to cause damage on the plantar in long-time measurement.

The human gait cycle can be divided into a stance phase and a swing phase. The stance phase is defined as the duration when the foot is on the ground, which can be subdivided into three phases: heel-strike, midstance, and push-off. Generally, the forefoot load (FL) increases substantially from the beginning of the midstance to the end of the push-off. In other words, midstance and push-off are the period when the forefoot is in contact with the ground.

In order to determine the FL, the midstance and push-off need to be identified. However, calculation for the center of the plantar load is required to recognize the phases using the trajectory of the force center, which is not easy [14]. The plantar load can be considered as equal to the sum of ground reaction forces (GRFs) which are acting between the foot and ground during stance phase. The GRFs can be computed by means of Newtonian mechanics. Hence, in this study, we adopted a different approach that identifies the midstance and push-off phases and then calculates the force localized to the foot, using inertial sensors which provide accelerations and angular velocities that are composition elements of Newtonian mechanics.

As reported in previous papers, many methods to estimate GRFs have been proposed other than Newtonian mechanics. For instance, a regression model was developed to predict peak plantar load from an acceleration-based activity monitor [15]. While the developed model predicted peak plantar load well, it required a dummy variable of the range of locomotion speed which was determined using electronic timing gates. Therefore, this model is workable only under laboratory settings. Also, GRF estimation studies using neural network models have increased recently but they require carefully chosen input variables and many training

data for the estimation model to reduce errors in the estimation [16, 17]. The Newton mechanics has been known to be able to calculate GRFs accurately in the most of the stance phase without any complicated process [18]. Yamazaki developed a method that calculates GRFs by solving the force equilibrium equations for each of the body segments of a mechanical model [19]. In his study, changes in body segment orientation and posture during walking were obtained by the optical motion capture system. Typically, the system uses cameras to obtain serial images of motions, which is not practical for daily use. However, it may be possible to alternate the optical motion capture system with the wearable motion sensor systems.

Wearable inertial motion sensors are composed of an acceleration sensor and a gyro sensor, and they have already been popular in biomedical applications, that is, measurement of physical activity in daily living. The wearable motion sensors are small enough to be attached anywhere and constrain or affect their user in any way, so they can be easily deployed in daily use [20, 21].

The purpose of this study was to evaluate the FL in daily walks of diabetic patients using a wearable motion sensor attached to each foot, so as to compare the FL between daily life environment and laboratory setting. In this paper, we first describe the process of FL estimation. Next, we validate the estimated FL by comparing it with FL measured by force sensors on the forefoot, which was assessed using the Pearson correlation coefficient. The estimated FL calculated using seven motion sensors of all the lower body segments, as well as only using a motion sensor of each foot, is validated here. Finally, we evaluate the FL of two diabetic patients estimated from foot motion data so as to determine the differences in the FL between their actual daily environment and the laboratory setting such as a short level corridor.

2. Methods

This study is composed of two main experiments. The first experiment is to validate estimated FL using correlation with FL measured by force sensors among healthy subjects. The walking measurements for the validation of the estimation algorithm were carried out in the following places: a level corridor, stairs, and a slope. The second experiment is to compare the FL between their actual daily environment and laboratory setting.

Written consent was obtained prior to the study, and all procedures were approved by the Research Ethics Committee of the Graduate School of Medicine, the University of Tokyo (number 11343).

2.1. Development of the Algorithm for Estimation of Forefoot Plantar Load

2.1.1. Subjects. Ten healthy subjects (4 males and 6 females; age: 32 ± 9 yr; weight: 61 ± 16 kg) without walking disorders participated in the experiment.

2.1.2. Instrumentation. Seven inertial motion sensors containing a 3-axis acceleration sensor and a 3-axis gyro sensor



FIGURE 1: Walking measurement for validation of the estimation algorithm. A motion sensor was attached to each of the lower body segment; in addition, 4 force sensors were attached to 1st and 2nd MTH (2 sensors each).



FIGURE 2: Force sensors on the 1st and 2nd MTH used for validation of the estimation algorithm.

(Logical Product Corporation, Fukuoka, Japan) were attached to several locations: sacrum, left and right thigh, left and right shank, and left and right foot (Figure 1). The motion sensors were secured to each body segment by Velcro straps so as to measure motion in the sagittal plane. Acceleration and angular velocity were recorded at a sampling rate of 100 Hz and low pass filtered using a fourth order, zero-lag critically damped filter with a cut-off frequency of 20 Hz [22]. It should be noted that synchronization with motion data of the seven body segments did not always work correctly. That was why one of the seven motion sensors tended not to collect data at a determined frequency. It was difficult to interpolate when much data were missed consecutively. Four triaxial force sensors (Touchence Inc., Tokyo, Japan) were attached to the 1st and 2nd metatarsal head (MTH) as shown in Figure 2 [23]. The force sensors are able to measure up to 40 N with a sampling rate of 100 Hz.

2.1.3. Protocol. Subjects walked at a self-selected forward speed in the following settings: a 15 m long corridor, stairs consisted of 10 steps which had a 300 mm tread and 180 mm height, and a 15 m long slope with an inclination of 4°. Ascending and descending motion were both performed on the stairs and slope. They walked wearing the shoes they use routinely for daily activities.

2.1.4. Estimation of Forefoot Plantar Load. In this section, first, we calculate vertical GRF based on Newton's equation of motion; then, we discriminate the midstance and push-off to estimate the FL. A seven-rigid-link model

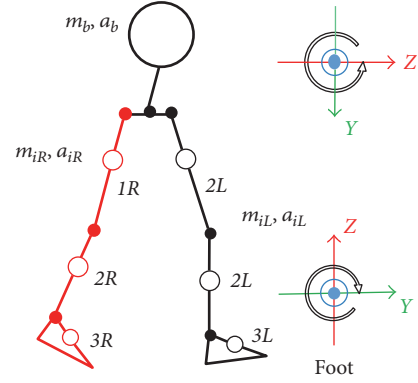


FIGURE 3: Rigid link model employing the present study and local coordinate system.

constructed by Yamazaki [19] was used in this study (Figure 3). All motions were assumed to take place in the sagittal plane. The plantar load N was computed by means of Newton's equation of motion, which states that the sum of all external forces balances the sum of the mass-acceleration products of all individual body segments as follows:

$$N = m_b(a_b + g) + \sum_{i=1}^3 m_i(a_{iR} + a_{iL} + 2g). \quad (1)$$

Here, m_b was the mass of the upper body, a_b was the vertical acceleration of the upper body, m_i was the mass of the i th leg segment, a_{iR} was the vertical acceleration of the i th right leg segment, a_{iL} was the vertical acceleration of the i th left leg segment, and g was the gravitational constant (9.8 ms^{-2}). The mass of each segment was calculated from the body weight based on the anthropometric study data [24]. Vertical acceleration was computed from the acceleration and integrated angular velocity (θ). The angular velocity integration was commenced from tilt angles of each body segment which were computed using static acceleration. Vertical acceleration of the foot could be expressed as

$$a_3 = a_{3z} \cos \theta_3 - a_{3y} \sin \theta_3, \quad (2)$$

where a_{3y} denoted the foot acceleration of the y -axis and a_{3z} denoted the foot acceleration of the z -axis. Vertical acceleration of the thigh could be written as

$$a_1 = a_{1z} \sin \theta_1 - a_{1y} \cos \theta_1, \quad (3)$$

where a_{1y} was the thigh acceleration of the y -axis and a_{1z} was the thigh acceleration of the z -axis. Vertical acceleration of the shank could be expressed as

$$a_2 = a_{2z} \sin \theta_2 - a_{2y} \cos \theta_2, \quad (4)$$

where a_{2y} was the shank acceleration of the y -axis and a_{2z} was the shank acceleration of the z -axis.

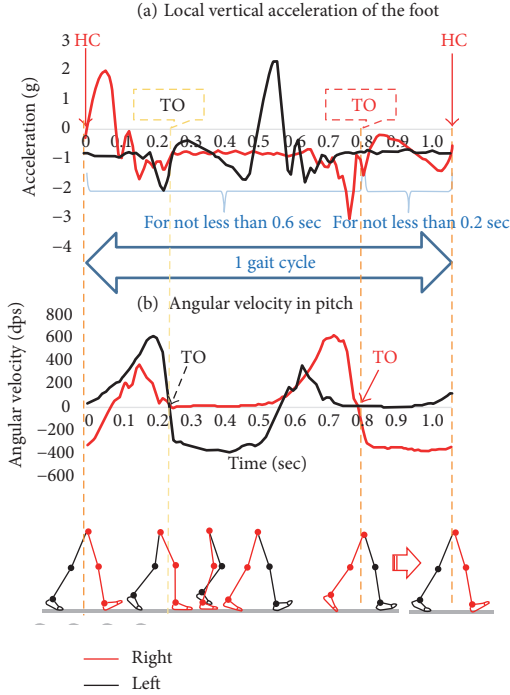


FIGURE 4: Algorithm discriminating IC and TO by foot acceleration and angular velocity.

To detect stance phase based on foot motion data, heel contact (HC) is defined as

$$a_{3zt} \cdot a_{3z(t+1)} \leq 0, \quad (5)$$

and the period from TO of the contralateral foot to HC of the ipsilateral foot is ≥ 0.2 sec, where a_{zt} denoted the foot acceleration of the z -axis at t sec. Toe off (TO) is defined as

$$r_{3xt} \cdot r_{3x(t+1)} \leq 0, \quad (6)$$

and the period from HC to TO of the ipsilateral foot is ≥ 0.6 sec, where r_{xi} denoted the angular velocity in pitch at t sec (Figure 4). The time involving stance phase and swing phase is determined based on the percentage of time involved in the stance phase and swing phase [25]. Also, the minimum time spent on the phases, which was determined empirically, was taken into account.

In order to recognize a period when the forefoot is contact with the ground in the stance phase, a period from the beginning of the midstance to TO needs to be identified. In this study, the beginning of midstance was defined as TO of the ipsilateral foot.

The pattern of the forefoot force while walking down the stairs was diverse among the subjects because the foot location touching a tread at the HC varied among them. Therefore, it is difficult to apply a consistent algorithm to all of the walking on a level corridor, stairs, and a slope. Hence, the descending stairs were excluded from the adaptation of the estimation algorithm.

2.1.5. Validation of Forefoot Load Estimation Algorithm. To validate the estimation algorithm, the estimated FL was compared with the FL measured by force sensors. In this study,

the estimation algorithm was validated using correlation between the estimated FL and the measured FL because we aimed to detect relative excessive load in intrasubject. The correlation was assessed by the Pearson correlation coefficient. First, we computed correlation during midstance and push-off of each step, which was equal to approximately 0.6 sec (60 samples). Then, we calculated the mean and standard deviation (SD) of the Pearson correlation coefficient over 30 steps (15 steps of each foot) excluding the 1st step and last. In the case of the stair walking, the mean and SD of the Pearson correlation coefficient over 9 steps (4 steps of one foot and 5 steps of the other) excluding the last step were assessed. The Pearson correlation coefficient was categorized (in absolute value) as $p \leq 0.35$: weak, $0.35 < p \leq 0.65$: moderate, $0.67 < p \leq 0.9$: strong, $0.9 < p$: excellent [26]. One of the four force data representing the maximum value during midstance and push-off was used as the reference data of estimated FL.

Finally, 18 of the 50 trials, which were measured without the errors in sampling, were included in the correlation analysis.

2.1.6. Applicability of the Algorithm. The estimated FL and FL measured by force sensors on the MTHs demonstrated from moderate to strong correlation during walking on a level corridor (Table 1(a)). The magnitude of correlation remained consistent even when the FL was estimated only using foot motion data. The mean of correlation coefficient of all the subject was 0.63.

In the other places, the correlation between the estimated FL and FL measured by force sensors on the MTHs showed an intersubject difference (Tables 1(b), 1(c), and 1(d)).

Finally, we could demonstrate that the estimation algorithm was applicable to walks on the level ground. However, the estimation algorithm was not adequate to use walks on stairs or slopes.

2.2. Plantar Load Measurement in Daily Living of Patients with Diabetes

2.2.1. Subjects. Two diabetic patients participated in the study and their characteristics are as shown in Table 2. This time, patients under 60 years old, who often go out and walk routinely, were included in this study. In addition, from the aspect of safety, patients with neuropathies or calluses were excluded.

2.2.2. Instrumentation. A motion sensor containing a 3-axis acceleration sensor and a 3-axis gyro sensor (ATR-Promotions Inc., Soraku, Japan) were attached to each shoe with strap (Figures 5 and 6). Acceleration and angular velocity were recorded at a sampling rate of 100 Hz.

2.2.3. Protocol

(1) Walking Measurement in Laboratory Setting. Subjects walked at a self-selected forward speed on a 15 m long corridor twice, wearing the shoes they use routinely for daily activities.

TABLE 1: Correlation between FL from force sensors on the forefoot and estimated FL from all the motion sensors (left part of the tables)/foot motion sensors (right part of the tables).

(a) Walking on a level corridor

All the motion data of the lower body segments			Only each foot motion data		
ID	Mean \pm SD of the Pearson correlation coefficient		ID	Mean \pm SD of the Pearson correlation coefficient	
	Left	Right		Left	Right
3	0.68 \pm 0.08	0.58 \pm 0.10	3	0.72 \pm 0.06	0.71 \pm 0.05
5	0.07 \pm 0.03	0.69 \pm 0.10	5	0.69 \pm 0.04	0.71 \pm 0.04
6	0.62 \pm 0.09	0.71 \pm 0.05	6	0.67 \pm 0.04	0.55 \pm 0.06
8	0.68 \pm 0.08	0.83 \pm 0.04	8	0.61 \pm 0.04	0.58 \pm 0.09
10	0.07 \pm 0.17	0.47 \pm 0.14	10	0.57 \pm 0.08	0.48 \pm 0.10

(b) Walking up stairs

All the motion data of the lower body segments			Only each foot motion data		
ID	Mean \pm SD of the Pearson correlation coefficient		ID	Mean \pm SD of the Pearson correlation coefficient	
	Left	Right		Left	Right
2	0.72 \pm 0.06	0.66 \pm 0.18	2	0.10 \pm 0.23	-0.21 \pm 0.04
4	0.65 \pm 0.11	0.43 \pm 0.16	4	0.39 \pm 0.30	0.10 \pm 0.56
6	0.67 \pm 0.05	0.74 \pm 0.04	6	0.67 \pm 0.05	0.74 \pm 0.04
8	0.74 \pm 0.07	0.44 \pm 0.07	8	0.68 \pm 0.09	0.64 \pm 0.10
10	0.38 \pm 0.15	0.42 \pm 0.14	10	0.05 \pm 0.19	0.44 \pm 0.16

(c) Walking up a slope

All the motion data of the lower body segments			Only each foot motion data		
ID	Mean \pm SD of the Pearson correlation coefficient		ID	Mean \pm SD of the Pearson correlation coefficient	
	Left	Right		Left	Right
3	0.42 \pm 0.28	0.27 \pm 0.39	3	0.72 \pm 0.03	0.57 \pm 0.07
4	0.07 \pm 0.15	0.55 \pm 0.13	4	0.43 \pm 0.13	0.54 \pm 0.19
5	0 \pm 0.13	0.23 \pm 0.09	5	0.57 \pm 0.09	0.57 \pm 0.12
8	0.54 \pm 0.35	0.60 \pm 0.34	8	0.42 \pm 0.21	0.23 \pm 0.36
10	0.30 \pm 0.19	0.11 \pm 0.31	10	0.29 \pm 0.25	0.26 \pm 0.20

(d) Walking down a slope

All the motion data of the lower body segments			Only each foot motion data		
ID	Mean \pm SD of the Pearson correlation coefficient		ID	Mean \pm SD of the Pearson correlation coefficient	
	Left	Right		Left	Right
5	0.48 \pm 0.11	0.67 \pm 0.07	5	0.72 \pm 0.03	0.75 \pm 0.09
8	0.76 \pm 0.08	0.74 \pm 0.08	8	0.38 \pm 0.25	0.32 \pm 0.23
10	-0.17 \pm 0.59	-0.07 \pm 0.46	10	0.17 \pm 0.35	0 \pm 0.30

Thirty steps during walking corridors were evaluated, which did not include the first and last steps.

(2) *Walking Measurement in Daily Life Environment.* After the subjects walked on the corridors, they were asked to record their foot motion while they walked wearing the shoes in their daily activity area. Also, they were asked to take notes where they were walking and whether they used vehicle when they traveled from place to place.

In daily walk data, consecutive steps for not less than 30 seconds were analyzed, because the period was assumed to

be longer than the common walking measurement time in laboratory settings.

(3) *Definition of the Excessive Forefoot Load.* A walking trial on a 15 m long corridor was performed twice to define the “excessive load” of each patient from either one of the trials. Estimated FL points deviating more than 2 standard deviations from the average maximum FL of 15 steps were defined as excessive FL. The frequency of the excessive FL during walking was compared between the two settings: a corridor and daily life environment.

TABLE 2: Characteristics of each patient.

	DM01	DM02
Age (yrs)	43	38
Sex	Male	Female
Diabetes type	2	1
Diabetes duration (yrs)	3	8
HbA1c (%)	8.3	7.2
Height (m)	1.73	1.57
Weight (kg)	105	55
Neuropathy (+/-)	—	—
Present other diseases	Hypertension Hyperlipidemia	—
Occupation	System engineer	Nutritionist



FIGURE 5: A motion sensor used for daily walk measurement.

3. Results

Excessive FL of DM01 and DM02 were defined as over 10.0 kgf and 3.2 kgf each (Table 3).

The FL which exceeded 10.0 kgf was not observed in his 30 steps when DM01 was walking on a level corridor. DM02 also did not have the FL over 3.2 kgf in her 30 steps on the level corridor.

In DM01, motion data for approximately 3.0 hours (10,800 seconds) was recorded. This included going to the train station from home by bus, going to have lunch by train, and moving to another station to get off the train. The total time spent on consecutive steps for not less than 30 seconds within the said hours was 731.2 seconds. In addition, the average time was 1.3 seconds for each gait cycle. The sum of all of the consecutive steps over 30 sec was 2126 steps, in which excessive FL occurred 151 times. Excessive FL happened most frequently during walking from home to the bus stop, and 48 of the 238 steps exceeded 10 kgf. A gait cycle took about 1.07 sec then. The maximum excessive FL of the 2126 steps was 14.1 kgf, which occurred for 18 seconds after he got off a train, when each gait cycle took approximately 1.2 seconds.

In DM02, motion data for approximately 3.2 hours (12,000 seconds) was recorded. This included walking to the station from the restaurant, going shopping to downtown by train, and going home. Total time spent on consecutive steps for not less than 30 seconds within the said hours was 2336.0 seconds. In addition, the average time was 1.2 seconds for each step cycle. It was determined that 4030 steps in total



FIGURE 6: Walking measurement for identification of the places where the excessive FL occurs in daily walks. A motion sensor was attached to each shoe.

TABLE 3: Excessive FL of each patient.

	DM01	DM02
Mass of the foot (kg)	1.2	0.6
Average estimated FL (kgf)	7.0	1.5
SD of estimated FL (kgf)	1.8	0.84
Excessive FL (kgf)	≥ 10.0 kgf	≥ 3.2 kgf

during the consecutive steps period and 762 steps within the 4030 steps demonstrated excessive FL. Excessive FL most frequently occurred while walking back home from downtown, during which time 186 of the 372 steps were counted as demonstrating excessive load. At this time, each gait cycle was approximately 1.04 seconds. The maximum excessive FL was 6.3 kgf which occurred while DM02 was walking on a concrete sidewalk, when one gait cycle took about 1.2 sec.

After all, the excessive FL was not observed in both patients in the laboratory setting. By contrast, both of them had excessive FL in their daily life environment. The excessive FL occurred at a rate of 1 time per about 14 steps in daily walks of DM01. Also, the excessive FL happened at a rate of 1 time per about 5 steps in daily walks of DM02.

4. Discussion

This is the first study to investigate the forefoot load of diabetic patients in a daily life environment using foot motion data.

Daily walk measurement using wearable motion sensors appears feasible and safely induces no adverse events in patients with diabetes. The smallness and lightness of the inertial wearable motion sensors were considered to allow daily measurement of daily walks in diabetic patients.

Daily walks of two diabetic patients were measured and consecutive steps not less than 30 seconds were analyzed. The sum of all of the consecutive steps that were timed did not occupy much of the recorded time of DM01 because he

was mainly traveling by buses and trains. DM01 had excessive FL at a rate of 1 per 5 steps on his way from his home to the bus stop. The daily walking data of DM02 included the time strolling around for shopping downtown, and consecutive steps that took less than 30 seconds were often observed. However, it took approximately 2 seconds for one gait cycle, which was relatively slow. Therefore, excessive FL can be assumed to have seldom occurred during walking when the purpose of the consecutive steps was not to move around [27]. DM02 had excessive FL most frequently when going home from downtown and the rate was 1 of 2 steps. It was observed that there was no excessive load when 30 steps were counted as having been walked on a corridor. Thus, a patient whose forefoot tends to receive excessive load could not be found unless the walking measurement is taken in a daily life environment. The situations in which excessive FL occurred may be different from a laboratory setting in terms of the walking speed or properties of the road surface in their daily life environment [28]. Therefore, these differences may suggest the occurrence of excessive FL.

The algorithm was able to estimate the forefoot load during walking on a level corridor with more than moderate accuracy. However, the estimation accuracy was not consistent among the subjects in stair walking and slope walking. If the peak of the FL comes early in the stance phase, correlation between FL and estimated FL was attenuated. Generally, the pattern of the FL and its magnitude would be different depending on places to be walked [29]. For instance, more GRF is applied on the forefoot because impact by a falling body when walking down the slope is greater than when walking on a level floor. These properties may result in attenuating the accuracy of FL estimation. The changes of posture when the center of body mass is raised can be captured accurately by the acceleration of the trunk. In addition, a previous study showed that the pattern of trunk acceleration in the stance phase was similar to GRF [30]. The accuracy of the estimation algorithm would be improved by a combination of trunk and feet acceleration.

Several limitations of this study need to be acknowledged. First, the estimation algorithm proposed here is not applicable when walking down stairs. Foot location at HC is different for each person; some people initiate their landing from the toe and others land from the heel. Hence, algorithm for the different types of landing needs to be established. Second, forefoot load in horizontal component was not estimated despite the fact that shear stress is associated with callus formation [31]. Future studies need to be conducted that consider the forefoot load of both components. Finally, FL under each foot cannot be determined when both feet are in contact with the ground in this study. However, FL of one foot cannot exceed the sum of each FL; thus, the developed algorithm does not underestimate the FL.

We should conduct future research that estimates the daily forefoot load of diabetic patients with/without frequent excessive FL and investigate the association between the frequent excessive FL and calluses. Such a future study would provide insights into the screening of patients at risk for DFU.

5. Conclusion

This study created an algorithm to estimate the forefoot load and revealed that excessive load not observed in laboratory settings using level floors did in fact occur during daily walks. In addition, this study demonstrated the feasibility of long-time FL measurement in patients' daily environment. Our next interest is to demonstrate whether excessive load is related to callus formation.

Conflicts of Interest

The authors report no relevant conflict of interests.

Acknowledgments

Part of this study was supported by the Japan Society for the Promotion of Science Grant-in-Aid for Science Research (PN: 16K12949). This paper is based on a master's thesis by Ayano Watanabe.

References

- [1] G. E. Reiber, L. Vileikyte, E. J. Boyko et al., "Causal pathways for incident lower-extremity ulcers in patients with diabetes from two settings," *Diabetes Care*, vol. 22, no. 1, pp. 157–162, 1999.
- [2] V. Falanga, "Wound healing and its impairment in the diabetic foot," *Lancet*, vol. 366, no. 9498, pp. 1736–1743, 2005.
- [3] J. A. Mayfield, G. E. Reiber, L. J. Sanders, D. Janisse, and L. M. Pogach, "Preventive foot care in people with diabetes," *Diabetes Care*, vol. 21, no. 12, pp. 2161–2177, 1998.
- [4] S. Jan, P. R. C. Ulbrecht, and G. M. Caputo, "Foot problems in diabetes: an overview," *Clinical Infection Diseases*, vol. 39, pp. S73–S82, 2004.
- [5] L. A. Lavery, E. J. Peters, and D. G. Armstrong, "What are the most effective interventions in preventing diabetic foot ulcers?," *International Wound Journal*, vol. 5, no. 3, pp. 425–433, 2008.
- [6] G. B. Dishan Singh and S. G. Trevino, "Callosities, corns, and calluses," *British Medical Journal*, vol. 312, no. 7043, pp. 1403–1406, 1996.
- [7] D. M. Anjos, L. P. Gomes, L. M. Sampaio, J. C. Correa, and C. S. Oliveira, "Assessment of plantar pressure and balance in patients with diabetes," *Archives of Medical Science*, vol. 6, no. 1, pp. 43–48, 2010.
- [8] M. Yavuz, A. Erdemir, G. Botek, G. B. Hirschman, L. Bardsley, and B. L. Davis, "Peak plantar pressure and shear locations: relevance to diabetic patients," *Diabetes Care*, vol. 30, no. 10, pp. 2643–2645, 2007.
- [9] S. Rao, C. L. Saltzman, and H. J. Yack, "Relationships between segmental foot mobility and plantar loading in individuals with and without diabetes and neuropathy," *Gait & Posture*, vol. 31, no. 2, pp. 251–255, 2010.
- [10] M. Yavuz, "American society of biomechanics clinical biomechanics award 2012: plantar shear stress distributions in diabetic patients with and without neuropathy," *Clinical Biomechanics (Bristol, Avon)*, vol. 29, no. 2, pp. 223–229, 2014.
- [11] M. Oe, K. Takehara, Y. Ohashi et al., "Incidence of foot ulcers in patients with diabetes at a university hospital in Tokyo over a 5-year period," *Diabetology International*, vol. 6, no. 1, pp. 55–59, 2015.

- [12] G. E. Reiber, D. G. Smith, C. Wallace et al., "Effect of therapeutic footwear on foot reulceration in patients with diabetes: a randomized controlled trial," *The Journal of the American Medical Association*, vol. 287, no. 19, pp. 2552–2558, 2002.
- [13] A. H. Razak, A. Zayegh, R. K. Begg, and Y. Wahab, "Foot plantar pressure measurement system: a review," *Sensors*, vol. 12, pp. 9884–9912, 2012.
- [14] Y. Jung, M. Jung, K. Lee, and S. Koo, "Ground reaction force estimation using an insole-type pressure mat and joint kinematics during walking," *Journal of Biomechanics*, vol. 47, no. 11, pp. 2693–2699, 2014.
- [15] J. M. Neugebauer, K. H. Collins, and D. A. Hawkins, "Ground reaction force estimates from ActiGraph GT3X+ hip accelerations," *PLoS One*, vol. 9, no. 6, article e99023, 2014.
- [16] S. E. Oh, A. Choi, and J. H. Mun, "Prediction of ground reaction forces during gait based on kinematics and a neural network model," *Journal of Biomechanics*, vol. 46, no. 14, pp. 2372–2380, 2013.
- [17] G. Leporace, L. A. Batista, L. Metsavaht, and J. Nadal, "Residual analysis of ground reaction forces simulation during gait using neural networks with different configurations," in *2015 37th Annual International Conference of the IEEE Engineering in Medicine and Biology Society (EMBC)*, pp. 25–29, IMBC in Milano, Italy, August, 2015.
- [18] M. Mojaddarasil, "Inverse dynamics and ground reaction force estimation during walking," in *RSI/ISM International Conference on Robotics and Mechatronics*, pp. 625–630, RSI/ISM in Tehran, Iran, 2014.
- [19] N. Yamazaki, "Comprehensive analysis of bipedal walking and simulation," *Biomechanism*, vol. 3, pp. 261–269, 1975.
- [20] L. Allet, R. H. Knols, K. Shirato, and E. D. de Bruin, "Wearable systems for monitoring mobility-related activities in chronic disease: a systematic review," *Sensors (Basel)*, vol. 10, no. 10, pp. 9026–9052, 2010.
- [21] M. A. Brodie, M. J. Coppens, S. R. Lord et al., "Wearable pendant device monitoring using new wavelet-based methods shows daily life and laboratory gaits are different," *Medical & Biological Engineering & Computing*, vol. 54, no. 4, pp. 663–674, 2016.
- [22] D. G. Robertson and J. J. Dowling, "Design and responses of Butterworth and critically damped digital filters," *Journal of Electromyography and Kinesiology*, vol. 13, no. 6, pp. 569–573, 2003.
- [23] A. Amemiya, H. Noguchi, M. Oe, H. Sanada, and T. Mori, "Establishment of a measurement method for in-shoe pressure and shear stress in specific regions for diabetic ulcer prevention," in *2016 38th Annual International Conference of the IEEE Engineering in Medicine and Biology Society (EMBC)*, pp. 16–20, EMBC in Florida, America, August, 2016.
- [24] M. Ae and T. Yokoi, "Estimation of inertia properties of the body segments in Japanese athletes," *Biomechanism*, no. 11, pp. 23–33, 1997.
- [25] J. S. Wang, C. W. Lin, Y. T. Yang, and Y. J. Ho, "Walking pattern classification and walking distance estimation algorithms using gait phase information," *IEEE Transactions on Biomedical Engineering*, vol. 59, no. 10, pp. 2884–2892, 2012.
- [26] R. Taylor, "Interpretation of the correlation coefficient: a basic review," *Journal of Diagnostic Medical Sonography*, vol. 6, no. 1, pp. 35–39, 1990.
- [27] J. Nilsson and A. Thorstensson, "Ground reaction forces at different speeds of human walking and running," *Acta Physiologica Scandinavica*, vol. 136, no. 2, pp. 217–227, 1989.
- [28] S. J. Dixon, A. C. Collop, and M. E. Batt, "Surface effects on ground reaction forces and lower extremity kinematics in running," *Medicine and Science in Sports and Exercise*, vol. 32, no. 11, pp. 1919–1926, 2000.
- [29] I. Takahama, M. Fujita, and H. Saeki, "An observation of reaction to the sole on a normal gait movement," *Precision Engineering*, vol. 44, no. 524, pp. 973–980, 1978.
- [30] H. Osaka, S. Watanabe, D. Fujita, and K. Kobara, "Appropriate location of an accelerometer for gait analysis : a comparative study based on cross-correlation coefficients," *Physiotherapy Science*, vol. 26, no. 6, pp. 785–789, 2011.
- [31] M. Hamatani, T. Mori, M. Oe et al., "Factors associated with callus in patients with diabetes, focused on plantar shear stress during gait," *Journal of Diabetes Science and Technology*, vol. 10, no. 6, pp. 1353–1359, 2016.

Research Article

Alcohol Consumption Is a Risk Factor for Lower Extremity Arterial Disease in Chinese Patients with T2DM

Shanshan Yang,^{1,2} Shuang Wang,³ Bo Yang,³ Jinliang Zheng,³
Yuping Cai,³ and Zhengguo Yang³

¹Institute of Geriatrics, Beijing Key Laboratory of Ageing and Geriatrics, State Key Laboratory of Kidney Disease, Chinese PLA General Hospital, 28 Fuxing Road, Beijing 100853, China

²Jinan Military Area CDC, Jinan, Shandong 250014, China

³Department of Nephrology and Endocrinology, PLA 148th Hospital, Zibo 255300, China

Correspondence should be addressed to Zhengguo Yang; yangzhanq@163.com

Received 7 March 2017; Revised 22 May 2017; Accepted 28 May 2017; Published 6 July 2017

Academic Editor: Nikolaos Papanas

Copyright © 2017 Shanshan Yang et al. This is an open access article distributed under the Creative Commons Attribution License, which permits unrestricted use, distribution, and reproduction in any medium, provided the original work is properly cited.

Objective. To investigate the relationship between alcohol consumption and diabetic lower extremity arterial disease (LEAD) in hospitalized patients with type 2 diabetes mellitus (T2DM). **Methods.** We evaluated 138 hospitalized patients with T2DM who consumed alcohol and 833 who did not. We used propensity score matching to reduce the confounding bias between groups. Additionally, a logistic regression analysis was performed with the matched data to evaluate the LEAD risk. **Results.** In total, 119 pairs of patients who did and did not consume alcohol were matched. According to the logistic regression analysis, patients who consumed >8 U of alcohol/day had a higher risk of LEAD (odds ratio (OR): 6.35, 95% confidence interval (CI): 1.78–22.65) than patients who did not consume alcohol. Additionally, after adjusting for age, gender, region, occupation, smoking status, body mass index, weight change, and duration of diabetes, the OR of peripheral artery disease after >20 years of alcohol consumption was 3.48 (95% CI: 1.09–11.15). Furthermore, we observed a significant dose-response relationship between alcohol consumption and LEAD. **Conclusions.** Alcohol consumption may be a risk factor of LEAD in patients with T2DM. Patients with T2DM should be advised to stop drinking, to prevent the onset of LEAD.

1. Introduction

Lower extremity arterial disease (LEAD) is one of the most common complications of diabetes and harms the peripheral arteries via multiple pathways [1]. LEAD is also associated with healing failure, amputation, cardiovascular events, and an increased risk of premature mortality [2, 3]. Furthermore, LEAD is a pathological process, and only one in four LEAD patients survives for more than 10 years. Approximately 10 million men and women in the United States suffer from LEAD [4], and in Chinese patients with diabetes older than 50 years, the prevalence of LEAD ranges from 16.9 to 23.8% [5]. Compared with individuals without diabetes mellitus (DM), patients with DM have a 2-fold higher risk of LEAD and of having an earlier onset age, a more serious illness, more lesions, and a worse prognosis [6]. The rate at

which patients with LEAD eventually require an amputation is as high as 33% [7]. In 1997, the medical cost of a diabetic foot ulcer in the United States was \$10,831 and the average hospital stay length was 8.9 days; the medical cost of an amputation was \$17,302 and the hospital stay length was 12 days, far exceeding the lengths of stay for coronary bypass surgery (9.9 days) and myocardial infarction (6.9 days) [8]. In China, the average duration of hospitalization for patients with LEAD undergoing amputation was 26 days and the average cost was 14,906 yuan [5].

Considering the serious health hazards of LEAD, a comprehensive identification of preventable risk factors of LEAD is important to improving patients' quality of life and reducing the associated medical costs. Smoking, ageing, race/ethnicity, increased levels of inflammatory markers, homocysteinaemia, and abdominal obesity are currently identified as risk factors

for LEAD [9]. However, the association between alcohol use and LEAD remains unclear. Alcohol consumers with peripheral artery disease (PAD) were reported to have a lower mortality than patients with PAD who did not consume alcohol. On the other hand, heavy drinking has been reported to be a risk factor for PAD, whereas other studies have not identified an association between alcohol use and LEAD [9–12]. In addition, in these studies, the measures of alcohol consumption were not consistent, and the demographic characteristics of the groups who did and did not consume alcohol differed significantly. Studies on this topic in the Chinese population are limited. Thus, we designed a study to assess the association between alcohol consumption and LEAD in Chinese patients with type 2 diabetes mellitus (T2DM) using U (an international measure of ethanol) to measure alcohol consumption and propensity score matching (PSM) to control for differences in characteristics between patients who did and did not consume alcohol.

2. Design and Methods

2.1. Study Sample. We used clinical data from the Department of Nephrology and Endocrinology, PLA 148th Hospital. Of the 1025 inpatients (from January 2010 to December 2012), we excluded 25 inpatients with type 1 DM and 11 adult inpatients with latent autoimmune diabetes, and we recruited 989 (507 men and 482 women) as our participants.

We collected data regarding each participant's gender, age, occupation, region of residence, alcohol and smoking habits, T2DM duration, and LEAD status.

2.2. Measurements. T2DM was defined according to the American Diabetes Association criteria [13]. LEAD was diagnosed as follows: (1) an ankle-brachial index (ABI) < 0.90, which is the systolic blood pressure at the ankle divided by the systolic blood pressure of the arm; (2) an ABI > 1.3 and a toe-brachial index (TBI) < 0.7; and (3) intermittent claudication, $0.9 < \text{ABI} < 1.3$, and an ABI that is reduced by 15–20% after an exercise tolerance test [14]. The ABI was measured in all subjects, and the TBI was measured in subjects with an ABI > 1.3 using a Vista AVS system (Summit Doppler Systems Inc., Golden, CO 80403, USA).

An alcohol user was defined as a regular drinker who consumed alcohol almost every day and had regularly consumed alcohol for more than half a year. This definition was used because the average alcohol consumption of occasional drinkers is difficult to determine [15]. The participants' alcohol use status was defined by asking the question "Are you a regular drinker who has used alcohol almost every day for more than a half year?" The duration and quantity of alcohol consumption were defined by asking the questions "How many years have you been a regular drinker?" and "Do you drink more than two standard glasses (approximately 250 ml) of white spirits or 2.5 bottles/5 cans (approximately 1,500 ml) of beer a day on average?" The answers to these questions were either "A. Yes" or "B. No." A volume of 1 U of consumed alcohol equals 10 ml or 8 g of ethanol, which corresponds to the amount of alcohol a normal (60 kg) adult can metabolize in 1 hour [16]. Thus, we defined

a heavy drinker as someone who consumed 8 U of alcohol a day on average, that is, a person who metabolized alcohol at least 8 hours every day.

This information was collected by a primary nurse. The patients' answers to the questions on alcohol use were confirmed by the patients and their relatives to ensure the accuracy of the information. Central obesity was defined as a waist circumference (WC) > 90 cm in men and > 80 cm in women [17].

2.3. Statistical Analysis. SPSS version 19.0 was used to analyse the data. The significance level for all tests was set at a two-tailed α value of 0.05. The differences in means and proportions were evaluated using Student's *t*-test and the chi-square test, respectively. Logistic regression models were used to identify the risk of alcohol use.

PSM [18] was used to match the groups of those who did and did not consume alcohol. Gender, age, region, occupation, smoking status, body mass index (BMI), WC, and the duration of T2DM were included as covariates. We used the nearest-neighbour matching to match former smokers with current smokers at a 1 : 1 ratio with a calliper width of 0.02 [19].

2.4. Ethical Considerations. The Committee for Medical Ethics of the Chinese PLA General Hospital examined and approved our study. Before completing the questionnaire, each involved participant signed an informed consent form.

3. Results

Nine hundred and eighty-nine (507 men and 482 women) inpatients were involved in our study before PSM. The average age was 56.8 ± 11.6 years (range: 14–93 years). The average ages of patients who did and did not consume alcohol were 52.3 ± 11.3 years (range: 28–85 years) and 57.5 ± 11.3 years (range: 14–93 years), respectively. The general characteristics (age, gender, origin, occupation, smoking status, BMI, and central obesity) of the participants are shown in Table 1. Compared with the group of alcohol consumers, the group of patients who did not consume alcohol comprised more women, more workers engaged in hard physical labour, fewer smokers, and patients who were older and had more central obesity and longer durations of T2DM (5.4 ± 6.0 years versus 7.5 ± 6.6 years; $P < 0.05$).

After PSM, 238 participant pairs were matched, and the two groups were balanced for age, gender, occupation, smoking status, BMI, central obesity, and T2DM duration (with and without alcohol consumption: 5.8 ± 6.3 years versus 5.9 ± 6.1 years, resp.; $P = 0.937$) (Table 1).

According to the logistic regression analysis, patients who consumed alcohol had a higher risk of LEAD (OR: 2.75, 95% CI: 1.11–6.80) than patients who did not after adjusting for age, gender, region, occupation, smoking status, BMI, WC, and T2DM duration. Regarding the risk of LEAD after adjusting for alcohol use ≤ 8 U/day and > 8 U/day, the odds ratios (ORs) were 2.07 (95% confidence interval (CI): 0.78–5.54, $P > 0.05$) and 6.35 (95% CI: 1.78–22.65, $P < 0.05$), respectively. We also observed a dose-response relationship between the units of alcohol consumed per

TABLE 1: Demographic characteristics of the participants according to alcohol use before and after PSM.

Group	Number (%) Total <i>n</i> = 971	Alcohol use (before PSM)			Alcohol use (after PSM)		
		Yes (<i>n</i> = 138)	No (<i>n</i> = 833)	<i>P</i>	Yes (<i>n</i> = 119)	No (<i>n</i> = 119)	<i>P</i>
Age (years)				<0.001			0.534
≤40	81 (8.3)	22 (15.9)	59 (7.1)		16 (13.4)	15 (12.6)	
60–69	529 (54.5)	79 (57.2)	450 (54.0)		68 (57.1)	76 (63.9)	
≥70	361 (37.2)	37 (26.8)	324 (38.9)		35 (29.4)	28 (23.5)	
Gender				<0.001			1.000
Male	498 (51.3)	136 (98.6)	362 (43.5)		117 (98.3)	117 (98.3)	
Female	473 (48.7)	2 (1.4)	471 (56.5)		2 (1.7)	2 (1.7)	
Occupation				0.01			0.562
White collar	103 (10.6)	22 (15.9)	81 (9.7)		84 (70.6)	77 (64.7)	
Light physical labourer	117 (12.0)	23 (16.7)	94 (11.3)		19 (16.0)	25 (21.0)	
Hard physical labourer	751 (77.3)	93 (67.4)	658 (79.0)		16 (13.4)	17 (14.3)	
Region				0.756			0.408
Shandong province	940 (96.8)	133 (96.4)	807 (96.9)		117 (98.3)	115 (96.6)	
Other province	31 (3.2)	5 (3.6)	26 (3.1)		2 (1.7)	4 (3.4)	
Smoker				<0.001			0.512
Yes	182 (18.7)	90 (65.2)	92 (11.0)		71 (59.7)	66 (55.5)	
No	789 (81.3)	48 (34.8)	741 (89.0)		48 (40.3)	53 (44.5)	
BMI				0.038			0.783
<24.00	368 (37.9)	39 (28.3)	329 (39.5)		36 (30.3)	32 (26.9)	
24.00–27.99	388 (40.0)	62 (44.9)	326 (39.1)		50 (42.0)	55 (46.2)	
≥28.00	215 (22.1)	37 (26.8)	178 (21.4)		33 (27.7)	32 (26.9)	
Central obesity				<0.001			0.697
Yes	625 (64.4)	66 (47.8)	559 (67.1)		60 (50.4)	57 (47.9)	
No	346 (35.6)	72 (52.2)	274 (32.9)		59 (49.6)	62 (52.1)	
Mean ± SD							
Age		52.3 ± 11.3	57.5 ± 11.3	<0.001	53.2 ± 11.9	51.9 ± 11.9	0.401
Duration of T2DM		5.4 ± 6.0	7.5 ± 6.6	0.001	5.8 ± 6.3	5.9 ± 6.1	0.937
BMI		25.8 ± 3.7	25.3 ± 4.1	0.143	25.8 ± 3.9	25.9 ± 3.9	0.861
WC		90.9 ± 8.4	88.3 ± 8.8	0.001	90.9 ± 8.7	90.7 ± 8.4	0.825

day and LEAD risk (after adjusting for age, gender, region, occupation, smoking status, BMI, WC, and T2DM duration, $P = 0.005$). In addition, compared with patients who did not consume alcohol, patients who had consumed alcohol for >20 years had a higher risk of LEAD after adjusting for various factors (OR: 3.48, 95% CI: 1.09–11.15), and a dose-response relationship between the number of years of alcohol use and the risk of LEAD was also observed ($P = 0.019$) (Table 2).

When alcohol consumption was analysed as a continuous outcome, models A to C showed that increased alcohol consumption was associated with an increased risk of LEAD (all $P < 0.05$, Table 2). However, the association between continuous years of alcohol consumption and LEAD was not significant after adjusting for various factors (Table 2). Furthermore, we utilized model D (adjusting for age, gender, region, occupation, smoking status, BMI, WC, T2DM duration, systolic blood pressure, cholesterol, and prevalent cardiovascular disease) to analyse participants with

cholesterol, blood pressure, and prevalent cardiovascular disease data ($n = 185$) and obtained similar results (Table S1 available online at <https://doi.org/10.1155/2017/8756978>).

The gender imbalance between alcohol consumers and nonconsumers is striking. We performed an analysis on male patients only (the number of alcohol-consuming women was too low for a separate analysis of female patients). Compared with male patients who did not consume alcohol, male patients who consumed alcohol had a higher risk of LEAD (OR: 3.17, 95% CI: 1.25–8.09) after adjusting for age, region, occupation, smoking status, BMI, WC, and T2DM duration. Regarding the risk of LEAD after adjusting for alcohol use ≤8 U/day and >8 U/day, the ORs were 2.43 (95% CI: 0.89–6.68, $P > 0.05$) and 7.03 (95% CI: 1.91–25.84, $P < 0.05$), respectively. We also observed a dose-response relationship between the units of alcohol consumed per day and LEAD risk (after adjusting for age, region, occupation, smoking status, BMI, WC, and T2DM duration, $P = 0.003$). In addition, compared with male patients who did not consume alcohol,

TABLE 2: OR (95% CI) of LEAD in participants according to alcohol use.

	<i>n</i> (%)	Model A OR (95% CI)	Model B OR (95% CI)	Model C OR (95% CI)
Alcohol use				
No (reference)	9 (7.6)	1	1	1
Yes	21 (17.6)	2.62 (1.15–5.99)	2.61 (1.09–6.23)	2.75 (1.11–6.80)
<i>P</i>		0.022	0.031	0.028
Alcohol consumption				
No (reference)	9 (7.6)	1	1	1
≤8 U/day	14 (15.7)	2.28 (0.94–5.54)	1.95 (0.76–5.02)	2.07 (0.78–5.54)
>8 U/day	7 (23.3)	3.72 (1.26–11.01)	6.33 (1.89–21.15)	6.35 (1.78–22.65)
<i>P</i> for trend		0.012	0.004	0.005
Alcohol use duration				
No (reference)	9 (7.6)	1	1	1
≤20 years	8 (15.1)	2.17 (0.79–5.99)	2.25 (0.86–5.90)	2.41 (0.88–6.60)
>20 years	13 (19.7)	3.00 (1.21–7.45)	3.40 (1.13–10.23)	3.48 (1.09–11.15)
<i>P</i> for trend		0.017	0.015	0.019
Continuous				
No (reference)		1	1	1
Alcohol consumption (U)		1.06 (1.00–1.12)	1.10 (1.03–1.18)	1.11 (1.04–1.19)
<i>P</i>		0.048	0.004	0.003
No (reference)		1	1	1
Alcohol use duration (years)		1.03 (1.01–1.06)	1.02 (0.99–1.04)	1.02 (0.99–1.05)
<i>P</i>		0.013	0.054	0.055

Model A: crude model; model B: adjusted for age, gender, region, and occupation; model C: adjusted for age, gender, region, occupation, smoking status, BMI, WC, and T2DM duration.

male patients who had consumed alcohol for >20 years had a higher risk of LEAD after adjusting for various factors (OR: 2.82, 95% CI: 1.07–7.91), and a dose-response relationship between the number of years of alcohol use and the risk of LEAD was also observed ($P = 0.039$) (Table 3).

When alcohol consumption was analysed as a continuous outcome, models A to C showed that increased alcohol consumption was associated with an increased risk of LEAD (all $P < 0.05$, Table 3). In addition, the association between continuous years of alcohol consumption and LEAD was not significant after adjusting for various factors (Table 3). Furthermore, we utilized model D (adjusting for age, origin, occupation, smoking status, BMI, WC, T2DM duration, systolic blood pressure, cholesterol, and prevalent cardiovascular disease) to analyse male participants with cholesterol, blood pressure, and prevalent cardiovascular disease data ($n = 182$) and obtained similar results (Table S2).

4. Discussion

In this study, we observed a significant association between alcohol consumption and LEAD in patients with T2DM. We used a standard and universal measure of alcohol consumption; in China, individuals usually drink white spirits distilled from sorghum or maize or beer, and “liang” (50 g) is usually used as the measurement for the amount of alcohol consumed [20]. These differences from Western countries make comparisons between nations difficult; however, we used the

standard and universal measure U, that is, 10 ml or 8 g of ethanol, to solve this problem. We also used PSM to comprehensively control and adjust for a wide range of potential confounders and to improve the comparability between the two groups.

As shown in a study by Mukamal et al. [10], older adults in Pennsylvania who consumed 1–13 drinks per week had a lower risk (OR: 0.56, 95% CI: 0.33–0.95) of hospitalization for LEAD; however, this reduced risk became insignificant when >13 drinks were consumed per week. This study used drinks per week as a measurement of alcohol consumption and did not present information about the quantity of alcohol consumed or the years of alcohol consumption. Vliegenthart et al. [11] observed an inverse relationship between alcohol consumption and PAD in nonsmoking women, but not in nonsmoking men; this difference may be related to the propensity of males to drink beer, wine, and liquor, whereas females predominantly drink wine and types of fortified wine. In addition, Xie et al. [21] observed an association between heavy drinking (>60 g/day) and a higher risk (OR: 2.878, 95% CI: 1.215–4.018) of a low ABI in Chinese men; this result is consistent with the findings of our study. Furthermore, heavy drinking has adverse effects on blood pressure and serum triglyceride levels [22], both of which may lead to LEAD.

This study had several limitations. As the information on alcohol consumption was based on recall, recall bias could not be completely excluded; however, the information was

TABLE 3: OR (95% CI) of LEAD in male participants according to alcohol use.

	<i>n</i> (%)	Model A OR (95% CI)	Model B OR (95% CI)	Model C OR (95% CI)
Alcohol use				
None (reference)	8 (6.8)	1	1	1
Yes	21 (17.9)	2.98 (1.26–7.04)	3.10 (1.25–7.67)	3.17 (1.25–8.09)
<i>P</i>		0.013	0.015	0.016
Alcohol consumption				
None (reference)	8 (6.8)	1	1	1
≤8 U/day	14 (16.1)	2.61 (1.04–6.54)	2.36 (0.88–6.26)	2.43 (0.89–6.68)
>8 U/day	7 (23.3)	4.15 (1.37–12.58)	7.32 (2.10–25.42)	7.03 (1.91–25.84)
<i>P</i> for trend		0.007	0.002	0.003
Alcohol use duration				
None (reference)	8 (6.8)	1	1	1
≤20 years	8 (15.1)	2.42 (0.86–6.85)	3.88 (1.25–12.07)	3.93 (1.19–12.96)
>20 years	13 (20.3)	3.47 (1.36–8.90)	2.74 (1.01–7.39)	2.82 (1.01–7.91)
<i>P</i> for trend		0.009	0.042	0.039
Continuous				
None (reference)		1	1	1
Alcohol consumption (U)		1.06 (1.00–1.13)	1.11 (1.04–1.18)	1.11 (1.04–1.19)
<i>P</i>		0.036	0.003	0.003
None (reference)		1	1	1
Alcohol use duration (years)		1.04 (1.01–1.07)	1.03 (1.00–1.05)	1.03 (1.00–1.06)
<i>P</i>		0.004	0.067	0.063

Model A: crude model; model B: adjusted for age, region, and occupation; model C: adjusted for age, region, occupation, smoking status, BMI, WC, and T2DM duration.

confirmed by patients and their relatives to ensure accuracy. Second, our sample may not be completely representative of patients with T2DM in China because our hospital is one of the best hospitals in Zibo, and the inpatients here have higher proportions of diabetic complications. However, the representativeness of our sample should not substantially affect the internal validity of this study. Third, the cholesterol, blood pressure, and prevalent cardiovascular disease data were missing for 229 participants, and thus, we did not include these three variables as confounders for PSM. Furthermore, we did not collect information about physical activity or homocysteine levels, which are also risk factors for LEAD [23]. However, we utilized model D (adjusting for age, gender, region, occupation, smoking status, BMI, WC, T2DM duration, systolic blood pressure, cholesterol, and prevalent cardiovascular disease) in participants with available cholesterol, blood pressure, and prevalent cardiovascular disease data ($n = 185$) and obtained similar results, as the effect of alcohol consumption on the LEAD risk was still significant after adjusting for these factors. Finally, we could not examine the hazard ratio of alcohol consumption with respect to LEAD because detailed information regarding the onset time of LEAD was not available.

In summary, our study observed a dose-response relationship between alcohol consumption and LEAD among inpatients with T2DM. We used a standard and universal measurement of alcohol consumption and increased the comparability of the two groups using the PSM method. Alcohol consumption may be a risk factor for LEAD in

patients with T2DM; however, further cohort studies should be conducted to verify the causal relationship. Based on our findings, patients with T2DM should be advised to stop drinking, or at least to avoid heavy drinking, to prevent the onset of LEAD.

Abbreviations

ABI:	Ankle-brachial index
BMI:	Body mass index
95% CI:	95% confidence interval
DM:	Diabetes mellitus
LEAD:	Lower extremity arterial disease
OR:	Odds ratio
PAD:	Peripheral artery disease
PSM:	Propensity score matching
T2DM:	Type 2 diabetes mellitus
TBI:	Toe-brachial index
WC:	Waist circumference.

Conflicts of Interest

The authors declare that they have no conflicts of interest.

Authors' Contributions

Dr. Shanshan Yang and Professor Zhengguo Yang conceived and designed the study; Shuang Wang, Bo Yang, Jinliang

Zheng, and Yuping Cai performed the experiments; Shanshan Yang and Shuang Wang analysed the data; and Shanshan Yang, Shuang Wang, and Zhengguo Yang contributed materials/analysis tools and wrote the paper. Shanshan Yang and Shuang Wang contributed equally to this work. This manuscript has been read and approved by all the authors, the requirements for authorship have been met, and each author believes that the manuscript represents honest work.

Acknowledgments

The authors would like to thank Lei Xu, Qian Li, Wei Jia, Xinli Cai, Lihui Liu, Ying Zhang, Jinjuan Zhao, and Xinai Yan from the 148th PLA Hospital for assisting with the research described in this study.

References

- [1] R. E. Hoyt, "Peripheral arterial disease in people with diabetes: response to consensus statement," *Diabetes Care*, vol. 27, no. 8, p. 2095, 2004.
- [2] J. Malmstedt, L. Karvestedt, J. Swedenborg, and K. Brismar, "The receptor for advanced glycation end products and risk of peripheral arterial disease, amputation or death in type 2 diabetes: a population-based cohort study," *Cardiovascular Diabetology*, vol. 14, no. 1, p. 93, 2015.
- [3] J. R. Brownrigg, N. C. Schaper, and R. J. Hinchliffe, "Diagnosis and assessment of peripheral arterial disease in the diabetic foot," *Diabetic Medicine*, vol. 32, no. 6, pp. 738–747, 2015.
- [4] J. Muasher, "Lower extremity arterial disease," *Journal of Vascular and Interventional Radiology*, vol. 23, no. 7, pp. 186–205, 2012.
- [5] C. D. Society, "Guidelines for prevention and treatment of type 2 diabetes mellitus in China," *Chinese Journal of Diabetes*, vol. 22, no. 8, pp. 2–42, 2014.
- [6] C. D. Society, "Guidelines for prevention and treatment of type 2 diabetes mellitus in China," *Chinese Journal of Diabetes*, vol. 20, no. 1, pp. S1–S37, 2012.
- [7] M. E. Levin, "Preventing amputation in the patient with diabetes," *Diabetes Care*, vol. 18, no. 10, pp. 1383–1394, 1995.
- [8] N. G. Mahon, P. O. Rahallaigh, J. B. O'Sullivan, M. B. Codd, H. A. McCann, and D. D. Sugrue, "Hospital cost of acute myocardial infarction in the thrombolytic era," *Irish Medical Journal*, vol. 93, no. 4, p. 122, 2000.
- [9] I. Wakabayashi and Y. Sotoda, "Alcohol drinking and peripheral arterial disease of lower extremity," *Nihon Arukōru Yakubutsu Igakkai Zasshi*, vol. 49, no. 1, pp. 13–27, 2014.
- [10] K. Mukamal, M. Kennedy, M. Cushman et al., "Alcohol consumption and lower extremity arterial disease among older adults the cardiovascular health study," *American Journal of Epidemiology*, vol. 167, no. 1, pp. 34–41, 2008.
- [11] R. Vliegenthart, J. M. Geleijnse, A. Hofman et al., "Alcohol consumption and risk of peripheral arterial disease: the Rotterdam Study," *American Journal of Epidemiology*, vol. 155, no. 4, pp. 332–338, 2002.
- [12] E. Sacanella and R. Estruch, "The effect of alcohol consumption on endothelial adhesion molecule expression," *Addiction Biology*, vol. 8, no. 4, pp. 371–378, 2004.
- [13] D. Power, "Standards of medical care in diabetes," *Diabetes Care*, vol. 29, no. 2, pp. S4–S36, 2006.
- [14] M. Ruizcanela and M. A. Martínezgonzález, "Lifestyle and dietary risk factors for peripheral artery disease," *Circulation Journal*, vol. 78, no. 3, pp. 553–559, 2014.
- [15] I. Wakabayashi, "Comparison of the relationships of alcohol intake with atherosclerotic risk factors in men with and without diabetes mellitus," *Alcohol and Alcoholism (Oxford)*, vol. 46, no. 3, pp. 301–307, 2011.
- [16] J. H. O'Keefe, S. K. Bhatti, A. Bajwa, J. J. Dinicolantonio, and C. J. Lavie, "Alcohol and cardiovascular health: the dose makes the poison...or the remedy," *Mayo Clinic Proceedings*, vol. 89, no. 3, pp. 382–393, 2014.
- [17] J. Xiao, X. Xing, J. Lu et al., "Prevalence and associated factors of microalbuminuria in Chinese individuals without diabetes: cross-sectional study," *BMJ Open*, vol. 3, no. 11, article e003325, 2013.
- [18] F. Thoemmes, "Propensity score matching in SPSS," *ArXiv Preprint*, vol. 6385, p. 1201, 2012.
- [19] P. C. Austin, "Optimal caliper widths for propensity-score matching when estimating differences in means and differences in proportions in observational studies," *Pharmaceutical Statistics*, vol. 10, no. 2, pp. 150–161, 2011.
- [20] G. S. Ma, D. H. Zhu, X. Q. Hu, D. C. Luan, L. Z. Kong, and X. G. Yang, "The drinking practice of people in China," *Acta Nutrimenta Sinica*, vol. 27, no. 5, pp. 362–365, 2005.
- [21] X. Xie, Y. T. Ma, Y. N. Yang et al., "Alcohol consumption and ankle-to-brachial index: results from the cardiovascular risk survey," *PLoS One*, vol. 5, no. 12, article e15181, 2010.
- [22] I. Wakabayashi, R. Kobaba-Wakabayashi, and H. Masuda, "Relation of drinking alcohol to atherosclerotic risk in type 2 diabetes," *Diabetes Care*, vol. 25, no. 7, pp. 1223–1228, 2002.
- [23] M. D. Gerhard-Herman, H. L. Gornik, C. Barrett et al., "2016 AHA/ACC guideline on the management of patients with lower extremity peripheral artery disease: a report of the American College of Cardiology/American Heart Association task force on clinical practice guidelines," *Journal of the American College of Cardiology*, vol. 69, no. 11, p. 1465, 2017.

Research Article

Therapeutic Effects of Static Magnetic Field on Wound Healing in Diabetic Rats

Jing Zhao,¹ Yong-guo Li,² Kai-qin Deng,³ Peng Yun,^{3,4} and Ting Gong³

¹Central Laboratory, Medical School of Yangtze University, Hubei 434003, China

²Department of Endocrinology, Central Hospital of Jingzhou City, Hubei 434001, China

³Department of Endocrinology, The First Affiliated Hospital of Yangtze University, Hubei 434000, China

⁴Department of Internal Medicine, The First Clinical Medical School of Yangtze University, Hubei 434000, China

Correspondence should be addressed to Peng Yun; tjyd_y123@163.com and Ting Gong; 28715026@qq.com

Received 3 January 2017; Accepted 27 February 2017; Published 26 March 2017

Academic Editor: Paul Valensi

Copyright © 2017 Jing Zhao et al. This is an open access article distributed under the Creative Commons Attribution License, which permits unrestricted use, distribution, and reproduction in any medium, provided the original work is properly cited.

Objective. To investigate the effects of static magnetic field (SMF) on cutaneous wound healing of Streptozotocin- (STZ-) induced diabetic rats. **Methods.** 20 STZ-induced diabetic rats were randomly divided into two groups (10 in each group): diabetic rats with SMF exposure group which were exposed to SMF by gluing one magnetic disk of 230 mT intensity and diabetic rats with sham SMF exposure group (sham group). 10 normal Wistar rats were used as the control group. One open circular wound with 2 cm diameter in the dorsum was generated on both normal and diabetic rats and then covered with sterile gauzes. Wound healing was evaluated by wound area reduction rate, mean time to wound closure, and wound tensile strength. **Results.** The wound area reduction rate in diabetic rats in comparison with the control group was significantly decreased ($P < 0.01$). Compared with sham magnet group, diabetic rats under 230 mT SMF exposure demonstrated significantly accelerated wound area reduction rate on postoperative days 7, 14, and 21 and decreased gross time to wound closure ($P < 0.05$), as well as dramatically higher wound tissue strength ($P < 0.05$) on 21st day. **Conclusion.** 230 mT SMF promoted the healing of skin wound in diabetic rats and may provide a non-invasive therapeutic tool for impaired wound healing of diabetic patients.

1. Introduction

Diabetes mellitus (DM) is a metabolic disorder that is characterized by chronic hyperglycaemia. It is a common and potentially disabling chronic disease. The condition is presently afflicting 382 million people worldwide [1]. This rise in prevalence of DM is likely to bring a concomitant increase in its complications among diabetic patients. One important complication of DM is the diabetic skin ulcer. Impaired wound healing of skin ulcer in diabetic patients is a common, serious and costly global health issue. It is a leading cause of admission, amputation and mortality in diabetic patients [2]. How to accelerate the wound healing in diabetic patients and relieve their suffering has become a great challenge to medical field. Static magnetic field (SMF) as alternative noninvasive method can produce satisfying therapeutic effects on different kinds of tissue defects [3, 4]. Previous study has showed that 220 mT SMF increased the

rate of healing by secondary intention in normal rats [5], but few study to date has examined SMF effect on diabetic wound healing. In this study, we examined the effects of an externally applied electromagnetic field, a 230 mT SMF generated by a permanent NeFeB magnet, to investigate the effects of SMF on cutaneous wound healing in Streptozotocin (STZ)-induced diabetic rats.

2. Methods

2.1. Experimental Diabetes. 26 adult male Wistar rats were provided by Animal Center of Wuhan University (Wuhan, China) and housed in a room with Controlled temperature ($23 \pm 1^\circ\text{C}$), relative humidity (50–60%), and alternately light-dark cycle (12h/12h), with access to standard pellet and clean water. Diabetes mellitus was induced by a subcutaneous injection of 65 mg/kg streptozocin (Sigma Chemicals, St. Louis, MO, USA; freshly dissolved in sterile saline, 0.9%).

Confirmation of hyperglycemia was made three days after STZ injection, and only STZ treated rats whose glucose concentration of the tail venous blood measured by One Touch SureStep Plus glucometer (Lifescan, Milpitas, CA, USA) was higher than 16.7 mmol/L (300 mg/dL) were considered as qualified diabetic models. Six rats were excluded from the study after confirmation of success of diabetic models because of low blood glucose levels. The rest of rats were randomized into two weight-matched groups (10 in each group): diabetic rats with SMF exposure group (SMF group) which were exposed to SMF by gluing one magnetic disk with 230 mT intensity and diabetic rats with sham SMF exposure group (Sham group). 10 normal Wistar rats were used as the Control group.

The current study was performed in adherence to the National Institutes of Health guidelines for the use of experimental animals, and all animal protocols were approved by the Committee for Ethical Use of Experimental Animals of the Yangtzes University.

2.2. Surgical Procedure and SMF Apparatus. Two weeks after establishment of diabetes, all rats were anesthetized with administered 50 mg/kg Pentobarbital Sodium. Standardized wounds were created on the backs of 30 rats. These wounds measured 2.0×2.0 cm and were produced under sterile conditions by excising skin, subcutaneous tissue, and panniculus carnosus. After achieving hemostasis, the wounds were covered with sterile gauzes. All surgical procedures were performed by the same investigator. For postoperative analgesia, beginning on the day of operation, 0.02 mg/kg fentanyl citrate (Enhua co., Xuzhou, China) was administered subcutaneously, 2 times daily, for 3 days. Rats were housed individually in plastic cages. The distance between cages was 30 cm, to prevent interaction between magnets. The sterile gauzes were replaced once a day. If the wound appeared infection, debrided the infected tissue and applied erythromycin ointment (Mayinglong co., Wuhan, China).

On the day after operation, all diabetic rats in SMF group had permanent NeFeB Magnetic disk (Solelectron magnets co., Hangzhou, China) measuring 3.0×3.0 cm placed over the wound directly on top of the gauzes (N pole toward the gauzes, The magnetic field strength at the site was 230 ± 5 mT, measured by gaussmeter). The other 10 diabetic rats in sham group had nonmagnetized disk placed.

2.3. Healing Parameters

2.3.1. Comparison of the Wound Area Reduction Rates. For surface area measurement, rats were anesthetized with ether inhalation, and then digital camera was used to photograph the wound of rats on postoperative day 7, 14 and 21. Keeping the lens from the target distance for 10 cm when took photos. Then the borders of the skin defect in the pictures were marked, and then the number of pixels within the bordered area was measured to calculate the wound area by using Photoshop CS5 software (Adobe, San Jose, CA, USA). Based on the measured wound area, the wound area reduction rate was calculated by means of the following expression: (former

TABLE 1: Comparison of wound healing rate between three groups ($\bar{x} \pm s$, %).

Group	7th days (n = 10)	14th days (n = 10)	21st days (n = 10)
SMF	25.5 ± 4.6 ^{#,*}	63.4 ± 5.5 ^{#,*}	87.7 ± 4.6 ^{#,*}
Sham	20.3 ± 4.1 [*]	52.9 ± 5.2 [*]	66.5 ± 7.3 [*]
Control	38.6 ± 3.7	86.1 ± 4.7	95.2 ± 1.8

[#] $P < 0.05$, statistically significant compared to the sham group; ^{*} $P < 0.01$, statistically significant compared to the control group.

size of the wound-current size of the wound)/(former size of the wound) $\times 100\%$ [6].

2.3.2. Comparison of Mechanical Strength of Wound Tissue.

Postoperative day 21, five rats in each group were randomly selected to be killed by anesthetic overdose and assessed for the dorsal pelt containing the healing scar was removed and cut at a right angle to the long axis of the wound into four 10-mm wide strips. The strips were placed in a buffered Ringer's solution (pH 7.4) and used within 30 minutes of recovering the pelt to assess breaking strength. Biomechanical tests were performed using an electronic universal testing machine (model INSTRON-5840, USA). Two sides of the strips were placed into custom-made mechanical grips. Grip length was selected as 10 mm on both sides and fine-grade sandpapers were placed inside the grips to prevent slipping. Test length of the slips was selected at 30 mm. Tests were performed at a constant speed of 1 mm/minute until breakage at the healing scar was observed. Force was measured with a 260-N load-cell attached to the testing frame.

2.3.3. Comparison of the Mean Time to Wound Closure. The wounds were allowed to heal by secondary intention and the time to complete closure was recorded for the rest five rats in each group.

2.4. Statistical Analysis. Statistical analyses were carried out using SPSS (version 14.0, SPSS, IL, USA). Continuous variables were expressed as mean values \pm SEM. The values were analyzed by one-way ANOVA and multiple comparisons. In a multiple comparison, difference between two groups was compared using the Student Newman Keuls- q test (SNK- q). χ^2 test for categorical dates. When P was less than 0.05, it was regarded as statistically significant.

3. Results

3.1. Comparison of Blood Glucose Level. As shown in Figure 1, in the process of the whole experiment, there were no statistical difference between the two diabetic groups ($P > 0.05$).

3.2. Comparison of Wound Area Reduction Rate. Table 1 showed that the SMF group and Sham group presented significant visual wound healing delayed compared with the Control group ($P < 0.01$, one-way ANOVA and q test).

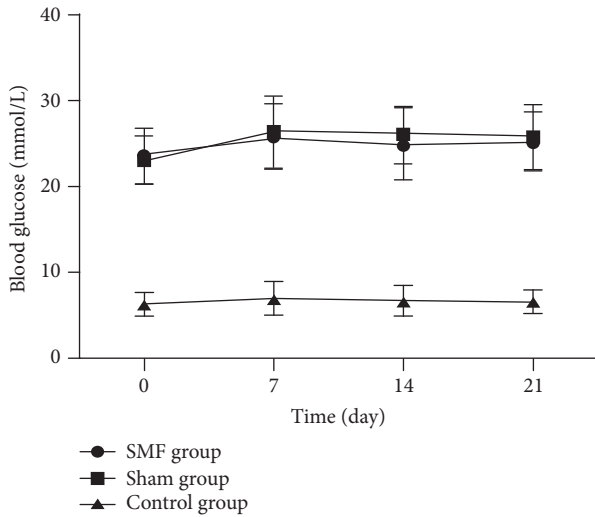


FIGURE 1: Trends of blood glucose levels in Control, SMF and Sham groups on days 0, 7, 14 and 21 after surgery.

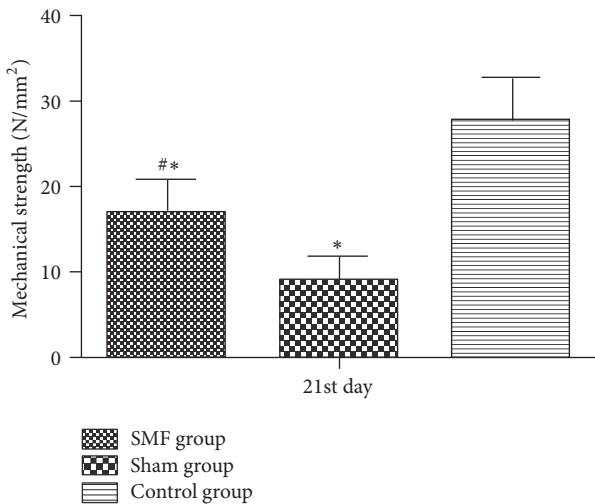


FIGURE 2: Comparison of mechanical strength in three groups on 21st day, # $P < 0.05$, statistically significant compared to the Sham group; * $P < 0.01$, statistically significant compared to the Control group.

Meanwhile, wound area reduction rate in group SMF at 7th, 14th and 21st days, respectively, was (25.5 ± 4.6)%, (63.4 ± 5.5)%, and (89.7 ± 5.2)%; they were significantly higher than those in sham magnet group (P value, resp., was 0.026, 0.005, and 0.001, q test).

3.3. Comparison of Mechanical Strength of Wound Tissue. Figure 2 showed that the mean skin wound mechanical strength values for group SMF, sham, and control, respectively, were 16.9 ± 3.8 N/mm², 8.8 ± 2.7 N/mm², and 26.7 ± 5.3 N/mm² (five rats were killed in each group). The stress values for diabetic rats were significantly lower than the control group ($P < 0.01$, one-way ANOVA and q test), and

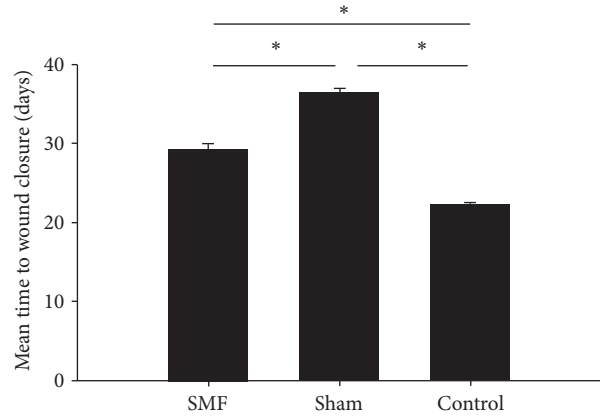


FIGURE 3: Comparison of mean time to wound closure in three groups, * $P < 0.05$, statistically significant compared to other group.

use of SMF increased the stress value in diabetic rats ($P = 0.012$, q test).

3.4. Comparison of the Mean Time to Wound Closure. The wound of partial diabetic rats was healed by second intention due to wound infection: one rat in SMF group, two rats in sham group, zero in control group; there was no significant difference between two diabetic groups ($\chi^2 = 0.480$, $P = 0.490$). As shown in Figure 3, the mean time to wound closure in the group treated with magnets was 29.5 ± 3.8 days compared with 36.5 ± 4.4 days for the sham magnet group and 22.3 ± 2.5 days for the control group (five rats were reserved in each group). Duration of healing time in diabetic rats was significantly greater than normal ($P < 0.01$, one-way ANOVA and q test). Application of SMF in diabetic rats significantly ($P = 0.028$, q test) reduced the mean time to wound closure.

4. Discussion

The present study suggested that exposure to a static magnetic field of 230 mT intensity significantly increased the rate of cutaneous wound healing and reduced the mean time to wound closure ($P < 0.05$). SMF exposure did not present overt impact on serum glucose of diabetic rats throughout the present experiment. It suggested that the capacity of SMF to promote wound healing was not dependent on the changes of serum glucose. These results were similar to Jing et al. previous research result [7]. But the wound healing rate and wound closure in our study were obviously slower than Jing et al. result; this may be due to the difference of intensity of magnetic field, wound dressing, and grouping method: higher magnetic field strength in our study (230 mT versus 180 mT); the wound dressing, respectively, was sterile gauze or hydrogel; we continuously observed wound healing process of each rat; however, only partially rats which executed every once in a while were observed in previous research [7]; the wound of partial diabetic rats was healed by second intention in our study.

In general, the wound healing process can be classified into three different phases: the inflammatory phase, proliferative phase, and remodeling phase. This process is a series of complicated reactions and interactions among cells and mediators, which can be affected by various factors [8]. Diabetes-induced impairment of wound healing is characterized by inhibition of inflammatory response, angiogenesis, fibroplasias, defects in collagen deposition, and differentiation of extracellular matrix. All these have been suggested to contribute to the observed impairment of diabetic wound healing. At present, the conventional treatments for diabetic wounds include platelet-derived products, epidermal growth factor, negative pressure suction, hyperbaric oxygen, and new type medical wound dressings. However, the clinical efficacy of these methods is controversial and some of the treatments (such as platelet derived products, antimicrobial dressings) are of poor cost-effectiveness [9]. As alternative noninvasive method, electromagnetic therapy has been used in the treatment of diabetic wound healing, but it is limited to basic research at present time. One of the findings showed that low-frequency pulsed electromagnetic field (PEMF) accelerated skin wound healing in diabetic rats [10]. But there is a problem with applying PEMF in experimental conditions because they cannot be focused on a specific target tissue. The coils wrapped around the cage that generates the magnetic field affect the animal's entire body. Animals placed in cages have stable positions according to the vector of a pulsed electromagnetic field. To lessen the stress of test animals, exposure times must be limited. Application of SMF is simple, and it achieves a permanent magnetic effect and a permanent vectorial effect. SMF is not related to electric energy, as no heat and electricity harm the tissues. At the same time, the magnetic force applied locally, but not to the whole body or surrounding tissues, has minimal exposure. This makes the SMF a useful tool for the long term. Medical applications of SMF have been generally reported as successful in musculoskeletal disease [11]. Investigations have elucidated the numerous actions of electromagnetic energy on bone including effects on cellular calcium and calcification, collagen and proteoglycans, and angiogenesis. Clinical investigations proved the benefit of electromagnetic therapy in the treatment of delayed unions, difficult fractures, and osteotomies. Animal experiments had shown that moderate field strength of SMF effectively increased the rate of wound healing; the coverage is from 15 mT to 350 mT [12, 13]. Recently, Ekici et al. study showed that high-power static magnetic fields (3900 to 4200 mT) which were placed perpendicular to the wound also increased wound tissue strength in the skin of the experimental model [14].

Mechanical strength is an important measure because it best describes the mechanical property of skin. This parameter of the skin also exhibits a progressive increase in continual tissue repair during the wound healing process [15]. In the present study, we also found that a 230 mT static magnetic treatment of the wound increased the wound breaking strength compared with sham magnet group. It implied that SMF could help to improve the quality of wound healing; similar results had also been reported in previous studies [7, 15].

The mechanism of magnetic field promoting wound healing is not very clear. Synthesizing relevant literature materials [16–18], it may include mainly three aspects: (1) the magnetic field has certain anti-inflammatory effects; (2) magnetic field can promote vascular endothelial cell proliferation and promote the formation of the epidermal neovascularization; (3) magnetic field can promote the formation of skin collagen to promote skin regeneration. In present study, we observed SMF increased wound healing in diabetic rats, but we had not compared it with conventional treatments in curative effect and explored its probable mechanism. These will be the direction of our next research.

In conclusion, according to our findings SMF of 230 mT intensity seems to improve wound healing in diabetic rats. This may provide a noninvasive therapeutic tool for impaired wound healing in diabetic patients.

Conflicts of Interest

The authors declared that they have no conflicts of interest to this work.

Authors' Contributions

Jing Zhao and Yong-guo Li contributed equally to this work.

Acknowledgments

This study was supported by the Scientific Research Program of Hubei Provincial Department of Education (Grant no. B2015443).

References

- [1] L. Guariguata, D. R. Whiting, I. Hambleton, J. Beagley, U. Linnenkamp, and J. E. Shaw, "Global estimates of diabetes prevalence for 2013 and projections for 2035," *Diabetes Research and Clinical Practice*, vol. 103, no. 2, pp. 137–149, 2014.
- [2] T. A. Motley, A. M. Gilligan, D. L. Lange, C. R. Waycaster, and J. E. Dickerson, "Cost-effectiveness of clostridial collagenase ointment on wound closure in patients with diabetic foot ulcers: Economic analysis of results from a multicenter, randomized, open-label trial," *Journal of Foot and Ankle Research*, vol. 8, no. 1, article 7, 2015.
- [3] H.-M. Yun, S.-J. Ahn, K.-R. Park et al., "Magnetic nanocomposite scaffolds combined with static magnetic field in the stimulation of osteoblastic differentiation and bone formation," *Biomaterials*, vol. 85, pp. 88–98, 2016.
- [4] K.-T. Lim, C.-S. Cho, Y.-H. Choung et al., "Influence of static magnetic field stimulation on cells for tissue engineering," *Tissue Engineering and Regenerative Medicine*, vol. 6, no. 1-3, pp. 250–258, 2009.
- [5] S. L. Henry, M. J. Concannon, and G. J. Yee, "The effect of magnetic fields on wound healing: experimental study and review of the literature," *Eplasty*, vol. 8, article e40, 2008.
- [6] D. Cukjati, S. Reberšek, and Miklavčič, "A reliable method of determining wound healing rate," *Medical and Biological Engineering and Computing*, vol. 39, no. 2, pp. 263–271, 2001.

- [7] D. Jing, G. Shen, J. Cai et al., "Effects of 180 mT static magnetic fields on diabetic wound healing in rats," *Bioelectromagnetics*, vol. 31, no. 8, pp. 640–648, 2010.
- [8] G. Broughton II, J. E. Janis, and C. E. Attinger, "The basic science of wound healing," *Plastic and Reconstructive Surgery*, vol. 117, no. 7, pp. 12S–34S, 2006.
- [9] F. L. Game, J. Apelqvist, C. Attinger et al., "Effectiveness of interventions to enhance healing of chronic ulcers of the foot in diabetes: a systematic review," *Diabetes/Metabolism Research and Reviews*, vol. 32, no. 1, pp. 154–168, 2016.
- [10] I. Goudarzi, S. Hajizadeh, M. E. Salmani, and K. Abrari, "Pulsed electromagnetic fields accelerate wound healing in the skin of diabetic rats," *Bioelectromagnetics*, vol. 31, no. 4, pp. 318–323, 2010.
- [11] A. Yadollahpour and S. Rashidi, "Therapeutic applications of electromagnetic fields in musculoskeletal disorders: a review of current techniques and mechanisms of action," *Biomedical and Pharmacology Journal*, vol. 7, no. 1, pp. 23–32, 2014.
- [12] C. Ohkubo, H. Okano, A. Ushiyama, and H. Masuda, "EMF effects on microcirculatory system," *Environmentalist*, vol. 27, no. 4, pp. 395–402, 2007.
- [13] R. Saunders, "Static magnetic fields: animal studies," *Progress in Biophysics and Molecular Biology*, vol. 87, no. 2-3, pp. 225–239, 2005.
- [14] Y. Ekici, C. Aydogan, C. Balcik et al., "Effect of static magnetic field on experimental dermal wound strength," *Indian Journal of Plastic Surgery*, vol. 45, no. 2, pp. 215–219, 2012.
- [15] D. A. Hollander, H. J. Erli, A. Theisen, S. Falk, T. Kreck, and S. Müller, "Standardized qualitative evaluation of scar tissue properties in an animal wound healing model," *Wound Repair and Regeneration*, vol. 11, no. 2, pp. 150–157, 2003.
- [16] G.-E. Costin, S. A. Birlea, and D. A. Norris, "Trends in wound repair: cellular and molecular basis of regenerative therapy using electromagnetic fields," *Current Molecular Medicine*, vol. 12, no. 1, pp. 14–26, 2012.
- [17] S. Xu, H. Okano, M. Nakajima, N. Hatano, N. Tomita, and Y. Ikada, "Static magnetic field effects on impaired peripheral vasomotion in conscious rats," *Evidence-Based Complementary and Alternative Medicine*, vol. 2013, Article ID 746968, 6 pages, 2013.
- [18] M. J. Callaghan, E. I. Chang, N. Seiser et al., "Pulsed electromagnetic fields accelerate normal and diabetic wound healing by increasing endogenous FGF-2 release," *Plastic and Reconstructive Surgery*, vol. 121, no. 1, pp. 130–141, 2008.

Clinical Study

Efficacy of Administration of an Angiotensin Converting Enzyme Inhibitor for Two Years on Autonomic and Peripheral Neuropathy in Patients with Diabetes Mellitus

Triantafyllos Didangelos, Konstantinos Tziomalos, Charalambos Margaritidis, Zisis Kontoninas, Ioannis Stergiou, Stefanos Tsotoulidis, Eleni Karlafti, Alexandros Mourouglakis, and Apostolos I. Hatzitolios

Diabetes Center, First Propedeutic Department of Internal Medicine, Medical School, Aristotle University of Thessaloniki, AHEPA Hospital, Thessaloniki, Greece

Correspondence should be addressed to Triantafyllos Didangelos; didang@med.auth.gr

Received 13 January 2017; Accepted 21 February 2017; Published 8 March 2017

Academic Editor: Ilias Migdalis

Copyright © 2017 Triantafyllos Didangelos et al. This is an open access article distributed under the Creative Commons Attribution License, which permits unrestricted use, distribution, and reproduction in any medium, provided the original work is properly cited.

Aim. To evaluate the effect of quinapril on diabetic cardiovascular autonomic neuropathy (CAN) and peripheral neuropathy (DPN). **Patients and Methods.** Sixty-three consecutive patients with diabetes mellitus [43% males, 27 with type 1 DM, mean age 52 years (range 22–65)], definite DCAN [abnormal results in 2 cardiovascular autonomic reflex tests (CARTs)], and DPN were randomized to quinapril 20 mg/day (group A, $n = 31$) or placebo (group B, $n = 32$) for 2 years. Patients with hypertension or coronary heart disease were excluded. To detect DPN and DCAN, the Michigan Neuropathy Screening Instrument Questionnaire and Examination (MNSIQ and MNSIE), measurement of vibration perception threshold with biothesiometer (BIO), and CARTs [R-R variation during deep breathing [assessed by expiration/inspiration ratio (E/I), mean circular resultant (MCR), and standard deviation (SD)], Valsalva maneuver (Vals), 30 : 15 ratio, and orthostatic hypotension (OH)] were used. **Results.** In group A, E/I, MCR, and SD increased (p for all comparisons < 0.05). Other indices (Vals, 30 : 15, OH, MNSIQ, MNSIE, and BIO) did not change. In group B, all CART indices deteriorated, except Vals, which did not change. MNSIQ, MNSIE, and BIO did not change. **Conclusions.** Treatment with quinapril improves DCAN (mainly parasympathetic dysfunction). Improved autonomic balance may improve the long-term outcome of diabetic patients.

1. Introduction

Diabetes mellitus (DM) is the most common cause of neuropathy and diabetic neuropathy (DN) comprises a heterogeneous group of disorders that can cause neuronal dysfunction throughout the human body. The Toronto Consensus Panel on DN divided in 2010 the disease into typical and atypical neuropathy [1]. Typical diabetic peripheral neuropathy (DPN) is “a symmetrical, length-dependent sensorimotor polyneuropathy attributable to metabolic and microvascular alterations as a result of chronic hyperglycemia exposure and cardiovascular risk covariates.” Atypical forms of DN differ in onset, course, manifestations, associations, and putative mechanisms and are likely to be associated with pain and/or dysautonomia. Peripheral and autonomic neuropathies are

the most common manifestations of DN, which often coexist. Diabetic peripheral neuropathy is the second most common form of DN and is estimated to affect 45–50% of all patients with DM [2]. The prevalence varies according to the severity and duration of hyperglycaemia but overall polyneuropathy is present in up to 50% of people with long-standing DM [3].

DPN represents a major health problem as it may present with excruciating neuropathic pain and is responsible for substantial morbidity, resulting from foot ulceration, amputations, and impaired quality of life, as well as with increased mortality. The manifestations of diabetic autonomic neuropathy (DAN) are manifold affecting all systems and organs innervated from autonomic system, but cardiovascular, urogenital, gastrointestinal, pupillomotor, thermoregulatory, and sudomotor systems are the most important. Diabetic

TABLE 1: Characteristics of patients at baseline.

	Group A (n = 31)	Group B (n = 32)	<i>P</i>
Age (years)	52.7 ± 16.4	51.9 ± 13.9	NS
Males (%)	48.4	37.5	NS
Diabetes mellitus duration (years)	17.8 ± 7.4	18.1 ± 8.2	NS
Type 1 diabetes mellitus (%)	45.2	40.6	NS
HbA _{1c} (%)	7.1 ± 2.2	7.2 ± 2.4	NS
Fasting plasma glucose (mg/dl)	125 ± 27	129 ± 19	NS
Total cholesterol (mg/dl)	189 ± 37	193 ± 51	NS
High density lipoprotein cholesterol (mg/dl)	46 ± 10	45 ± 10	NS
Low density lipoprotein cholesterol (mg/dl)	107 ± 36	118 ± 49	NS
Triglycerides (mg/dl)	185 ± 70	171 ± 68	NS
Creatinine (mg/dl)	0.97 ± 0.19	0.98 ± 0.25	NS
Estimated glomerular filtration rate (ml/min/1.73 m ²)	112 ± 34	109 ± 37	NS
Uric acid (mg/dl)	5.4 ± 1.3	6.1 ± 2.1	NS

cardiovascular autonomic neuropathy (DCAN) is characterized by autonomic dysfunction of the cardiovascular system. It is the most prevalent and well-studied form of DAN [4]. It is characterized by alterations in the control of heart rate and vascular hemodynamics. The prevalence of DCAN ranges from 2.5 to 50% in different cohorts. The prevalence of confirmed DCAN is around 20% and rises up to 65% with age and DM duration. DCAN has been shown to negatively impact mortality due to its relationship with serious comorbidities (including silent myocardial ischemia, coronary heart disease (CHD), stroke, diabetic nephropathy, and increased perioperative morbidity) [4]. Thus, the management of DCAN has important implications for the prognosis of DM.

Despite the significant individual and social burden associated with diabetic neuropathy, its treatment remains unsatisfactory. This is in part due to the innately unpredictable and complex nature of the disease, combined with limited systematic diagnostic testing, which differs from diabetic retinopathy and nephropathy, where the disease is more predictable and the diagnostic tests more straightforward. In the current study, we chose to use the most valid and accurate diagnostic tests [Michigan Neuropathy Screening Instrument Questionnaire and Examination (MNSIQ and MNSIE) and Cardiovascular Reflex Tests (CRTs)] for the evaluation of neuropathy in well characterized and highly selected patients. Moreover, there are currently no FDA-approved therapies for diabetic neuropathy and only 3 approved therapies for painful DPN. No treatment results in complete resolution of the underlying pathophysiological abnormalities and treatment of DN is an unmet need in clinical practice. Only strict metabolic control appears to have a beneficial effect on the prevention and delay of the onset of DN and to reduce the prevalence of established DN [5–8].

The aim of the present study was to evaluate the efficacy and safety of the administration of an angiotensin converting enzyme (ACE) inhibitor, quinapril 20 mg/day, for two years on DCAN and DPN in patients with type 1 and 2 DM.

2. Research Design and Methods

2.1. Patient Selection. This open, parallel-group, controlled study included 63 adult patients with long-standing types 1 and 2 DM, who were recruited from the outpatient diabetes clinics in AHEPA University hospital and Hippokration hospital of Thessaloniki, Greece. The study was approved by the institutional ethics committee and all subjects gave written informed consent. The study started in 1999. All patients were asymptomatic, had a normal electrocardiogram, and were normotensive (blood pressure ≤ 130/85 mmHg). They also had normal renal function and were under no medication other than insulin. CHD was excluded on the basis of normal thallium 201 myocardial perfusion imaging. All patients were well characterized and highly selected. Patients were randomized to receive either quinapril 20 mg/day (group A, *n* = 31) or no treatment (group B, *n* = 32). Demographic characteristics of the patients are shown in Table 1.

2.2. Cardiovascular Autonomic Reflex Tests (CARTs). The Monitor ONE NDX device (QMED Industries, Clark, NJ, USA) was used for the measurement of the autonomic nervous function (ANF) indices. ANF was assessed according to the consensus statement of the American Diabetes Association and the American Academy of Neurology [9] and the Toronto Consensus Panel on Diabetic Neuropathy [10] taking into account various factors such as concomitant illnesses and lifestyle (exercise, hypoglycemia, smoking, and caffeine intake). The following tests were performed as previously described: (1) beat to beat variation of R-R interval assessed by (a) expiration/inspiration index (E/I Index), (b) mean circular resultant (MCR) vector analysis (probably the most reliable ANF index), and (c) standard deviation (SD) and (2) Valsalva maneuver (Valsalva Index), (3) variation of R-R interval during postural change (30:15 Index), and (4) variation of systolic blood pressure during postural change (standing). The presence of definite DCAN was established if

TABLE 2: Changes in cardiovascular autonomic reflex tests during the study in patients who received quinapril (group A) and in those who did not (group B).

	Group A (n = 31)			Group B (n = 32)			p (group A versus group B at end of treatment)
	Baseline	End of treatment	p (versus baseline)	Baseline	End of treatment	p (versus baseline)	
E/I index	1.11 ± 0.06	1.23 ± 0.12	0.011	1.09 ± 0.06	1.04 ± 0.04	0.007	<0.001
MCR	18.1 ± 6.2	38.7 ± 20.5	0.006	14.2 ± 4.2	8.1 ± 4.5	0.01	<0.001
SD	31.1 ± 11.9	56.6 ± 23.0	0.004	28.2 ± 9.9	15.5 ± 7.4	<0.05	<0.001
Valsalva index	1.48 ± 0.28	1.56 ± 0.33	NS	1.52 ± 0.22	1.50 ± 0.28	NS	NS
30:15 index	1.15 ± 0.12	1.18 ± 0.12	NS	1.15 ± 0.06	1.08 ± 0.04	<0.05	<0.001
OH	16.0 ± 11.8	10.4 ± 6.1	NS	18.5 ± 4.5	28.0 ± 6.3	0.018	<0.001

E/I: expiration/inspiration; MCR: mean circular resultant; SD: standard deviation; OH: orthostatic hypotension.

TABLE 3: Changes in indices of diabetic peripheral neuropathy during the study in patients who received quinapril (group A) and in those who did not (group B).

	Group A (n = 31)			Group B (n = 32)		
	Baseline	End of treatment	p (versus baseline)	Baseline	End of treatment	p (versus baseline)
Michigan Neuropathy Screening Instrument	2.6 ± 0.4	2.4 ± 0.3	NS	2.4 ± 0.4	2.5 ± 0.5	NS
Vibration perception threshold	23 ± 8	20 ± 7	NS	25 ± 8	24 ± 9	NS

at least 2 of the above-mentioned CARTs were abnormal. The normal values adopted were those reported by Ziegler et al. [11].

2.3. Michigan Neuropathy Screening Instrument (MNSI). MNSI has 2 steps to assess history of neuropathic symptoms and physical examination to evaluate the appearance and sensation of feet. An objective test with 4 questions included foot skin inspection for deformities, dry skin, calluses, infections, fissures and ulcer, ankle reflex, and vibration sensation tested by a 128 HZ tuning fork placed over great toe (MNSIQ). The test was performed by an experienced physician. A score ≥ 2 was considered abnormal. Abnormality in each item is graded between 0.5 and 1 and at least more than 2 abnormal items are needed to reach the score of neuropathy [12].

All tests were performed in the same day by an experienced physician blinded to the treatment. All patients had both definite DCAN (2 or more CARTs abnormal) and definite DPN.

3. Statistical Analysis

All data were analyzed with the statistical package SPSS (version 17.0; SPSS, Chicago, IL, USA). Data are presented as percentages for categorical variables and as mean and standard deviation for continuous variables. Differences in categorical variables between groups at baseline were assessed with the chi-square test. Differences in continuous variables between groups at baseline and at the end of follow-up were

assessed with the independent samples *t*-test. Paired samples *t*-test was used for comparisons of DPN and DCAN indices between and after treatment. In all cases, a two-tailed $p < 0.05$ was considered significant.

4. Results

After 2 years of follow-up, improvement was recorded in group A in all indices of deep breathing test (E/I, MCR, SD) versus baseline (Table 2). The other indices, Valsalva Index, 30:15, and orthostatic hypotension did not change versus baseline (Table 2).

In group B, all indices displayed significant deterioration in comparison to baseline at month 24 of follow-up except the Valsalva Index that remained unchanged throughout the study (Table 2).

At the end of follow-up, all indices in group A, except Valsalva Index, were better than in group B (Table 2).

All indices of DPN did not change during the study in either group A or group B and did not differ between the 2 groups at the end of follow-up (Table 3).

5. Discussion

The present study demonstrated for the first time that treatment with quinapril for 2 years improves parasympathetic function of DCAN as expressed with the indices of deep breathing test. We did not observe any significant improvement or deterioration in DPN, according to MNSI and BIO indices.

In the present study, we used CARTs, MNSI, and BIO as the most valid and appropriate tests to diagnose definite neuropathy. This study design was adopted because we wanted to assess the clear effect of ACE inhibition on DCAN and DPN without interference of any other disease except DM or any potential drug-induced change in autonomic nervous system function parameters. Despite the fact that many new methods have been described for the diagnosis of DCAN such as heart rate variability, metaiodobenzylguanidine scan, and corneal confocal microscopy, they are not included in the criteria for the diagnosis of DCAN according to the San Antonio conference and the new proposal from the Toronto panel. The criteria suggested from these 2 conferences are that 2 or more of the following cardiovascular reflex tests should be abnormal: (1) deep breathing test, (2) Valsalva maneuver, (3) 30:15 index, and (4) orthostatic hypotension.

The present study included only well characterized, highly selected normotensive patients with definite diagnosed DCAN and DPN free of CHD (based on a normal scintigraphy test), diabetic cardiomyopathy, nephropathy, arrhythmias, or heart failure of any etiology. In our previous study with a 6-month duration, we found an improvement in indices of 24 h HRV without any change in indices of CARTs [13]. In another study from our group, we also observed after 1 year of treatment with quinapril improvement of DCAN and left ventricular dysfunction [14]. However, the former study was criticized because of lack of control group. The Steno-2 trial reported that a multifactorial cardiovascular risk intervention (including ACE inhibition) appeared to reduce the prevalence of autonomic dysfunction by 63% [15]. In the former study, glucose-lowering therapy appeared to have the least impact in preventing DCAN compared with antihypertensive drugs, lipid-lowering agents, antiplatelet therapy, and vitamin and mineral supplementation [15]. In another recent study, patients received α -lipoic acid plus ACE inhibition and there was an improvement in DCAN after 4 years of treatment [16]. Therefore, it is difficult to evaluate the effect of ACE inhibition in the latter two studies, since other treatments were also administered. To the best of our knowledge, the current study is the first that shows the effects of monotherapy with an ACE inhibitor on DCAN.

At baseline, the values of most standard CARTs were below the lower limit of normal. The values of parasympathetic related tests were more adversely affected at baseline than those of sympathetic related tests. It is argued that indices of the deep breathing test (E:I index, SD, and MCR of R-R intervals), considered to be related to vagal tone, were negatively affected and are the earliest markers of DCAN deterioration. So, maybe, they are the first to improve with appropriate treatment, as observed in the current study. Valsalva maneuver is a more complex test; it encompasses a complex reflex arc involving both sympathetic and vagal pathways to the heart, sympathetic pathways to the vascular tree, and baroreceptors in the chest and lungs [11]. Thus, it is reasonable that the Valsalva Index is affected after total and significant autonomic nervous system entanglement, which probably occurs later than the 2 year follow-up period of our study.

Indices of DPN did not change during the 2-year follow-up period. Only 2 randomized, double-blind, placebo-controlled studies evaluated this topic. One trial from Malik et al. reported that peroneal nerve motor conduction velocity increased after 12 months of treatment with trandolapril compared with placebo [17]. Vibration perception threshold, autonomic function and the neuropathy symptom, and deficit score showed no improvement in either group. Our experience with administration of quinapril for 6 months in a randomized, double-blind, placebo-controlled trial was an improvement in indices of 24 h HRV with no change in vibration perception threshold. But, in the study by Malik et al., values from indices of CARTs were much lower than in ours and in our study indices of CARTs during 6 months of treatment did not improve and we did not evaluate nerve conduction velocity. The obvious question is why no pathogenetic treatment for DPN has proved sufficiently efficacious to achieve regulatory approval. Ziegler and Luff suggested that trials were hampered by a generally poor design and short follow-up and by being limited to patients with advanced DPN [18]. They suggested that trials involving patients with early DPN, conducted over 3–5 years to establish a delay or arrest in the progression of neuropathy, rather than reversal, were more likely to be successful [18].

Previous studies in experimental models [19, 20] have shown a reduction in the progression of DN. These effects are mainly mediated through the vasodilating properties of ACE inhibitors, when used for improvement of nerve flow velocity. A beta blockade-like effect of quinapril was observed in a previous study; that is, quinapril compared with lisinopril decreased the heart rate (-12% , $p < 0.01$) in patients with mild to moderate hypertension [21]. In the lisinopril group, no change in heart rate was observed [21]. So, quinapril appears to combine beta blockade-like and ACE inhibition properties, without the side effects of β -blocking agents. This was the reason why we chose to use in the current study quinapril among other ACE inhibitors.

Moreover, formation of advanced glycosylated end products (AGEs) in DM appears to play a crucial role in the pathogenesis of microvascular complications and maybe in the “metabolic memory” observed in large studies. It has been proposed that the pathophysiological cascades triggered by AGEs have a dominant, hyperglycemia-independent role in the onset of the microvascular complications of diabetes [22]. Furthermore, ACE inhibition, in experimental trials, reduces the accumulation of AGEs in DM [23, 24] and maybe that is another mechanism of action of these drugs against the development of microvascular complications in DM. Moreover, a beneficial effect of ACE inhibitors has been suggested in many studies on retinopathy and nephropathy.

Data supporting the role of glycemic control in both the primary and secondary prevention of DPN in patients with type 1 DM comes from the Diabetic Control and Complications Trial (DCCT) [5]. In the intensive glucose control arm, a 60% reduction in the incidence of DPN and a 45% reduction in the incidence of DCAN were observed [5]. In the Epidemiology of Diabetes Interventions and Complications (EDIC) study, despite no difference in glycemic control, the prevalence and incidence of DPN and CAN were significantly

reduced in patients who received prior intensive insulin treatment compared with patients who received standard insulin therapy during the DCCT [5]. This protective effect of prior intensive glycemic control, termed metabolic memory, persisted until 13 to 14 years after the end of the DCCT [5]. For CAN, differences in glycosylated hemoglobin levels during the DCCT explained almost all the protective effects of intensive versus standard therapy on the risk of incident CAN, supporting early commencement of intensive treatment in T1D [5]. In T2DM, there is less evidence of benefits of intensive glycemic control on DN. The United Kingdom Prospective Diabetes Study (UKPDS) emphasized the impact of glycemic control on microvascular complications in type 2 DM and reported a lower rate of impaired vibration perception threshold (VPT) with intensive therapy versus standard therapy, even though this effect became significant only after 15 years of follow-up (relative risk 0.60, 95% confidence interval 0.39–0.94) [25]. Furthermore, a Cochrane review of 17 randomized trials concluded that strict glycemic control prevented neuropathy in patients with type 1 DM but a trend towards reduced incidence in type 2 DM was not significant [26].

Our group proposed for the first time the management of DCAN with ACE inhibitors and reported an increase in indices of 24h HRV, which have been considered as the earliest markers of autonomic dysfunction [13]. In the present study, we report a clear effect of quinapril in well characterized patients with types 1 and 2 DM with definite DCAN and DPN.

Another drug class that has been studied in the context of DCAN and DPN is aldose reductase inhibitors (ARIs). In a previous study from our group, tolrestat, an ARI, improved indices of CARTs in patients with definite DCAN after 2 years of treatment [27]. In a meta-analysis, Hu et al. evaluated the efficacy and safety of ARIs for the treatment of CAN in DM, based on CARTs [28]. From their analysis of 10 studies, the authors concluded that ARIs improved cardiac autonomic function [28].

Additional data for the beneficial effect of ACE inhibition on DCAN were reported in the NATHAN-1 trial [16]. The authors used as efficacy measures the Neuropathy Impairment Score of the lower limbs (NIS-LL) and heart rate during deep breathing (HRDB) [16]. Participants treated with a-lipoic acid for 4 years who received ACE inhibitors showed a greater improvement in HRDB after 4 years [16].

Many other drugs have been used in the management of DN and further studies are necessary for identifying the best combinations of treatments for diabetic neuropathy [29].

Foot problems from underlying DN are a major cause for developing ulcers, Charcot foot abnormalities, injuries, infections, and lower extremity amputation and this is a lifetime risk for patients with DM. As neuropathy progresses, impairment of body balance and gait abnormalities may be encountered and all these in addition to motor dysfunction may predispose to falls and fractures. Moreover, DCAN could predispose to these adverse events. The economic cost from foot problems is big worldwide and in Greece [30]. Patients with diabetic neuropathy should be routinely counseled about their disease, in particular focusing on patient concerns and expectations. Moreover, the role of strict glycemic control

should be emphasized. Thus, patients should be advised on the need for meticulous foot hygiene, appropriate footwear, and mobility support as needed.

In conclusion, in the present study, DCAN (mainly parasympathetic dysfunction) improved after 2 years of treatment with quinapril. Improved autonomic balance may be of clinical importance in the long-term outcome of patients with DM. A clear effect of quinapril on DCAN has been demonstrated. Strict glycemic control is the only confirmed treatment for prevention and delaying the development of diabetic neuropathy today. ACE inhibition and especially quinapril could be an alternative tool for the treatment of DN and the beneficial effect could be more prominent if the treatment begins at the early stages of neuropathy.

Additional Points

Novelty Statement. (i) The present study shows the efficacy and safety of treatment with angiotensin converting enzyme (ACE) inhibitors in patients with cardiovascular autonomic neuropathy (CAN), especially in patients with type 2 diabetes mellitus at early stages of the disease, in whom coronary heart disease and hypertension are much more common than in type 1 diabetes mellitus. (ii) Moreover, many studies suffer from inadequate definition of diabetic cardiovascular autonomic neuropathy (DCAN) or supporting data for the presence of DCAN. (iii) The present study explores in highly selected patients this association and is the first to report an improvement in DCAN after treatment with an ACE inhibitor for 2 years.

Ethical Approval

The study was approved by the Ethics Committee of the Medical School of the Aristotle University of Thessaloniki.

Competing Interests

The authors have no conflict of interest to declare.

References

- [1] S. Tesfaye, A. J. Boulton, P. J. Dyck et al., "Diabetic neuropathies: update on definitions, diagnostic criteria, estimation of severity, and treatments," *Diabetes Care*, vol. 33, pp. 2285–2293, 2010.
- [2] J. E. Shaw and P. Z. Zimmet, "The epidemiology of diabetic neuropathy," *Diabetes Reviews*, vol. 7, no. 4, pp. 245–252, 1999.
- [3] P. J. Dyck, W. J. Litchy, K. A. Lehman, J. L. Hokanson, J. L. Low, and P. C. O'Brien, "Variables influencing neuropathic endpoints: the rochester diabetic neuropathy study of healthy subjects," *Neurology*, vol. 45, no. 6, pp. 1115–1121, 1995.
- [4] A. I. Vinik and T. Erbas, "Diabetic autonomic neuropathy," *Handbook of Clinical Neurology*, vol. 117, pp. 27–294, 2013.
- [5] R. Pop-Busui, W. H. Herman, E. L. Feldman et al., "DCCT and EDIC studies in type 1 diabetes: lessons for diabetic neuropathy regarding metabolic memory and natural history," *Current Diabetes Reports*, vol. 10, no. 4, pp. 276–282, 2010.
- [6] C. L. Martin, J. W. Albers, and R. Pop-Busui, "Neuropathy and related findings in the diabetes control and complications

- trial/epidemiology of diabetes interventions and complications study," *Diabetes Care*, vol. 37, no. 1, pp. 31–38, 2014.
- [7] I. M. Stratton, A. I. Adler, H. A. W. Neil et al., "Association of glycaemia with macrovascular and microvascular complications of type 2 diabetes (UKPDS 35): prospective observational study," *British Medical Journal*, vol. 321, no. 7258, pp. 405–412, 2000.
 - [8] Y. Ohkubo, H. Kishikawa, E. Araki et al., "Intensive insulin therapy prevents the progression of diabetic microvascular complications in Japanese patients with non-insulin-dependent diabetes mellitus: a randomized prospective 6-year study," *Diabetes Research and Clinical Practice*, vol. 28, no. 2, pp. 103–117, 1995.
 - [9] American Diabetes Association and American Academy of Neurology, "Consensus statement: report and recommendations of the San Antonio Conference on Diabetic Neuropathy," *Diabetes Care*, vol. 11, pp. 592–597, 1988.
 - [10] V. Spallone, D. Ziegler, R. Freeman et al., "Cardiovascular autonomic neuropathy in diabetes: clinical impact, assessment, diagnosis, and management," *Diabetes/Metabolism Research and Reviews*, vol. 27, no. 7, pp. 639–653, 2011.
 - [11] D. Ziegler, G. Laux, K. Dannehl et al., "Assessment of cardiovascular autonomic function: age-related normal ranges and reproducibility of spectral analysis, vector analysis, and standard tests of heart rate variation and blood pressure responses," *Diabetic Medicine*, vol. 9, no. 2, pp. 166–175, 1992.
 - [12] W. H. Herman, R. Pop-Busui, B. H. Braffett et al., "Use of the Michigan Neuropathy Screening Instrument as a measure of distal symmetrical peripheral neuropathy in Type1 diabetes: results from the Diabetes Control and Complications Trial/Epidemiology of Diabetes Interventions and Complications," *Diabetic Medicine*, vol. 29, no. 7, pp. 937–944, 2012.
 - [13] A. G. Kontopoulos, V. G. Athyros, T. P. Didangelos et al., "Effect of chronic quinapril administration on heart rate variability in patients with diabetic autonomic neuropathy," *Diabetes Care*, vol. 20, no. 3, pp. 355–361, 1997.
 - [14] T. P. Didangelos, G. A. Arsos, D. T. Karamitsos, V. G. Athyros, S. D. Georga, and N. D. Karatzas, "Effect of quinapril or losartan alone and in combination on left ventricular systolic and diastolic functions in asymptomatic patients with diabetic autonomic neuropathy," *Journal of Diabetes and its Complications*, vol. 20, no. 1, pp. 1–7, 2006.
 - [15] P. Gæde, P. Vedel, N. Larsen, G. V. H. Jensen, H.-H. Parving, and O. Pedersen, "Multifactorial intervention and cardiovascular disease in patients with type 2 diabetes," *The New England Journal of Medicine*, vol. 348, no. 5, pp. 383–393, 2003.
 - [16] D. Ziegler, P. A. Low, R. Freeman, H. Tritschler, and A. I. Vinik, "Predictors of improvement and progression of diabetic polyneuropathy following treatment with α -lipoic acid for 4 years in the NATHAN 1 trial," *Journal of Diabetes and Its Complications*, vol. 30, no. 2, pp. 350–356, 2016.
 - [17] R. A. Malik, S. Williamson, C. Abbott et al., "Effect of angiotensin-converting-enzyme (ACE) inhibitor trandolapril on human diabetic neuropathy: randomised double-blind controlled trial," *Lancet*, vol. 352, no. 9145, pp. 1978–1981, 1998.
 - [18] D. Ziegler and D. Luff, "Clinical trials for drugs against diabetic neuropathy: can we combine scientific needs with clinical practicalities?" *International Review of Neurobiology*, vol. 50, pp. 431–463, 2002.
 - [19] E. P. Davidson, L. J. Coppey, A. Holmes, and M. A. Yorek, "Effect of inhibition of angiotensin converting enzyme and/or neutral endopeptidase on vascular and neural complications in high fat fed/low dose streptozotocin-diabetic rats," *European Journal of Pharmacology*, vol. 677, no. 1–3, pp. 180–187, 2012.
 - [20] L. J. Coppey, E. P. Davidson, T. W. Rinehart et al., "ACE inhibitor or angiotensin II receptor antagonist attenuates diabetic neuropathy in streptozotocin-induced diabetic rats," *Diabetes*, vol. 55, no. 2, pp. 341–348, 2006.
 - [21] A. Papageorgiou, A. Karayiannis, V. Athyros, S. Douma, K. Petidis, and C. Zamboulis, "A comparative study of the efficacy and safety of quinapril and lisinopril in patients with mild to moderate hypertension," *Drug Investigation*, vol. 7, no. 1, pp. 13–17, 1994.
 - [22] N. C. Chilelli, S. Burlina, and A. Lapolla, "AGEs, rather than hyperglycemia, are responsible for microvascular complications in diabetes: a 'glycooxidation-centric' point of view," *Nutrition, Metabolism and Cardiovascular Diseases*, vol. 23, no. 10, pp. 913–919, 2013.
 - [23] J. M. Forbes, M. E. Cooper, V. Thallas et al., "Reduction of the accumulation of advanced glycation end products by ACE inhibition in experimental diabetic nephropathy," *Diabetes*, vol. 51, pp. 3274–3282, 2002.
 - [24] J. M. Forbes, S. R. Thorpe, V. Thallas-Bonke et al., "Modulation of soluble receptor for advanced glycation end products by angiotensin-converting enzyme-1 inhibition in diabetic nephropathy," *Journal of the American Society of Nephrology*, vol. 16, no. 8, pp. 2363–2372, 2005.
 - [25] R. R. Holman, S. K. Paul, M. A. Bethel, D. R. Matthews, and H. A. W. Neil, "10-Year follow-up of intensive glucose control in type 2 diabetes," *The New England Journal of Medicine*, vol. 359, no. 15, pp. 1577–1589, 2008.
 - [26] B. C. Callaghan, A. A. Little, E. L. Feldman, and R. A. C. Hughes, "Enhanced glucose control for preventing and treating diabetic neuropathy," *Cochrane Database of Systematic Reviews*, vol. 6, Article ID CD007543, 2012.
 - [27] T. P. Didangelos, D. T. Karamitsos, V. G. Athyros, and G. I. Kourtoglou, "Effect of aldose reductase inhibition on cardiovascular reflex tests in patients with definite diabetic autonomic neuropathy over a period of 2 years," *Journal of Diabetes and its Complications*, vol. 12, no. 4, pp. 201–207, 1998.
 - [28] X. Hu, S. Li, G. Yang, H. Liu, G. Boden, and L. Li, "Efficacy and safety of aldose reductase inhibitor for the treatment of diabetic cardiovascular autonomic neuropathy: systematic review and meta-analysis," *PLoS ONE*, vol. 9, no. 2, Article ID e87096, 2014.
 - [29] S. Javed, U. Alam, and R. A. Malik, "Treating diabetic neuropathy: present strategies and emerging solutions," *Review of Diabetic Studies*, vol. 12, no. 1–2, pp. 63–83, 2015.
 - [30] I. Migdalis, G. Rombopoulos, M. Hatzikou, C. Manes, N. Kypraios, and N. Tentolouris, "The cost of managing type 2 diabetes mellitus in greece: a retrospective analysis of 10-year patient level data 'the HERCULES study'," *International Journal of Endocrinology*, vol. 2015, Article ID 520759, 7 pages, 2015.

Research Article

NLRP3 Inflammasome Expression and Signaling in Human Diabetic Wounds and in High Glucose Induced Macrophages

Xiaotian Zhang,¹ Jiezhai Dai,¹ Li Li,² Hua Chen,¹ and Yimin Chai¹

¹Department of Orthopedic Surgery, Shanghai Sixth People's Hospital, Jiao Tong University, Shanghai, China

²Department of Orthopedic Surgery, Shanghai First People's Hospital, Jiao Tong University, Shanghai, China

Correspondence should be addressed to Hua Chen; chuadr@aliyun.com and Yimin Chai; chaiyimin@vip.163.com

Received 21 September 2016; Revised 27 November 2016; Accepted 6 December 2016; Published 10 January 2017

Academic Editor: Ilias Migdalis

Copyright © 2017 Xiaotian Zhang et al. This is an open access article distributed under the Creative Commons Attribution License, which permits unrestricted use, distribution, and reproduction in any medium, provided the original work is properly cited.

Introduction. To investigate the contribution and mechanism of NLRP3 inflammasome expression in human wounds in diabetes mellitus and in high glucose induced macrophages. **Methods.** In the present study, we compared the expression of NLRP3 inflammasome in debridement wound tissue from diabetic and nondiabetic patients. We also examined whether high glucose induces NLRP3 inflammasome expression in cultures THP-1-derived macrophages and the influence on IL-1 β expression. **Results.** The expressions of NLRP3, caspase1, and IL-1 β , at both the mRNA and protein level, were significantly higher in wounds of diabetic patients compared with nondiabetic wounds ($P < 0.05$). High glucose induced a significant increase in NLRP3 inflammasome and IL-1 β expression in THP-1-derived macrophages. M1 macrophage surface marker with CCR7 was significantly upregulated after high glucose stimulation. siRNA-mediated silencing of NLRP3 expression downregulates the expression of IL-1 β . **Conclusion.** The higher expression of NLRP3, caspase1, and secretion of IL-1 β , signaling, and activation might contribute to the hyperinflammation in the human diabetic wound and in high glucose induced macrophages. It may be a novel target to treat the DM patients with chronic wound.

1. Introduction

Diabetes mellitus affects more than 170 million people worldwide with the number expected to increase [1]. Impaired wound healing is a major complication and chronically contributes to a poor quality of life associated with pain, suffering, and disability [2]. Enhanced activation of inflammatory pathology accumulation clearly contributes to the healing impairment. IL-1 β is a proinflammatory cytokine that is produced by various cells such as neutrophils, macrophages, fibroblasts, and keratinocytes. Excessive IL-1 β production is closely linked to chronic inflammatory disease, including diabetes, atherosclerosis, and gout [3]. An important evidence of IL-1 β is reported in mice showing that IL-1 β has a negative effect on angiogenesis in wound healing [4, 5]. NLRP3 is one of the NLR family members. Once activated, procaspase1 is recruited to the NLRP3 inflammasome and cleaved to produce active caspase1 and then cleaves and activates the potent proinflammatory cytokines IL-1 β and IL-18. Caspase1 is key constituent of this inflammasome together with NLRP3

and an adapter protein termed apoptosis-associated speck-like protein containing a caspase recruitment domain (ASC) [6].

The stimuli to activate the NLRP3 inflammasome during infection include bacterial, viral, and fungal pathogens [7]. Moreover, the activation of NLRP3 inflammasome is induced by endogenous and exogenous danger signals, such as lipopolysaccharide (LPS) and high glucose (HG). During impaired healing associated with diabetes, wounds display prolonged accumulation of macrophages associated with elevated levels of proinflammatory cytokines [8]. However, the role of the NLRP3 inflammasome in high glucose induced macrophages remains unclear.

Recent studies have suggested NLRP3 inflammasome/IL-1 β pathway plays a critical role in the pathogenesis of type 2 diabetes mellitus [9], and other evidences have previously shown that sustained NLRP3 inflammasome activity contributes to impairing wound healing in diabetic mice [10]. However, little is known about the role of the NLRP3 inflammasome in human diabetic wounds. Thus, in the

present study, we examined NLRP3 inflammasome expression in human diabetic wounds and in high glucose induced macrophages.

2. Materials and Methods

2.1. Patients. A chronic wound is a wound that does not heal in an orderly set of stages and in a predictable amount of time the way most wounds do; wounds that do not heal within three months are often considered chronic [11]. In this study, we included type 2 diabetes with chronic wounds located anywhere on the foot and non-DM patients (controls) with a leg wound lasting for at least three months. We collected wound tissue from diabetic ($n = 6$) and nondiabetic wound ($n = 6$) during initial debridement as part of standard of care. Patients' evaluation included a medical history, physical examination, and wound site measurements (location, size, and clinical infection). Serum glucose and HbA1c levels were extracted from patients.

Inclusion criteria included age 18 and older; ulcer size $>2 \text{ cm}^2$ and $<25 \text{ cm}^2$; ulcer duration more than three months; no clinical signs of infection; and adequate circulation to the affected extremity.

Exclusion criteria were chronic wound caused by pressure ulcer, vasculitis, pyoderma gangrenosum, and diseases that cause ischemia; osteomyelitis or index ulcer probing to bone; currently receiving radiation or chemotherapy; known or suspect malignancy of current ulcer. This study was approved by the Ethic Review Board of Shanghai Six People's Hospital affiliated to Shanghai Jiao Tong University. Written informed consent was obtained from all of the enrolled participants.

2.2. Cell Culture, Differentiation, and High Glucose Stimulation. The THP-1 cell line was obtained from the Cell Bank of the Chinese Academy of Sciences (Shanghai, China) and maintained at $2\text{--}10 \times 10^5$ cells/mL in the RPMI 1640 medium supplemented with 10% fetal bovine serum, 100 U/mL penicillin, and 0.1 mg/mL streptomycin at 37°C with 5% CO_2 . The differentiation of THP-1 cells into macrophages was induced with phorbol myristate acetate (PMA) for 72 h. After washing with phosphate-buffered saline (PBS), the THP-1-derived macrophages were exposed to a high glucose environment. Control group (NC) were incubated in a medium containing 10% FBS, 2 mmol L-glutamine, 50 $\mu\text{g}/\text{ml}$ gentamicin, and 5.5 mmol glucose for 48 h designed to resemble normal glucose levels observed in healthy subjects. High glucose group (HG) were incubated in a medium containing 10% FBS, 2 mmol L-glutamine, 50 $\mu\text{g}/\text{ml}$ gentamicin, and 30 mmol glucose for 48 h.

2.3. Collection of Wound Tissue. During a sharp debridement, biopsies were taken from tissue located near the center of the wound. Immediately, it was frozen in liquid nitrogen for mRNA and protein analyses.

2.4. RNA Analysis. Total RNA was isolated from all the snap frozen wound tissue and macrophages with Trizol (Invitrogen). The first strand cDNA was synthesized with 2 μg total RNA using a reverse transcriptase kit from (Promega).

Quantitative PCR was performed in 20 μl total reaction mix using PCR master mix (Life Technology) on an ABI ViiA7 (Life Technology) following the manufacturer's cycling parameters. Relative gene expression was determined using the $2^{-\Delta\text{CT}}$ method and β -actin was used as endogenous control.

2.5. Western Blot. Expression of NLRP3 proteins was evaluated by Western blot. Primary antibodies for NLRP3 were purchased from Cell Signaling (Danvers, MA, USA). Secondary peroxidase conjugated antibodies were obtained by Abcam (Cambridge, UK). The protein signals were visualized by chemiluminescence (ECL, Promega), quantified by scanning densitometry, and were expressed as integrated intensity, relative to β -actin (Cell Signaling), measured on stripped blots.

2.6. Elisa. IL-1 β was measured in the supernatants of wound homogenates or cell culture medium using human-specific ELISA assay kits (from Anogen and RayBiotech, resp.) and following the manufacturer's instructions. IL-1 β levels were expressed as pg/mL of wound lysate.

2.7. Immunofluorescence. Sections were incubated overnight with primary antibodies against CD68 and NLRP3. Sections were then incubated with FITC- and tetramethylrhodamine isothiocyanate-conjugated isotype specific secondary antibodies.

2.8. Characterization of Cell Surface Markers by Flow Cytometry. After collecting macrophages, 5×10^5 cells were resuspended in 50 μL of sterile PBS. Then, cells were simultaneously incubated with anti-CCR7 2 μg or anti-206 6 μg for 45 min on ice, respectively. After incubation and three rounds of wash in the same buffer, cells were incubated with FITC anti-mouse antibody for 25 min on ice. The samples were analyzed using BD FACSCalibur and the results were analyzed using FlowJo software.

2.9. Data Analysis. Data are presented as mean \pm SD. Comparisons between different groups were analyzed by one-way ANOVA test. A P value < 0.05 was considered significant. All statistical analyses were performed using GraphPad Prism software.

3. Results

Six patients had diabetes mellitus for >5 years (mean 2 h glucose of 13.7 ± 2.2 mg/dL and HbA1c of $7.8\% \pm 1.2\%$) with six non-DM patients on routine standard care for a chronic wound of at least three months of duration and showed no signs of clinical infection. All the clinical data and laboratory data were documented in Tables 1 and 2. In diabetic wound group, two were in ankle, one was in midfoot, and three were in forefoot. None of them was in plantar surface. Patient did not report the existence of other diabetic complications, such as peripheral neuropathy, nephropathy, retinopathy, and vascular disease. In control group, patients did not suffer from other diseases.

TABLE 1: Clinical characteristics of diabetic patients and controls.

	Diabetic patients (N = 6)	Control (N = 6)	P
Age (years)	51.0 ± 11.4	43.7 ± 8.8	P > 0.05
Body mass (kg)	69.3 ± 9.3	65.5 ± 8.5	P > 0.05
Body mass index (kg/m ²)	25.4 ± 2.5	23.7 ± 1.3	P > 0.05
Duration of diabetes (years)	6.7 ± 3.5	—	—
Insulin (n/N)	3/6	—	—
Antidiabetic drug (n/N)	3/6	—	—

TABLE 2: Laboratory data of diabetic patients and controls.

	Diabetic patients (N = 6)	Control (N = 6)	P
Fasting blood glucose (mmol/L)	8.7 ± 1.1	5.4 ± 0.5	P < 0.01
2 h blood glucose (mmol/L)	13.7 ± 2.2	6.5 ± 0.9	P < 0.01
HbA1c (%)	7.8 ± 1.2	5.2 ± 0.5	P = 0.01
LDL-C (mmol/L)	2.8 ± 0.2	2.5 ± 0.1	P > 0.05
SCr (μmol/L)	73.7 ± 13.0	68.2 ± 8.8	P > 0.05
BUN (μmol/L)	4.7 ± 0.9	3.8 ± 0.6	P > 0.05
GFR (ml/min)	98.4 ± 10.3	117.8 ± 33.3	P > 0.05

3.1. Expression of NLRP3, Caspase1, and IL-1β in Human Diabetic Wound. Total RNA was isolated from all the snap frozen wound tissue of patients with diabetic wound or non-diabetic wound for this analysis of NLRP3, caspase1, and IL-1β mRNA expression. A significantly higher level of NLRP3, caspase1, and IL-1β was found in patients of diabetic wound compared to nondiabetic wound ($P < 0.05$) (Figures 1(a), 1(b), and 1(c)). Consistent with mRNA expression pattern, a similar expression profile of protein expression of NLRP3, caspase1, and IL-1β was observed between diabetic wound and nondiabetic wound (Figures 1(d)–1(g)).

3.2. Wound Biopsy Immunostained for NLRP3 and the Macrophages Marker CD68. Immunofluorescent staining for NLRP3 was performed in chronic wound paraffin section. It confirmed protein expression of the NLRP3, in the majority of CD68⁺ wound macrophages (Figures 1(h), 1(i), and 1(j)).

3.3. High Glucose Induces the Production of NLRP3, Caspase1, and IL-1β in Macrophages. With the confirmed previous reports that NLRP3 inflammation signaling pathway is responsive to high glucose in macrophages, we treated the human THP-1-derived macrophages for 3 d with 30 mmol/L glucose.

Compared to normal control group, NLRP3, caspase1, and IL-1β were significantly increased at both the mRNA and protein levels when induced by 30 mmol/L glucose ($P < 0.05$) (Figures 2(a)–2(g)).

3.4. Effects of High Glucose on the Expression of Surface Markers on Macrophages. M1 macrophages usually express a high level of cell surface markers such as CCR7, while M2 macrophages express a higher level of mannose receptor (CD206) [12]. We accessed the impacts of high glucose on the expressions of these surface markers by FCM. As expected, an expression of CCR7 was significantly upregulated on macrophages after high glucose stimulation (Figure 3(a)). In addition, the level of CD206 was lower when the macrophages have been exposed to high glucose concentrations (Figure 3(b)).

3.5. Inhibition of NLRP3 Decreases IL-1β Activity in High Glucose Induced Macrophages. We knocked down NLRP3 levels by siRNA-mediated gene silencing. A scrambled siRNA was used as a control. Transfection with siNLRP3 was evidently effective in high glucose conditions, as reflected by decreased IL-1β expression at both the mRNA and protein levels (Figures 4(a) and 4(b)).

4. Discussion

An impaired diabetic wound healing process is a worldwide problem and a major cause of morbidity and mortality in diabetic patients [13]. It is typically associated with persistent inflammation response due to infiltration of immune cells and cytokines [14]. Several inflammatory cytokines are activated during the process of wound healing. An antagonistic relationship appears to exist within the wound microenvironment between the pathways of proinflammatory cytokines such as IL-1β and TNF-α and anti-inflammatory growth factors/cytokines/hormones, as in the case of TGF-β/IL-1ra//IL-10/E2. The role of this counterbalance in the pathogenesis of disturbed wound healing during diabetes remains to be fully elucidated [15].

In this study, we investigated the NLRP3 inflammasome in human diabetic wounds, and our results suggested the upregulation of NLRP3, caspase1, and IL-1β mRNA in human diabetic wounds. Consistent with this, significantly higher protein levels of NLRP3, caspase1, and IL-1β were also observed in diabetic wound group. Taken together, these data suggest that NLRP3 inflammation activation might be involved in the pathogenesis of wound healing impairment.

NLRP3 inflammasome is one of the largest as well as the most studied cytosolic inflammasomes, comprised of NLRP3, adapter molecule ASC, and procaspase1. During activation, procaspase1 is recruited to the NLRP3 inflammasome and cleaved to produce active caspase1 and then cleaves and activates the potent proinflammatory cytokines IL-1β. Considering a regulatory role of NLRP3 in inflammation and adaptive immune repose, its aberrant expression or function has been reported in many inflammatory diseases. Luo et al. [16] found NLRP3 may play an important role in the pathogenesis of diabetic cardiomyopathy, and silencing NLRP3 ameliorated cardiac remodeling and dysfunction. Chen et al. [17] showed that activation of the NLRP3 inflammasome regulates IL-1 family cytokine secretion and causes the development of tubulointerstitial inflammation in diabetic nephropathy. The chronic inflammation associated with obesity has been

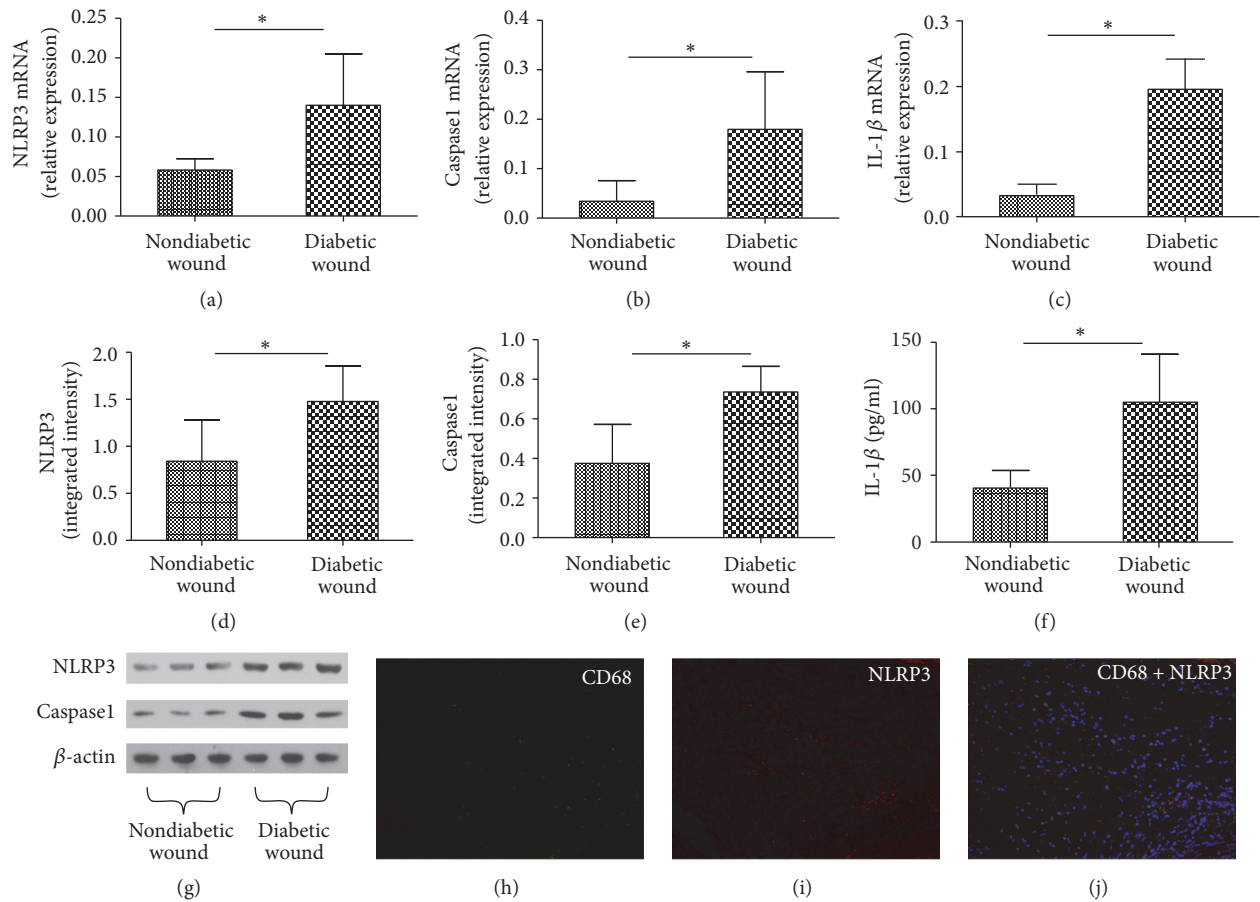


FIGURE 1: mRNA and protein expression of NLRP3, caspase1, and IL-1 β in diabetic wound and nondiabetic wound. RNA was measured by real-time PCR (a, b, and c) and proteins were measured by Western blot (d, e, and g) or Elisa (f), respectively. Wound biopsy immunostained for NLRP3 and the macrophages marker CD68 (h, i, and j). Values are mean \pm SD; * $P < 0.05$.

shown to contribute directly to the development of insulin resistance and ultimately type 2 diabetes and also affects diabetic microvascular complications [18]. As NLRP3 is involved in IL-1 β processing, we also analyzed IL-1 β release. In our study, both IL-1 β mRNA and protein were upregulated in the wounds of diabetic patients, when compared with nondiabetic wounds.

Although the role of NLRP3 inflammasome activation in diabetes has been demonstrated, the molecular targets utilizing high glucose during NLRP3 inflammasome activation in macrophages are not well understood. The pathophysiological relevance of NLRP3 inflammasome in human diabetic wound was accessed in the cultured biopsies. In the diabetic wound, NLRP3 colocalized with macrophages. Moreover, our ex vivo experiments suggest the upregulation of NLRP3, caspase1, and IL-1 β mRNA and protein in high glucose induced macrophages. This findings support a role for NLRP3 inflammasome in macrophages in human diabetic wound, linking high glucose accumulation and inflammation with the impaired wound healing.

In our study, we find that high glucose not only predominantly induces macrophages to secrete inflammatory cytokines but induces M1 polarization as evidenced by

the expression of surface markers on macrophages. The expression of M1 surface marker CCR7 was upregulated, and the expression of M2 surface marker CD206 was low after high glucose treatment. Diabetic wounds are typically associated with a persistent inflammatory response that involves accumulation of macrophages. There is a switch from proinflammatory to prohealing macrophages phenotypes during normal wound healing and the diabetic wound environment impairs the switch to a healing-associated macrophages phenotype. IL-1 β is a critical proinflammatory cytokine in the process of proinflammatory macrophage (M1) phenotype. The sustained production of IL-1 β in the diabetic wound environment acts as a positive feedback loop to sustain the proinflammatory macrophage phenotype and blocks the induction of a healing-associated macrophage phenotype [19]. In the previous study, Mirza et al. [4] applied IL-1 β -blocking antibody locally to wounds in vivo and found inhibiting IL-1 β downregulates the proinflammatory macrophage phenotype and upregulates expression of prohealing factors in wounds of diabetic mice and improves healing of these wounds. In our study, high glucose stimulation can induce macrophages polarization into M1 phenotype partly through the NLRP3/IL-1 β pathway and this might

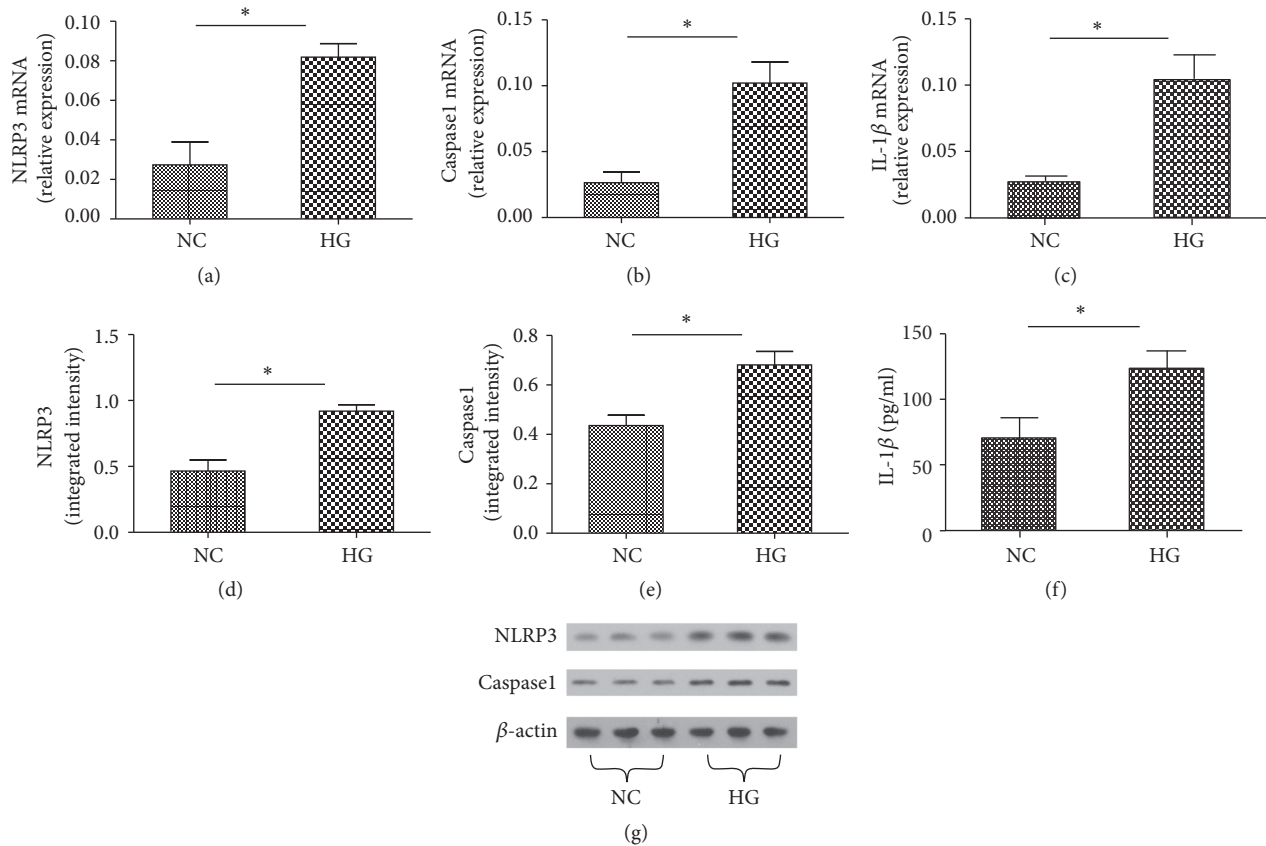


FIGURE 2: mRNA and protein expression of NLRP3, caspase1, and IL-1 β with high glucose stimulation. RNA was measured by real-time PCR (a, b, and c) and proteins were measured by Western blot (d, e, and g) or Elisa (f), respectively. Values are mean \pm SD; * $P < 0.05$.

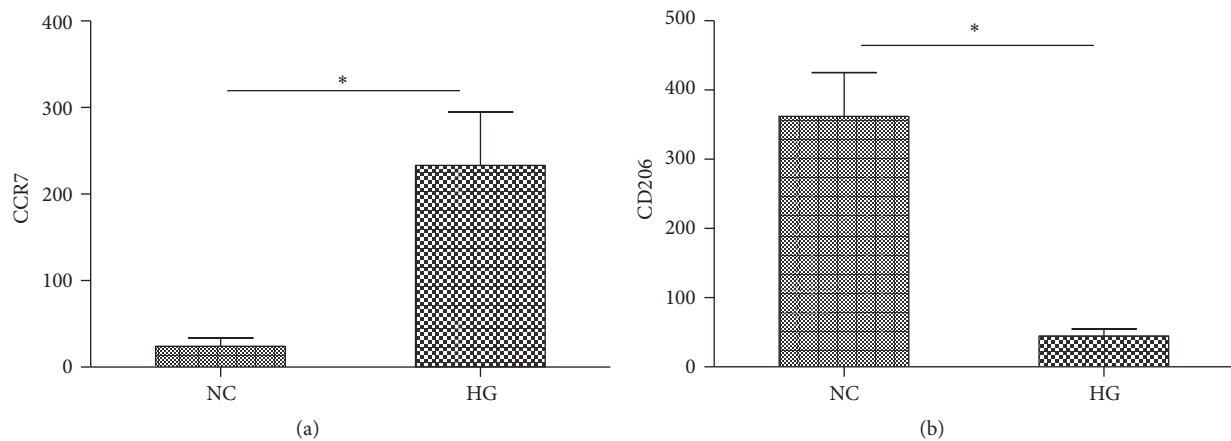


FIGURE 3: Cell surface CCR7 (a) and CD206 (b) expression in human macrophages exposed to high level of glucose. * $P < 0.05$.

be one of the mechanisms responsible for the diabetic complications.

NLRP3 is unique in its ability to recognize molecular patterns associated with host-derived signals that are abundant in obese individuals, including excess ATP, glucose, and ROS [20]. The expression of NLRP3, caspase1, and IL-1 β was significantly increased by high glucose concentration. When knocking down NLRP3 levels by siRNA-mediated

gene silencing, a decreased expression of IL-1 β in high glucose induced macrophages was noted. Song et al. [21] reported Mangiferin treatment attenuated the expressions of NLRP3 and reduced IL-1 β production in the presence of high glucose. Caspase1 mediated cleavage is the limiting step for processing IL-1 β into its secreted active forms [22]. Previous studies reported the activation of NLRP3/ASC/caspase1 inflammasome culminated in the production of IL-1 β [23].

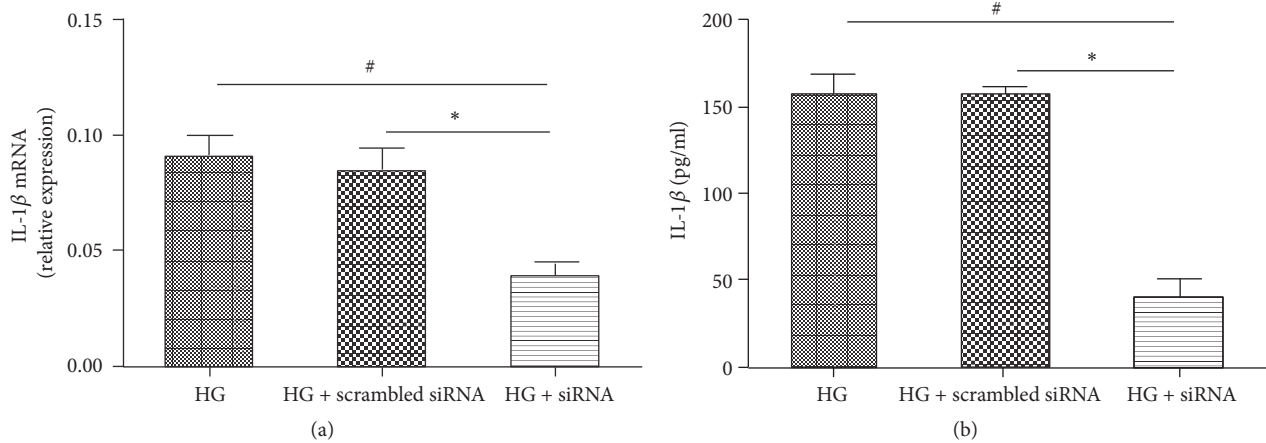


FIGURE 4: IL-1 β expression related to NLRP3 in macrophages transfected with siNLRP3. Cells are either silenced with siNLRP3 or treated with a scrambled control RNA and then exposed to high glucose. RNA and protein expression of IL-1 β were measured by real-time PCR (a) or Elisa (b), respectively. Values are mean \pm SD; # $P < 0.05$, * $P < 0.05$.

ASC act as the indispensable adaptor that connects NLRP3 and procaspase1 [24]. These clear evidences showed that IL-1 β secretion is regulated by the NLRP3 inflammasome in high glucose induced macrophages.

5. Conclusion

In conclusion, the present study demonstrated a significant higher expression of NLRP3, caspase1, and secretion of IL-1 β in the human diabetic wound and in high glucose induced macrophages, suggesting that NLRP3 inflammasome activation might contribute to the hyperinflammation in wound healing. High glucose induced macrophages polarization into M1 phenotype was partly dependent on NLRP3/IL-1 β activation. The results indicated that NLRP3 inflammation may be a novel target to treat the diabetic patients with chronic wound.

Ethical Approval

This study was approved by the Ethic Review Board of Shanghai Six People's Hospital affiliated to Shanghai Jiao Tong University.

Competing Interests

All the authors declare that they have no conflict of interests.

Authors' Contributions

Xiaotian Zhang and Jiezhi Dai contributed equally as first authors.

Acknowledgments

Sponsorship for this study and article processing charges was by Foundation of Shanghai Sixth People's Hospital (ynlc201505).

References

- [1] S. Wild, G. Roglic, A. Green, R. Sicree, and H. King, "Global prevalence of diabetes: estimates for the year 2000 and projections for 2030," *Diabetes Care*, vol. 27, no. 5, pp. 1047–1053, 2004.
- [2] R. Marfella, F. C. Sasso, M. R. Rizzo et al., "Dipeptidyl peptidase 4 inhibition may facilitate healing of chronic foot ulcers in patients with type 2 diabetes," *Experimental Diabetes Research*, vol. 2012, Article ID 892706, 11 pages, 2012.
- [3] E. Ozaki, M. Campbell, and S. L. Doyle, "Targeting the NLRP3 inflammasome in chronic inflammatory diseases: current perspectives," *Journal of Inflammation Research*, vol. 8, pp. 15–27, 2015.
- [4] R. E. Mirza, M. M. Fang, W. J. Ennis, and T. J. Kohl, "Blocking interleukin-1 β induces a healing-associated wound macrophage phenotype and improves healing in type 2 diabetes," *Diabetes*, vol. 62, no. 7, pp. 2579–2587, 2013.
- [5] E. M. Weinheimer-Haus, R. E. Mirza, and T. J. Koh, "Nod-like receptor protein-3 inflammasome plays an important role during early stages of wound healing," *PLoS ONE*, vol. 10, no. 3, Article ID e0119106, 2015.
- [6] F. Martinon, K. Burns, and J. Tschoop, "The inflammasome: a molecular platform triggering activation of inflammatory caspases and processing of proIL-1 β ," *Molecular Cell*, vol. 10, no. 2, pp. 417–426, 2002.
- [7] J.-J. Kim and E.-K. Jo, "NLRP3 inflammasome and host protection against bacterial infection," *Journal of Korean Medical Science*, vol. 28, no. 10, pp. 1415–1423, 2013.
- [8] R. Blakytyn and E. Jude, "The molecular biology of chronic wounds and delayed healing in diabetes," *Diabetic Medicine*, vol. 23, no. 6, pp. 594–608, 2006.
- [9] A. F. Mcgettrick and L. A. J. O'Neill, "NLRP3 and IL-1 β in macrophages as critical regulators of metabolic diseases," *Diabetes, Obesity & Metabolism*, vol. 15, no. s3, pp. 19–25, 2013.
- [10] A. Bitto, D. Altavilla, G. Pizzino et al., "Inhibition of inflammasome activation improves the impaired pattern of healing in genetically diabetic mice," *British Journal of Pharmacology*, vol. 171, no. 9, pp. 2300–2307, 2014.
- [11] T. A. Mustoe, "Dermal ulcer healing: advances in understanding," in *Proceedings of the Euroconference on Tissue Repair*

and Ulcer/Wound Healing: Molecular Mechanisms, Therapeutic Targets and Future Directions, Paris, France, March 2005.

- [12] A. C. Labonte, A.-C. Tosello-Trampont, and Y. S. Hahn, "The role of macrophage polarization in infectious and inflammatory diseases," *Molecules and Cells*, vol. 37, no. 4, pp. 275–285, 2014.
- [13] S. D. Hunt and F. Elg, "Clinical effectiveness of hemoglobin spray (Granulox[®]) as adjunctive therapy in the treatment of chronic diabetic foot ulcers," *Diabetic Foot & Ankle*, vol. 7, Article ID 33101, 2016.
- [14] H. Feng, J. Gu, F. Gou et al., "High Glucose and Lipopolysaccharide Prime NLRP3 Inflammasome via ROS/TXNIP Pathway in Mesangial Cells," *Journal of Diabetes Research*, vol. 2016, Article ID 6973175, 11 pages, 2016.
- [15] F. Al-Mulla, S. J. Leibovich, I. M. Francis, and M. S. Bitar, "Impaired TGF- β signaling and a defect in resolution of inflammation contribute to delayed wound healing in a female rat model of type 2 diabetes," *Molecular BioSystems*, vol. 7, no. 11, pp. 3006–3020, 2011.
- [16] B. Luo, B. Li, W. Wang et al., "Rosuvastatin alleviates diabetic cardiomyopathy by inhibiting NLRP3 inflammasome and MAPK pathways in a type 2 diabetes rat model," *Cardiovascular Drugs and Therapy*, vol. 28, no. 1, pp. 33–43, 2014.
- [17] S. Chen, C. Sheng, D. Liu et al., "Enhancer of zeste homolog 2 is a negative regulator of mitochondria-mediated innate immune responses," *Journal of Immunology*, vol. 191, no. 5, pp. 2614–2623, 2013.
- [18] J. Klen, K. Goričar, A. Janež, and V. Dolžan, "NLRP3 inflammasome polymorphism and macrovascular complications in type 2 diabetes patients," *Journal of Diabetes Research*, vol. 2015, Article ID 616747, 6 pages, 2015.
- [19] R. E. Mirza, M. M. Fang, E. M. Weinheimer-Haus, W. J. Ennis, and T. J. Koh, "Sustained inflammasome activity in macrophages impairs wound healing in type 2 diabetic humans and mice," *Diabetes*, vol. 63, no. 3, pp. 1103–1114, 2014.
- [20] M. A. Mori, O. Bezy, and C. R. Kahn, "Metabolic syndrome: is Nlrp3 inflammasome a trigger or a target of insulin resistance?" *Circulation Research*, vol. 108, no. 10, pp. 1160–1162, 2011.
- [21] J. Song, J. Li, F. Hou, X. Wang, and B. Liu, "Mangiferin inhibits endoplasmic reticulum stress-associated thioredoxin-interacting protein/NLRP3 inflammasome activation with regulation of AMPK in endothelial cells," *Metabolism: Clinical and Experimental*, vol. 64, no. 3, pp. 428–437, 2015.
- [22] T. Jourdan, G. Godlewski, R. Cinar et al., "Activation of the Nlrp3 inflammasome in infiltrating macrophages by endocannabinoids mediates beta cell loss in type 2 diabetes," *Nature Medicine*, vol. 19, no. 9, pp. 1132–1140, 2013.
- [23] S.-C. Zheng, X.-X. Zhu, Y. Xue et al., "Role of the NLRP3 inflammasome in the transient release of IL-1 β induced by monosodium urate crystals in human fibroblast-like synoviocytes," *Journal of Inflammation*, vol. 12, no. 1, article 30, pp. 1–9, 2015.
- [24] A. Babelova, K. Moreth, W. Tsalastra-Greul et al., "Biglycan, a danger signal that activates the NLRP3 inflammasome via toll-like and P2X receptors," *Journal of Biological Chemistry*, vol. 284, no. 36, pp. 24035–24048, 2009.

Research Article

Investigation of the Effects and Mechanisms of Mai Tong Formula on Lower Limb Macroangiopathy in a Spontaneous Diabetic Rat Model

Guangming Gong, Haipo Yuan, Ya Liu, and Luguang Qi

Endocrinology Department, Teaching Hospital of Chengdu University of Traditional Chinese Medicine, Chengdu 610075, China

Correspondence should be addressed to Guangming Gong; 13980506075@163.com

Received 20 September 2016; Accepted 19 October 2016

Academic Editor: Nikolaos Papanas

Copyright © 2016 Guangming Gong et al. This is an open access article distributed under the Creative Commons Attribution License, which permits unrestricted use, distribution, and reproduction in any medium, provided the original work is properly cited.

A new Chinese herbal formula called Mai Tong Formulae (MTF) has recently been used to treat lower limb macroangiopathy in type 2 diabetes mellitus (T2DM) patients. In this study, we investigated the effect of MTF on lower limb macroangiopathy in a spontaneous diabetic rat model (GK rats). We found that MTF treatment significantly reduced serum fasting blood glucose (FBG), triglycerides (TG), total cholesterol (TC), IL6, and VEGF and increased serum insulin in this model. Histological and ultrastructural observations showed that MTF treatment significantly reduced vascular endothelial cell shedding and improved endothelium injuries. We further detect proteome alteration following MTF treatment. 25 differential proteins (DPs) abnormally expressed in GK rats were normalized by MTF treatment. These DPs significantly are enriched in biological processes and pathways that regulate muscle contraction and cGMP-PKG signaling pathway and so on. Additional protein-protein interaction (PPI) network analyses of the DPs showed that Fasn and Prkar2a are involved in the AMPK signaling pathway, and Gnas, Myh11, and Myh6 are involved in vascular smooth muscle contraction; these 5 DPs were validated by Western blotting. These results indicate that MTF treatment effectively treats lower limb macroangiopathy by regulating key proteins involved in AMPK signaling pathway and vascular smooth muscle contraction.

1. Introduction

The prevalence of diabetes mellitus is increasing dramatically worldwide. Reports showed that, in 2015, over 8% of adult people worldwide suffer from type 2 diabetes mellitus (T2DM) (International Diabetes Federation, 2015) [1]. Lower limb macroangiopathy is a major complication T2DM which is caused by various pathogenic factors, including blood glucose levels, peripheral neuropathy, oxidative stress, and ischemia [2, 3]. Lower limb macroangiopathy can develop into lower limb ulcers, which decrease quality of life and contribute to high morbidity, mortality, and healthcare costs [4]. Currently, there is no medication to cure T2DM or macroangiopathy complications. In Western medicine, some blood glucose-lowering drugs, such as rosiglitazone and glibenclamide, have been used to alleviate the symptoms of T2DM but significant side effects and drug resistance exist [5]. Therefore, the development of novel longer-lasting, targeted therapeutics is urgently needed.

In China, traditional herbal formulas have been used for centuries to treat T2DM [6, 7]. Many herbal extracts can reduce blood glucose and improve complications associated with T2DM [8–11], and, compared to Western medications, many Chinese herbs have fewer side effects [12]. However, the complexity and various actions of herbal components have limited their application worldwide.

Recently, a new herbal formula called Mai Tong Formula (MTF) has been used to treat lower limb macroangiopathy and diabetic foot ulcers (DFU) in T2DM patients and has a curative effect on hyperglycemia, atherosclerosis, nephropathy, and inflammation [13]. However, the effect of MTF treatment on lower limb macroangiopathy has not been evaluated systematically, and no studies have explored the molecular mechanism of this herbal formula. Herein, we aim to explore the effect and molecular mechanism of MTF using a spontaneous diabetic rat model (GK rats). First, we evaluated the effect of MTF by measuring several blood biochemical indicators and histological observation; then, we employed

quantitative proteomic assays using isobaric tags for relative and absolute quantitation (iTRAQ), combined with high performance liquid chromatography-tandem mass spectrometry (HPLC-MS/MS), to detect proteome alteration from MTF treatment. Additional bioinformatics analyses were used to analyze the differential proteins (DPs) to investigate the key pathways underlying the mechanism of MTF treatment.

2. Materials and Methods

2.1. Animal Model and MTF Preparation. MTF is composed of dozens of herbs, including Huangqi (*Radix Astragali*), Sangshen (*Fructus Mori*), Danggui (*Angelica sinensis*), Danshen (*Salvia miltiorrhiza* Bge.), Zexie (*Alisma plantago-aquatica* Linn.), and Yinhuateng (*Lonicera japonica* Thunb.). All herbs were decocted with water, filtered, and brought to a final concentration of 1.0 g/mL.

Experimental protocols were approved by the Experimental Animal Care and Ethics Committees of the Teaching Hospital of Chengdu University of Traditional Chinese Medicine. Seven normal rats and 14 spontaneous diabetic rat models (Goto-kakizaki rats, GK rats) were purchased from SLRC Laboratory Animal Co., Ltd. (Shanghai, China). All rats were 8-week-old females with a body weight between 150 g and 210 g (certification number: SCXK (hu) 2003-0003). Seven normal rats were used as a control group and were given 2 mL intragastric saline vehicle (0.9%) once a day for 12 weeks. 14 GK rats were randomized and divided into two groups: (1) the model group ($n = 7$) was given 2 mL of intragastric saline vehicle (0.9%) once a day for 12 weeks; (2) the MTF group ($n = 7$) was given 29 g/kg MTF decoction once a day for 12 weeks. All rats were anesthetized and sacrificed under the experimental protocols described above and all efforts were made to minimize suffering.

2.2. Blood Indicators Examination. We removed the rats' tails and obtained samples to measure fasting blood glucose (FBG), blood triglycerides (TG), and blood total cholesterol (TC) levels in the 12th week of testing (AU5800, Beckman Coulter, USA). Serum insulin was measured by radioimmunoassay (HTA Co., Ltd., Beijing, China, number 2013009) using 2 mL inner canthus blood. Vascular endothelial growth factor (VEGF) and serum interleukin 6 (IL6) were measured by double-antibody sandwich ELISA (BOSTER Inc., Wuhan, China, number 2013006) using 2 mL inner canthus blood.

2.3. Pathologic Histology. For histological observation, rat femoral arteries were excised and fixed in 10% neutral formalin paraffin-embedded after dehydration; then, sections of tissue were stained with hematoxylin and eosin and images were obtained by light microscopy (Olympus, Tokyo, Japan). For ultrastructural observation, the femoral arteries were excised and fixed in 3% glutaraldehyde (4°C), dehydrated, embedded, and cut into semithin sections for optical localization; ultrathin sections were stained and visualized by electron microscopy (JEM-1010 (HC), JEOL).

2.4. Proteomic Analysis. 0.7 g of femoral arteries from 7 rats of each group (0.1 g per rat) was collected for protein extraction; then, protein (100 μ g) was digested with trypsin for 12 h at 37°C (protein/enzyme = 100/3.3). After iTRAQ (AB Science) labeling, equal amounts of labeled peptides from each group were mixed and resolved into 15 fractions by high performance liquid chromatography (HPLC), followed by Q Exactive mass spectrometry (Thermo Fisher Scientific). The resulting MS/MS data were qualitatively and quantitatively analyzed by Mascot 2.3.01 with the following parameters: protein identification using the nonredundant International Protein Index rat protein database (version 3.72) and full trypsin digest with a maximum of 1 missed cleavage. Peptide tol. and MS/MS tol. were 0.05 Da. Scaffold software was used to identify the differential proteins (Dps). Proteins with $P < 0.05$ fold change higher than 1.2 or lower than 0.833 were DPs.

2.5. Western Blotting Analysis. Cell lysates were separated by SDS-PAGE in 8% Tris-glycine gels (Invitrogen Life Technologies, Carlsbad, CA, USA) and transferred to a nitrocellulose membrane. Blots were probed with specific antibodies [diluted with 5% bovine serum albumin (BSA) to 1:1000]. Membranes were probed with horseradish peroxidase-labeled anti-rabbit secondary antibody (diluted with 5% BSA to 1:1000; Cell Signaling Technology, Inc., Danvers, MA, USA). Antibody binding was detected by using an enhanced chemiluminescence detection kit (Amersham International PLC, Buckinghamshire, UK).

2.6. Data Preprocessing. The data are presented as mean \pm standard deviation. Statistical comparisons among the three experimental groups were made using unpaired Student's t -tests. The GO and KEGG pathway enrichment analysis of DPs were performed using the Database for Annotation, Visualization, and Integrated Discovery (DAVID) [14]. The protein-protein interaction (PPI) networks were constructed using the String 10.0 database [15].

3. Results

3.1. Blood Indicators Examination and Pathologic Histology. From 0 to 12 weeks, compared with the control group, the rats in the model group were inactive, withered, and lusterless and had sparse fur, experienced diarrhea, and consumed more food and water. These symptoms in the MTF group were significantly alleviated.

We detected FBG, TG, and TC for all three experimental groups in the 12th week. As the results show in Figures 1(a), 1(b), and 1(c), the levels of FBG, TG, and TC in the model group were significantly higher than in the control group ($P < 0.01$), and, compared to model group, FBG, TG, and TC levels in the MTF group significantly improved ($P < 0.01$). As shown in Figure 1(d), serum insulin levels in the model group were significantly lower than in the control group ($P < 0.01$), and, compared to the model group, serum insulin levels in the MTF group were significantly increased ($P < 0.01$). As shown in Figures 1(e) and 1(f), serum VEGF and IL6 levels were significantly higher than in the control group ($P < 0.01$),

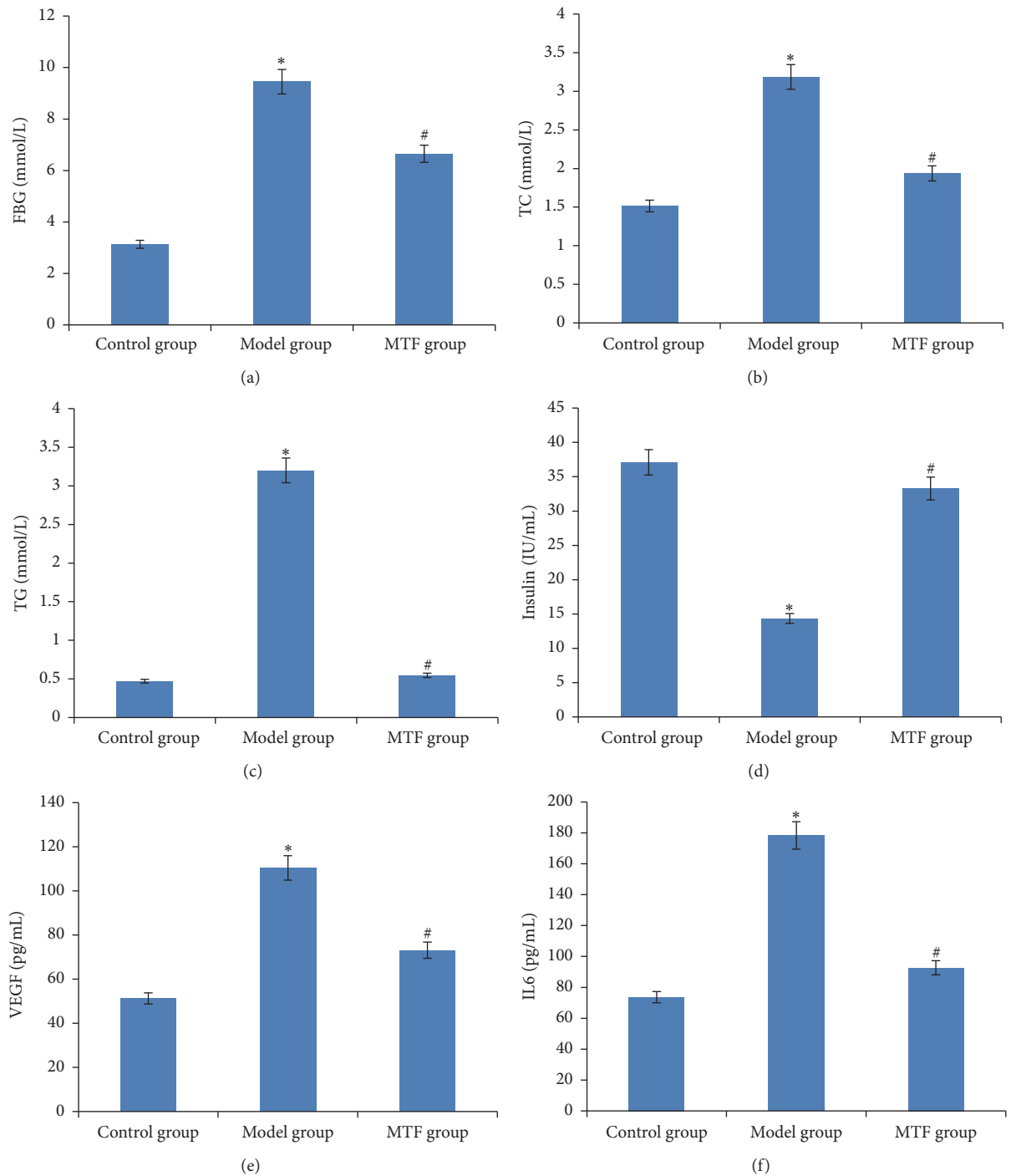


FIGURE 1: Blood indicators across three groups. (a) Level of FBG in blood; (b) level of TC in blood; (c) level of TG in blood; (d) level of insulin in blood; (e) level of VEGF in blood; (f) level of IL6 in blood. *Significant difference between the control and model group ($P < 0.01$). #Significant difference between the model and MTF group ($P < 0.01$).

and, compared to the model group, serum VEGF and IL6 levels were significantly reduced ($P < 0.01$).

Histological images from the model and MTF groups are shown in Figures 2(a), 2(b), 2(c), and 2(d). In the model group, there was a large amount of vascular endothelial cell

shedding, and the area of exfoliated endothelial cells was greater than 80%; however, in the MTF group, the exfoliated endothelial cells were distributed locally and the area was lower than 30%. The internal elastic lamina and vascular adventitia did show distinct changes in either group. The

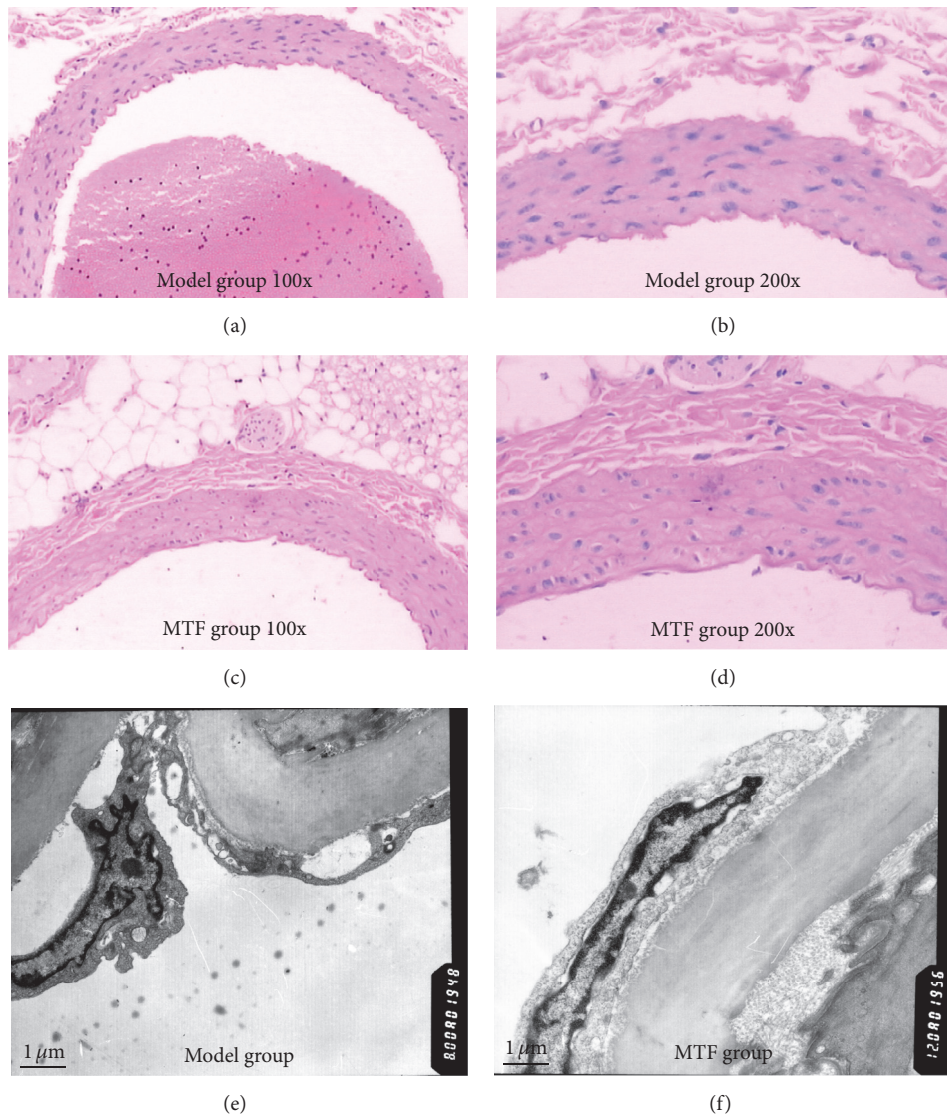


FIGURE 2: Histomorphological and ultrastructural observations of the femoral artery. (a) Histomorphological observation of model group (magnification $\times 100$); (b) histomorphological observation of model group (magnification $\times 200$); (c) histomorphological observation of MTF group (magnification $\times 100$); (d) histomorphological observation of MTF group (magnification $\times 200$); (e) ultrastructural observation of model group; (f) ultrastructural observation of MTF group.

results of ultrastructural observation are shown in Figures 2(e) and 2(f). In the model group, endothelial cell shedding, nuclear atypia, and chromatin edge accumulation were seen. Compared with the model group, the ultrastructure of endothelial cells in the treatment group was more complete.

3.2. Proteomics Analysis of the Three Groups. To explore the molecular mechanism of MTF, the femoral arteries of the three groups were collected for proteomics analysis using an iTRAQ approach. A total of 764 proteins were identified (see Table S1 in Supplementary Material available online at <http://dx.doi.org/10.1155/2016/8076796>); there were 78 DPs between the control and model groups and 76 DPs between the model and MTF groups (see Tables S2 and S3). As shown

in Figure 3(a), 40 overlapping DPs were found between the two DP comparisons (control versus model and model versus MTF). Deep analysis of these 40 overlapping DPs revealed that 25 DPs were abnormally expressed in the model group and normalized in the MTF group (named MTF-normalized DPs); 11 DPs were upregulated in the model group and downregulated in the MTF group; and 14 DPs were downregulated in the model group and upregulated in the MTF group (Table 1). We further investigated the related biological functions of the MTF-normalized DPs by using the David database. As shown in Table 2, the 25 DPs were significantly enriched in metabolic processes, cellular chemical homeostasis, muscle contraction, the cGMP-PKG signaling pathway, and endocrine and other factor-regulated calcium reabsorption pathways.

TABLE 1: DPs normalized by MTF treatment.

#	Accession number	Symbol	Molecular weight	Ratio (model/control)	Ratio (MTF/model)
Up expressed in model then down expressed in MTF	IPI00189809	Myh6	224 kDa	1.32	0.57
	IPI00200352	Crip2	23 kDa	1.23	0.76
	IPI00869592	Mylk	217 kDa	1.23	0.81
	IPI00208061	Atp1b3	32 kDa	1.41	0.66
	IPI00199872	Gnas	46 kDa	1.41	0.71
	IPI00230787	Car2	29 kDa	1.23	0.81
	IPI00231662	Cyb5r3	34 kDa	1.62	0.54
	IPI00231968	Anxa4	36 kDa	1.23	0.76
	IPI00764167	myh11	228 kDa	1.32	0.81
	IPI00390595	Stk25	48 kDa	1.41	0.76
	IPI00421517	Des	53 kDa	1.32	0.81
	Down expressed in model then up expressed in MTF	IPI00191090	Bgn	42 kDa	0.76
IPI00200661		Fasn	273 kDa	0.62	1.52
IPI00205332		Etfa	35 kDa	0.81	1.23
IPI00213036		C4a	192 kDa	0.71	1.23
IPI00231139		Tkt	71 kDa	0.41	2.46
IPI00231368		Txn1	12 kDa	0.81	1.23
IPI00326305		Atp1a1	113 kDa	0.44	1.52
IPI00365985		Hsp90b1	93 kDa	0.71	1.32
IPI00421539		Aco2	85 kDa	0.47	1.41
IPI00470254		Ezr	69 kDa	0.81	1.23
IPI00470288		Ckb	43 kDa	0.71	1.32
IPI00480639		C3	186 kDa	0.81	1.23
IPI00768626		Cdh5	87 kDa	0.71	1.52
IPI00196684		Prkar2a	46 kDa	0.57	1.32

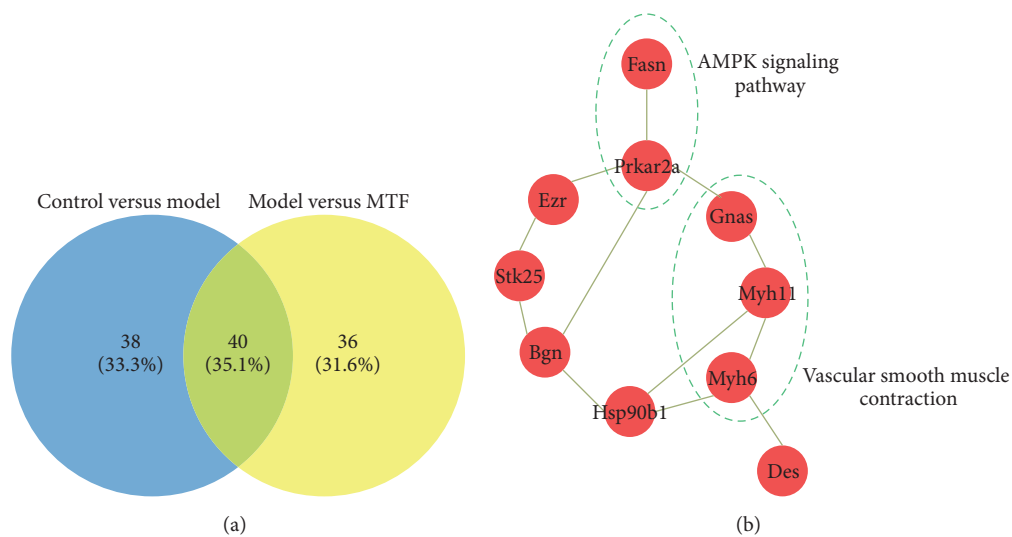


FIGURE 3: Venny plot of DPs between each group and the PPI network of the DPs normalized by MTF treatment. (a) Venny plot of DPs between each group (control versus model and model versus MTF); (b) PPI network of the DPs normalized by MTF treatment. Line: interaction; red node: DPs.

TABLE 2: GO and pathway enrichment analysis of the DPs normalized by MTF treatment database.

Database	Description	Protein number	<i>P</i>	
Gene ontology	Metabolic process	16	$5.59E - 04$	
	Single-organism metabolic process	11	$2.76E - 03$	
	Small molecule metabolic process	8	$4.84E - 03$	
	Regulation of sodium ion transport	3	$2.09E - 02$	
	Cellular monovalent inorganic cation homeostasis	3	$2.09E - 02$	
	Cellular potassium ion homeostasis	2	$2.09E - 02$	
	Sodium ion export from cell	2	$2.09E - 02$	
	Chemical homeostasis	6	$2.09E - 02$	
	Cellular chemical homeostasis	5	$2.09E - 02$	
	Membrane repolarization	2	$2.09E - 02$	
	Inorganic ion homeostasis	5	$2.09E - 02$	
	Positive regulation of striated muscle contraction	2	$2.50E - 02$	
	Regulation of biological quality	8	$2.50E - 02$	
	Cellular sodium ion homeostasis	2	$3.38E - 02$	
	Response to organic substance	8	$3.38E - 02$	
	Muscle contraction	3	$4.78E - 02$	
	KEGG pathway	Gastric acid secretion	5	$2.44E - 06$
		Proximal tubule bicarbonate reclamation	3	$2.47E - 04$
		Thyroid hormone synthesis	3	$4.23E - 03$
		Bile secretion	3	$4.23E - 03$
Cardiac muscle contraction		3	$4.50E - 03$	
Pancreatic secretion		3	$6.79E - 03$	
Thyroid hormone signaling pathway		3	$1.03E - 02$	
Adrenergic signaling in cardiomyocytes		3	$1.61E - 02$	
cGMP-PKG signaling pathway		3	$2.20E - 02$	
Aldosterone-regulated sodium reabsorption		2	$2.24E - 02$	
Carbohydrate digestion and absorption		2	$2.24E - 02$	
Endocrine and other factor-regulated calcium reabsorption		2	$2.50E - 02$	
Mineral absorption		2	$2.50E - 02$	

3.3. *PPI Network of the DPs.* To investigate the relationship between the 25 MTF-normalized DPs, we constructed a PPI network using a 10.0 database. As shown in Figure 3(b), the PPI network included 10 DPs and 12 interactions between them. In this PPI network, Fasn and Prkar2a and their interaction were found to be involved in the AMPK signaling

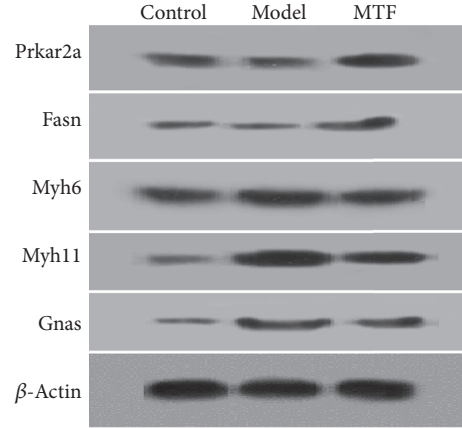


FIGURE 4: Western blots of the five DPs (Prkar2a, Fasn, Gnas, Myh11, and Myh6).

pathway; these two DPs were downregulated in the model group and upregulated in the MTF group. Gnas, Myh11, and Myh6 and their interactions were also found to be involved in vascular smooth muscle contraction; these three DPs were upregulated in the model group and downregulated in the MTF group.

3.4. *Validation of Representative DPs by Western Blotting.* To verify proteomic analysis data, five DPs (Fasn, Prkar2a, Gnas, Myh11, and Myh6) were validated using Western blotting. As shown in Figure 4, the expression of all five DPs was consistent with the iTRAQ data. Fasn and Prkar2a were downregulated in the model group and upregulated in the MTF group. Gnas, Myh11, and Myh6 were upregulated in the model group and downregulated in the MTF group.

4. Discussion

Lower limb macroangiopathy is a major complication associated with diabetes mellitus and has been shown to precede amputation in up to 90% of cases [16]. Current studies have indicated that continuous metabolic and chronic hemodynamic alterations in the blood of patients with T2DM could damage the endothelium, resulting in structural and functional changes and leading to thickening of the basement membrane and sclerosis of vascular walls, which can cause lower limb macroangiopathy [17, 18]. Many biological processes are involved in the pathogenesis of macroangiopathy, including oxidative stress, collagen deposition, angiogenesis, ECM remodeling, and vascular remodeling [19–21]. Improvement of these biological processes may be fundamental to treating lower limb macroangiopathy in T2DM.

In this study, we evaluated the efficacy and the molecular mechanism underlying MTF treatment. Our results showed that MTF treatment significantly reduced serum FBG, TG, and TC levels and significantly increased serum insulin levels in GK rats. We also found that MTF treatment significantly reduced levels of VEGF, which is associated with atherosclerosis, vascular ischemia, hypoxia, and AGE accumulation in

T2DM [22]. This reduction in VEGF indicates that MTF treatment may address antiatherosclerosis. Moreover, we found that MTF treatment also significantly reduced IL6 levels in GK rats, suggesting anti-inflammation effects [23], since IL6 is associated with vascular smooth muscle contraction in rat models of diabetes [24]. Based on visual inspections, we found a significant reduction in vascular endothelial cell shedding and improvement in endothelium injuries. Ultrastructural observation showed that MTF treatment also significantly improved necrosis in vascular endothelial cells. Taken together, these results indicate that MTF alleviates angiogenesis and affects vascular remodeling.

To characterize the molecular mechanism of MTF treatment, a proteomics analysis was used to explore multitarget characteristics. Abnormal expression of 25 DPs was normalized by MTF treatment in the GK rats. Functional enrichment analysis showed that these DPs were significantly involved in cellular chemical homeostasis, muscle contraction, cGMP-PKG signaling pathways, and endocrine and other factor-regulated calcium reabsorption, all of which are significantly associated with T2DM [25–31]. Moreover, we constructed a PPI network of these DPs, and, in this PPI network, Fasn and Prkar2a and their interaction were found to be involved in the AMPK signaling pathway. These 2 proteins have been proven to play key roles in macroangiopathy in T2DM. Fasn is a fatty-acid synthase, which may target endothelial nitric-oxide synthase (eNOS) in the plasma membrane by adding palmitate to eNOS; in this scenario, eNOS could generate NO in vascular tissue, and, in its absence, NO could decrease vasodilatation effectively leading to limb/nerve ischemia and macroangiopathy in T2DM [29]. Prkar2a is known to be a key upstream regulatory factor for Fasn [30, 32]. Three proteins (Gnas, Myh11, and Myh6) were found to be involved in vascular smooth muscle contraction, which is associated with vascular ischemia and poor local blood flow in macroangiopathy in T2DM [24]. These results indicate that MTF treatment could significantly improve vascular smooth muscle contraction.

T2DM is a complex disease that involves protein imbalance and the disturbance of multiple biological pathways. This study has shown that MTF can normalize many proteins and corresponding biological processes/pathways associated with T2DM. In accordance with our experimental results, we speculate a mechanistic pathway in vascular tissue that could be affected by MTF treatment (Figure 5). In this pathway, MTF could upregulate the expression of Prkar2a and Fasn, leading to eNOS palmitoylation, which would increase NO concentration and finally improve macroangiopathy. In addition, MTF could downregulate the expression of Gnas, Myh11, and Myh6 (which are associated with vascular ischemia), thus leading to improvement in macroangiopathy.

Competing Interests

The authors declare that they have no competing interests.

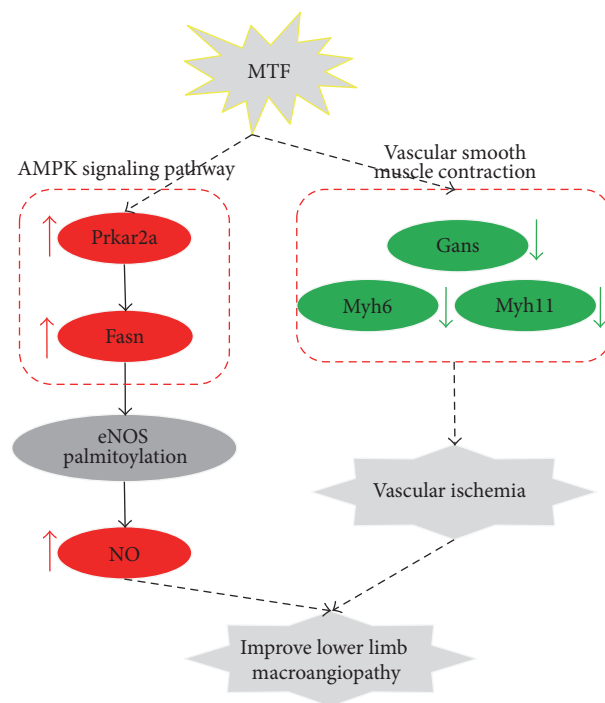


FIGURE 5: Mechanism of MTF treatment for lower limb macroangiopathy in T2DM.

References

- [1] International Diabetes Federation (IDF), *IDF Diabetes Atlas, Update 2015*, International Diabetes Federation (IDF), Brussels, Belgium, 7th edition, 2015.
- [2] K. Markakis, F. L. Bowling, and A. J. M. Boulton, "The diabetic foot in 2015: an overview," *Diabetes/Metabolism Research and Reviews*, vol. 32, Supplement 1, pp. 169–178, 2016.
- [3] W. Clayton Jr. and T. A. Elasy, "A review of the pathophysiology, classification, and treatment of foot ulcers in diabetic patients," *Clinical Diabetes*, vol. 27, no. 2, pp. 52–58, 2009.
- [4] R. Sinha, W. J. A. van den Heuvel, and P. Arokiasamy, "Factors affecting quality of life in lower limb amputees," *Prosthetics and Orthotics International*, vol. 35, no. 1, pp. 90–96, 2011.
- [5] S. Noor, R. U. Khan, and J. Ahmad, "Understanding diabetic foot infection and its management," *Diabetes & Metabolic Syndrome: Clinical Research & Reviews*, 2016.
- [6] A. L. Lee, B. C. Chen, C. H. Mou, M. F. Sun, and H. R. Yen, "Association of Traditional Chinese Medicine therapy and the risk of vascular complications in patients with type II diabetes mellitus: a nationwide, retrospective, Taiwanese-registry, cohort study," *Medicine*, vol. 95, no. 3, article e2536, 2016.
- [7] G.-D. Sun, C.-Y. Li, W.-P. Cui et al., "Review of herbal Traditional Chinese Medicine for the treatment of diabetic nephropathy," *Journal of Diabetes Research*, vol. 2016, Article ID 5749857, 18 pages, 2016.
- [8] J. C. W. Tam, C. H. Ko, C. Zhang et al., "Comprehensive proteomic analysis of a Chinese 2-herb formula (Astragali Radix and Rehmanniae Radix) on mature endothelial cells," *Proteomics*, vol. 14, no. 17-18, pp. 2089–2103, 2014.
- [9] S.-S. Luan, F. Yu, B.-Y. Li et al., "Quantitative proteomics study of protective effects of grape seed procyanidin B2 on diabetic

- cardiomyopathy in db/db mice,” *Bioscience, Biotechnology and Biochemistry*, vol. 78, no. 9, pp. 1577–1583, 2014.
- [10] Q. Cai, B. Li, F. Yu et al., “Investigation of the protective effects of phlorizin on diabetic cardiomyopathy in db/db mice by quantitative proteomics,” *Journal of Diabetes Research*, vol. 2013, Article ID 263845, 9 pages, 2013.
- [11] F. Yu, B.-Y. Li, X.-L. Li et al., “Proteomic analysis of aorta and protective effects of grape seed procyanidin B2 in db/db mice reveal a critical role of milk fat globule epidermal growth factor-8 in diabetic arterial damage,” *PLoS ONE*, vol. 7, no. 12, Article ID e52541, 2012.
- [12] S. Cai, W. Sun, Y. Fan et al., “Effect of mulberry leaf (*Folium Mori*) on insulin resistance via IRS-1/PI3K/Glut-4 signalling pathway in type 2 diabetes mellitus rats,” *Pharmaceutical Biology*, vol. 54, no. 11, pp. 2685–2691, 2016.
- [13] L. Ma, L. Huang, H. Pei et al., “Pharmacological effects of the water fraction of key components in the traditional chinese prescription Mai Tong Fang on 3T3-L1 adipocytes and ob/ob Diabetic Mice,” *Molecules*, vol. 19, no. 9, pp. 14687–14698, 2014.
- [14] D. W. Huang, B. T. Sherman, and R. A. Lempicki, “Systematic and integrative analysis of large gene lists using DAVID bioinformatics resources,” *Nature Protocols*, vol. 4, no. 1, pp. 44–57, 2009.
- [15] D. Szklarczyk, A. Franceschini, S. Wyder et al., “STRING v10: protein-protein interaction networks, integrated over the tree of life,” *Nucleic Acids Research*, vol. 43, no. 1, pp. D447–D452, 2015.
- [16] S. Jhamb, V. N. Vangaveti, and U. H. Malabu, “Genetic and molecular basis of diabetic foot ulcers: clinical review,” *Journal of Tissue Viability*, vol. 25, no. 4, pp. 229–236, 2016.
- [17] E. M. Yubero-Serrano, J. Delgado-Lista, J. F. Alcala-Diaz et al., “A dysregulation of glucose metabolism control is associated with carotid atherosclerosis in patients with coronary heart disease (CORDIOPREV-DIAB study),” *Atherosclerosis*, vol. 253, pp. 178–185, 2016.
- [18] F. Semeraro, A. Cancarini, R. dell’Omo, S. Rezzola, M. R. Romano, and C. Costagliola, “Diabetic retinopathy: vascular and inflammatory disease,” *Journal of Diabetes Research*, vol. 2015, Article ID 582060, 16 pages, 2015.
- [19] P. Madeddu, “Therapeutic angiogenesis and vasculogenesis for tissue regeneration,” *Experimental Physiology*, vol. 90, no. 3, pp. 315–326, 2005.
- [20] U. Förstermann and T. Münzel, “Endothelial nitric oxide synthase in vascular disease: from marvel to menace,” *Circulation*, vol. 113, no. 13, pp. 1708–1714, 2006.
- [21] R. Blakytyn and E. Jude, “The molecular biology of chronic wounds and delayed healing in diabetes,” *Diabetic Medicine*, vol. 23, no. 6, pp. 594–608, 2006.
- [22] R. L. Avery and G. M. Gordon, “Systemic safety of prolonged monthly anti-vascular endothelial growth factor therapy for diabetic macular edema: a systematic review and meta-analysis,” *JAMA Ophthalmology*, vol. 134, no. 1, pp. 21–29, 2016.
- [23] D. Baltzis, I. Eleftheriadou, and A. Veves, “Pathogenesis and treatment of impaired wound healing in diabetes mellitus: new insights,” *Advances in Therapy*, vol. 31, no. 8, pp. 817–836, 2014.
- [24] W.-B. Tang, Y.-Q. Zhou, T. Zhao et al., “Effect of interleukin-6 (IL-6) on the vascular smooth muscle contraction in abdominal aorta of rats with streptozotocin-induced diabetes,” *Chinese Journal of Physiology*, vol. 54, no. 5, pp. 318–323, 2011.
- [25] W. J. Jeffcoate and K. G. Harding, “Diabetic foot ulcers,” *The Lancet*, vol. 361, no. 9368, pp. 1545–1551, 2003.
- [26] L. B. Bockus and K. M. Humphries, “cAMP-dependent protein kinase (PKA) signaling is impaired in the diabetic heart,” *Journal of Biological Chemistry*, vol. 290, no. 49, pp. 29250–29258, 2015.
- [27] S. Guner, E. Arioglu, A. Tay et al., “Diabetes decreases mRNA levels of calcium-release channels in human atrial appendage,” *Molecular and Cellular Biochemistry*, vol. 263, no. 1, pp. 143–150, 2004.
- [28] S. Zhu, R. S. Guleria, C. M. Thomas et al., “Loss of myocardial retinoic acid receptor α induces diastolic dysfunction by promoting intracellular oxidative stress and calcium mishandling in adult mice,” *Journal of Molecular and Cellular Cardiology*, vol. 99, pp. 100–112, 2016.
- [29] X. Wei, J. G. Schneider, S. M. Shenouda et al., “De Novo lipogenesis maintains vascular homeostasis through endothelial nitric-oxide synthase (eNOS) palmitoylation,” *Journal of Biological Chemistry*, vol. 286, no. 4, pp. 2933–2945, 2011.
- [30] J. Chen, J. Ren, Q. Jing et al., “TSH/TSHR signaling suppresses Fatty Acid Synthase (FASN) expression in adipocytes,” *Journal of Cellular Physiology*, vol. 230, no. 9, pp. 2233–2239, 2015.
- [31] C. R. Triggle, H. Ding, T. J. Anderson, and M. Pannirselvam, “The endothelium in health and disease: a discussion of the contribution of non-nitric oxide endothelium-derived vasoactive mediators to vascular homeostasis in normal vessels and in type II diabetes,” *Molecular and Cellular Biochemistry*, vol. 263, no. 1, pp. 21–27, 2004.
- [32] T. A. M. Almabrouk, M. A. Ewart, I. P. Salt, and S. Kennedy, “Perivascular fat, AMP-activated protein kinase and vascular diseases,” *British Journal of Pharmacology*, vol. 171, no. 3, pp. 595–617, 2014.

Review Article

Sweet Bones: The Pathogenesis of Bone Alteration in Diabetes

Mohammed Al-Hariri

Department of Physiology, College of Medicine, University of Dammam, P. O. Box 2114-31451, Dammam, Saudi Arabia

Correspondence should be addressed to Mohammed Al-Hariri; mohd_alhariri@yahoo.com

Received 17 July 2016; Accepted 15 September 2016

Academic Editor: Ilias Migdalis

Copyright © 2016 Mohammed Al-Hariri. This is an open access article distributed under the Creative Commons Attribution License, which permits unrestricted use, distribution, and reproduction in any medium, provided the original work is properly cited.

Diabetic patients have increased fracture risk. The pathogenesis underlying the status of bone alterations in diabetes mellitus is not completely understood but is multifactorial. The major deficits appear to be related to a deficit in mineralized surface area, a decrement in the rate of mineral apposition, decreased osteoid surface, depressed osteoblast activity, and decreased numbers of osteoclasts due to abnormal insulin signaling pathway. Other prominent features of diabetes mellitus are an increased urinary excretion of calcium and magnesium, accumulation of advanced glycation end products, and oxidative stress leading to sweet bones (altered bone's strength, metabolism, and structure). Every diabetic patient should be assessed for risk factors for fractures and osteoporosis. The pathogenesis of the bone alterations in diabetes mellitus as well as their molecular mechanisms needs further study.

1. Introduction

Diabetes mellitus is a common chronic hyperglycemic, prevalent disease, with significant associated mortality and morbidity that affects millions of population worldwide. It is associated with a variety of complications that are well known to healthcare providers. In time, the bones may also be affected, in addition to many other organs. However, the status of bones as well as their disorders in patients with diabetes mellitus has received very little attention. This is surprising because bone disease in diabetes mellitus is probably as old as the disease itself since descriptions of bone disease in diabetes can be traced as far back as the 1920s and is as old as insulin itself [1]. Vestergaard et al. (2009) concluded that diabetes, whether type 1 diabetes (T1D) or type 2 diabetes (T2D), seems to carry an increased risk of fractures [2]. Recent studies have identified an impairment of bone quality and a higher risk of fracture, in those with T2D [3].

During the last two decades, studies reported that T2D is associated with up to three times increased risk of fracture [4, 5].

2. Pathogenesis of Sweet Bones

There are different mechanisms that can be proposed to explain the pathogenesis of sweet bones in diabetes mellitus, summarised in Figure 1.

Insulin signaling has a metabolic and mitogenic effect on osteoblast cells. Current evidence in experimental models with impaired insulin signaling exhibited both metabolic and bone phenotypes, including obesity, insulin intolerance/resistance, and symptoms of low bone mass [6] and the qualitatively different effects of T1D and T2D on bone mass are consistent with the opposing insulin-secretory states [hypoinsulinaemia versus hyperinsulinaemia] [7].

Diabetes could impact bone through several mechanisms, some of which may have contradictory effects. There are many reasons why diabetics are likely to develop bone disease and sustain fractures [8]. Many studies have suggested that low bone mineral density (BMD) is already apparent at the time of diagnosis [9, 10].

In T1D, for instance, patients may not attain the full potential of peak adult bone mass because of lower insulin-like growth factor 1 levels and the catabolic effects of frequent uncontrolled hyperglycemia during critical growth period [11]. Altered vitamin D and calcium metabolism due to hyperglycemia in diabetes mellitus can lead to low bone mass and increase chances of fractures [12, 13].

A number of studies demonstrated that osteopenia and osteoporosis are frequent complications of T1D [14], as a result of increased oxidative stress [15], as well as to the alteration of osteoblastic function [16].

Since almost 40% of the skeletal calcium is accumulated between the ages of 10 and 15 years, precisely the time when

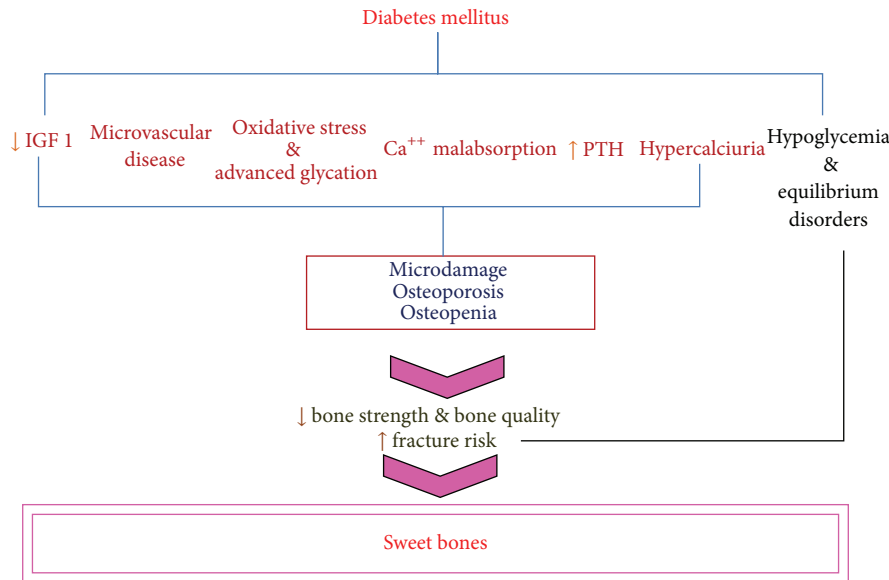


FIGURE 1: The pathogenesis of bone alteration in diabetes.

diabetes control may not be optimal, developing diabetes at this critical juncture may adversely affect the potential to achieve peak adult bone mass. It was reported that a significant number of patients with diabetes may have associated hypovitaminosis-D and calcium malabsorption or both [17, 18], low body mass, overt or subclinical malabsorption such as cystic fibrosis or celiac sprue [19, 20], and a higher incidence of subclinical eating behavior disorders, contributing to poor weight maintenance and/or relative malnutrition [21].

With the increasing life expectancy of many diabetic patients, the age related decline in osteoblast function contributes to the pathogenesis of bone loss and recurrent fractures [22].

Diabetes mellitus is known to cause advanced glycation of a variety of proteins that may also include glycation of type I collagen in bone and thus compromise its integrity [11].

Furthermore, peripheral vascular disease is common in this disease which may also contribute to the bone disease and fractures. Reduced interstitial bone fluid flow as a result of diabetic microvascular disease may result in osteocyte apoptosis and reduced osteocyte density leading to increased fragility of bone [23].

In contrast, the occurrence of bone disease in T2D presents an apparent paradox [8], but Takeuchi (2009) in his review reported that bone fragility due to poor bone quality is a major problem in patients with T2D [24]. It has been documented that T2D cases with high bone turnover assuredly predisposed to osteoporosis [25]. Obesity prevalent in T2D is strongly associated with higher BMD probably through mechanical loading and hormonal factors including insulin, estrogen, and leptin [26, 27].

A long-term T1D model showed that diabetic bones display specific defects of bone mineralization, including decreased hydroxyapatite crystal perfection, decreased calcium-to-phosphate composition of the ash, and decreased ash content in certain bones such as the tibial metaphysis.

It also found that the bones from diabetic animals exhibited reduced strength-related properties, along with a compensatory increase in stiffness, suggesting a possible alteration in bone crystal structure [28].

In a number of T1D animal studies, histomorphometric analyses have shown that, irrespective of the model used, insulin-deficient rats may exhibit reduced or absent bone formation and this decline is appreciated in relation to all bone surfaces examined [29, 30].

The major deficits in the insulin-deficient models appear to be related to a deficit in mineralized surface area, a decrement in the rate of mineral apposition, decreased osteoid surface, depressed osteoblast activity, and decreased numbers of osteoclasts [31], leading to an overall depression in remodeling of bone in the untreated insulin-deficient state.

Moreover, unlike patients with T1D, T2D patients have higher levels of insulin-like growth factor 1, which is known to stimulate bone formation. Indeed, there is suggestive evidence that age related bone loss is attenuated and bone turnover is either normal or reduced in patients with T2D ([32] and [33]). However, the existence of an elevated fracture risk in T2D, despite the underlying hyperinsulinaemia, suggests the involvement of other potential pathogenic influences (e.g., hyperglycemia, diabetic complications, and lifestyle factors) on bone [7]. In the experimental model, the skeletal fragility in T2D may arise from reduced transverse bone accrual and increased osteoclastogenesis during growth that is accelerated by the diabetic/hyperinsulinemic milieu [34]. Therefore, bone density at relevant measurement sites may not reflect the true quality of the skeleton in patients with T2D; in other words the quantity of bone may be normal but the quality is not.

All of these confounding variables may have independent negative impacts upon bone mineral acquisition in diabetes mellitus and, ultimately, on peak bone mass. On the other hand, low levels of insulin associated with T1D

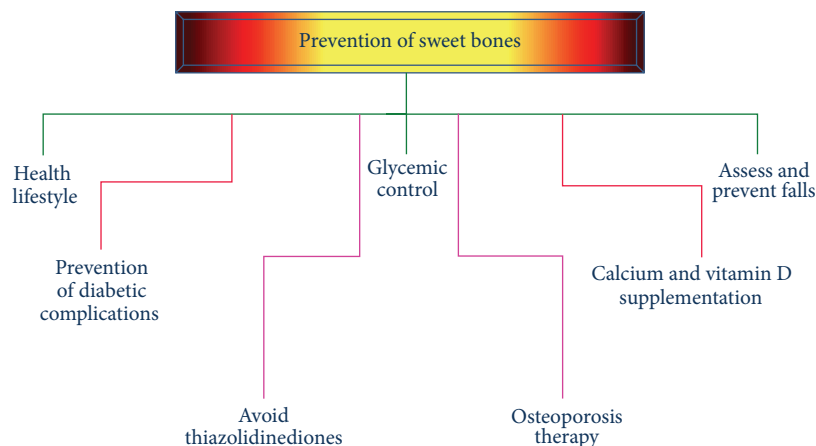


FIGURE 2: Preventive measures of sweet bones.

and the progression of T2D may cause reductions in BMD. Hyperglycemia generates a higher concentration of advanced glycation end products in collagen that may reduce bone strength [35].

T1D in humans has frequently been shown to be associated with reduced bone mass [36] and a reduced bone mineral content [37]. The percentage of patients reported to have osteopenia ranges from 18 to 54% [38]. Low turnover osteopenia with reduced mineral content has also been well documented in experimental models of T1D, such as streptozotocin-induced diabetes [39]. Another prominent feature of human and experimental T1D is an increased urinary excretion of calcium and magnesium [40].

Plasma calcium concentration in the rat is normally maintained in the face of such renal losses; a decreased bone mineral content may therefore represent an unfortunate consequence of the marked hypercalciuria serving to maintain normocalcaemia under these conditions [40].

Delayed and impaired fracture's healing in patients with diabetes mellitus has been described in many studies [41, 42]. Diabetes impairs the production of critical growth factors such as transforming growth factor-beta, insulin-like growth factor 1, vascular endothelial growth factor, and platelet-derived growth factor at the fracture site during the early phases of diabetic fracture healing which has been associated with decreased cell differentiation and proliferation [43, 44]. Previous studies have demonstrated a reduction in collagen synthesis in diabetic rats [45] which ultimately influences bone healing.

Some fractures that frequently occur in diabetic patients may not be related to the systemic effect of diabetes on the skeleton but rather may be due to hypoglycemia, neuropathy, loss of proprioception balance, and coordination that are common in this disease and an important risk factor for falling [46, 47].

3. Prevention of Sweet Bones

Prevention of any disease is a laudable goal. When this is applied to diabetes mellitus, it gains further importance

because of the fact that this disease is gaining epidemic proportion and the cost of treatment of its complications. Sweet bone can be prevented or delayed by making some changes in lifestyle and weight loss, accompanied by increased physical activity to prevent bone loss. Intensive insulin therapy is the standard treatment for T1D and seems to be associated with improved skeletal health [48, 49]. Systematic screening for diabetic complications such as polyneuropathy, retinopathy, and nephropathy is important. Laser therapy might prevent progression of advanced retinopathy and help to maintain vision [50]. Deficiencies of calcium and vitamin D in patients with diabetes mellitus should be treated. Vitamin D supplementation should ensure a serum 25-hydroxyvitamin D level of 75 nmol/L [51]. Attention should be paid to the use of thiazolidinediones, especially in postmenopausal women with T2D. It causes bone loss accompanied by decreased osteoblast activity and bone formation [52]. Assessment of osteoporosis is similar in patients with and without diabetes mellitus. Selection of specific osteoporosis drugs is frequently based on comorbidities [53] (Figure 2).

4. Conclusion

Nevertheless, awareness of sweet bone in a patient with diabetes mellitus is important in clinical practice. Early recognition and appropriate intervention are essential in avoiding sweet bones and its consequences in diabetic patient.

Every diabetic patient should be assessed for risk factors for fractures and osteoporosis according to the guidelines established by The International Society for Clinical Densitometry and The National Osteoporosis Foundation. The pathogenesis of the bone alterations in diabetes mellitus as well as their molecular mechanisms needs further study.

Competing Interests

The author declares that there is no conflict of interests regarding the publication of this paper.

References

- [1] R. T. Dauphine, B. L. Riggs, and D. A. Scholz, "Back pain and vertebral crush fractures: an unemphasized mode of presentation for primary hyperparathyroidism," *Annals of Internal Medicine*, vol. 83, no. 3, pp. 365–367, 1975.
- [2] P. Vestergaard, L. Rejnmark, and L. Mosekilde, "Diabetes and its complications and their relationship with risk of fractures in type 1 and 2 diabetes," *Calcified Tissue International*, vol. 84, no. 1, pp. 45–55, 2009.
- [3] J. N. Farr and S. Khosla, "Determinants of bone strength and quality in diabetes mellitus in humans," *Bone*, vol. 82, pp. 28–34, 2016.
- [4] M. Janghorbani, R. M. Van Dam, W. C. Willett, and F. B. Hu, "Systematic review of type 1 and type 2 diabetes mellitus and risk of fracture," *American Journal of Epidemiology*, vol. 166, no. 5, pp. 495–505, 2007.
- [5] P. Vestergaard, "Discrepancies in bone mineral density and fracture risk in patients with type 1 and type 2 diabetes—a meta-analysis," *Osteoporosis International*, vol. 18, no. 4, pp. 427–444, 2007.
- [6] S. N. Pramojane, M. Phimphilai, N. Chattipakorn, and S. C. Chattipakorn, "Possible roles of insulin signaling in osteoblasts," *Endocrine Research*, vol. 39, no. 4, pp. 144–151, 2014.
- [7] S. Adami, "Bone health in diabetes: considerations for clinical management," *Current Medical Research and Opinion*, vol. 25, no. 5, pp. 1057–1072, 2009.
- [8] D. A. Nelson and S. J. Jacober, "Why do older women with diabetes have an increased fracture risk?" *The Journal of Clinical Endocrinology & Metabolism*, vol. 86, no. 1, pp. 29–31, 2001.
- [9] P.-J. López-Ibarra, M. M. C. Pastor, F. Escobar-Jiménez et al., "Bone mineral density at time of clinical diagnosis of adult-onset type 1 diabetes mellitus," *Endocrine Practice*, vol. 7, no. 5, pp. 346–351, 2001.
- [10] B. Piepkorn, P. Kann, T. Forst, J. Andreas, A. Pfützner, and J. Beyer, "Bone mineral density and bone metabolism in diabetes mellitus," *Hormone and Metabolic Research*, vol. 29, no. 11, pp. 584–591, 1997.
- [11] M. E. Garay-Sevilla, L. E. Nava, J. M. Malacara, K. Wróbel, K. Wróbel, and U. Pérez, "Advanced glycosylation end products (AGEs), insulin-like growth factor-1 (IGF-1) and IGF-binding protein-3 (IGFBP-3) in patients with Type 2 diabetes mellitus," *Diabetes/Metabolism Research and Reviews*, vol. 16, no. 2, pp. 106–113, 2000.
- [12] H. Tanaka, T. Hamano, N. Fujii et al., "The impact of diabetes mellitus on vitamin D metabolism in predialysis patients," *Bone*, vol. 45, no. 5, pp. 949–955, 2009.
- [13] R. Ziegler, "Diabetes mellitus and bone metabolism," *Hormone and Metabolic Research, Supplement*, vol. 26, pp. 90–94, 1992.
- [14] F. Lumachi, V. Camozzi, V. Tombolan, and G. Luisetto, "Bone mineral density, osteocalcin, and bone-specific alkaline phosphatase in patients with insulin-dependent diabetes mellitus," *Annals of the New York Academy of Sciences*, vol. 1173, supplement 1, pp. E64–E67, 2009.
- [15] Y. Hamada, H. Fujii, R. Kitazawa, J. Yodoi, S. Kitazawa, and M. Fukagawa, "Thioredoxin-1 overexpression in transgenic mice attenuates streptozotocin-induced diabetic osteopenia: a novel role of oxidative stress and therapeutic implications," *Bone*, vol. 44, no. 5, pp. 936–941, 2009.
- [16] D. Lozano, L. F. de Castro, S. Dapía et al., "Role of parathyroid hormone-related protein in the decreased osteoblast function in diabetes-related osteopenia," *Endocrinology*, vol. 150, no. 5, pp. 2027–2035, 2009.
- [17] B. Basha, D. S. Rao, Z.-H. Han, and A. M. Parfitt, "Osteomalacia due to vitamin D depletion: a neglected consequence of intestinal malabsorption," *The American Journal of Medicine*, vol. 108, no. 4, pp. 296–300, 2000.
- [18] A. A. Tahrani, A. Ball, L. Shepherd, A. Rahim, A. F. Jones, and A. Bates, "The prevalence of vitamin D abnormalities in South Asians with type 2 diabetes mellitus in the UK," *International Journal of Clinical Practice*, vol. 64, no. 3, pp. 351–355, 2010.
- [19] D. R. Curran, J. R. McArdle, and J. S. Talwalkar, "Diabetes mellitus and bone disease in cystic fibrosis," *Seminars in Respiratory and Critical Care Medicine*, vol. 30, no. 5, pp. 514–530, 2009.
- [20] S. L. Elkin, A. Fairney, S. Burnett et al., "Vertebral deformities and low bone mineral density in adults with cystic fibrosis: a cross-sectional study," *Osteoporosis International*, vol. 12, no. 5, pp. 366–372, 2001.
- [21] K. M. Thrailkill, "Diabetes care for adolescents," in *Diabetes in Women: Adolescence, Pregnancy and Menopause*, Lippincott Williams & Wilkins, Philadelphia, Pa, USA, 3rd edition, 2004.
- [22] A. M. Parfitt, Z.-H. Han, S. Palnitkar, D. S. Rao, M.-S. Shih, and D. Nelson, "Effects of ethnicity and age or menopause on osteoblast function, bone mineralization, and osteoid accumulation in iliac bone," *Journal of Bone and Mineral Research*, vol. 12, no. 11, pp. 1864–1873, 1997.
- [23] S. J. Qiu, S. Palnitkar, and D. S. Rao, "Age-related changes in osteocyte density and distribution in human cancellous bone," *Journal Of Bone & Mineral Research*, vol. 14, supplement 1, p. S308, 1999.
- [24] Y. Takeuchi, "Overview: derangement of bone metabolism in diabetes mellitus," *Clinical Calcium*, vol. 19, no. 9, pp. 1247–1255, 2009.
- [25] P. Pooruk, N. Kittimanon, P. Janthorn, and N. Bunyaratavej, "The impacts of type 2 diabetes mellitus on bone markers in the elderly Thai women," *Journal of the Medical Association of Thailand*, vol. 92, pp. S45–S48, 2009.
- [26] T. Thomas, B. Burguera, L. J. Melton III et al., "Role of serum leptin, insulin, and estrogen levels as potential mediators of the relationship between fat mass and bone mineral density in men versus women," *Bone*, vol. 29, no. 2, pp. 114–120, 2001.
- [27] D. T. Felson, Y. Zhang, M. T. Hannan, and J. J. Anderson, "Effects of weight and body mass index on bone mineral density in men and women: the Framingham study," *Journal of Bone and Mineral Research*, vol. 8, no. 5, pp. 567–573, 1993.
- [28] T. A. Einhorn, A. L. Boskey, C. M. Gundberg, V. J. Vigorita, V. J. Devlin, and M. M. Beyer, "The mineral and mechanical properties of bone in chronic experimental diabetes," *Journal of Orthopaedic Research*, vol. 6, no. 3, pp. 317–323, 1988.
- [29] J. Verhaeghe, A. M. H. Suiker, B. L. Nyomba et al., "Bone mineral homeostasis in spontaneously diabetic BB rats. II. Impaired bone turnover and decreased osteocalcin synthesis," *Endocrinology*, vol. 124, no. 2, pp. 573–582, 1989.
- [30] J. Verhaeghe, W. J. Visser, T. A. Einhorn, and R. Bouillon, "Osteoporosis and diabetes: lessons from the diabetic BB rat," *Hormone Research in Paediatrics*, vol. 34, no. 5-6, pp. 245–248, 1990.
- [31] J. Verhaeghe, A. M. H. Suiker, W. J. Visser, E. Van Herck, R. Van Bree, and R. Bouillon, "The effects of systemic insulin, insulin-like growth factor-I and growth hormone on bone growth and turnover in spontaneously diabetic BB rats," *Journal of Endocrinology*, vol. 134, no. 3, pp. 485–492, 1992.

- [32] J. C. Krakauer, M. J. McKenna, N. F. Buderer, D. Sudhaker Rao, F. W. Whitehouse, and A. Michael Parfitt, "Bone loss and bone turnover in diabetes," *Diabetes*, vol. 44, no. 7, pp. 775–782, 1995.
- [33] G. Hampson, C. Evans, R. J. Petitt et al., "Bone mineral density, collagen type 1 α 1 genotypes and bone turnover in premenopausal women with diabetes mellitus," *Diabetologia*, vol. 41, no. 11, pp. 1314–1320, 1998.
- [34] Y. Kawashima, J. C. Fritton, S. Yakar et al., "Type 2 diabetic mice demonstrate slender long bones with increased fragility secondary to increased osteoclastogenesis," *Bone*, vol. 44, no. 4, pp. 648–655, 2009.
- [35] R. G. Paul and A. J. Bailey, "Glycation of collagen: the basis of its central role in the late complications of ageing and diabetes," *International Journal of Biochemistry and Cell Biology*, vol. 28, no. 12, pp. 1297–1310, 1996.
- [36] P. L. Selby, "Osteopenia and diabetes," *Diabetic Medicine*, vol. 5, no. 5, pp. 423–428, 1988.
- [37] P. McNair, C. Christiansen, M. S. Christensen et al., "Development of bone mineral loss in insulin-treated diabetes: a 1 1/2 years follow-up study in sixty patients," *European Journal of Clinical Investigation*, vol. 11, no. 1, pp. 55–59, 1981.
- [38] Y. Seino and H. Ishida, "Diabetic osteopenia: pathophysiology and clinical aspects," *Diabetes/Metabolism Reviews*, vol. 11, no. 1, pp. 21–35, 1995.
- [39] H. Ishida, Y. Seino, T. Taminato et al., "Circulating levels and bone contents of bone γ -carboxyglutamic acid-containing protein are decreased in streptozocin-induced diabetes: possible marker for diabetic osteopenia," *Diabetes*, vol. 37, no. 6, pp. 702–706, 1988.
- [40] A. B. Anwana and H. O. Garland, "Renal calcium and magnesium handling in experimental diabetes mellitus in the rat," *Acta Endocrinologica*, vol. 122, no. 4, pp. 479–486, 1990.
- [41] R. T. Loder, "The influence of diabetes mellitus on the healing of closed fractures," *Clinical Orthopaedics and Related Research*, no. 232, pp. 210–216, 1988.
- [42] L. Cozen, "Does diabetes delay fracture healing?" *Clinical Orthopaedics and Related Research*, vol. 82, pp. 134–140, 1972.
- [43] W. A. Tyndall, H. A. Beam, C. Zarro, J. P. O'Connor, and S. S. Lin, "Decreased platelet derived growth factor expression during fracture healing in diabetic animals," *Clinical Orthopaedics and Related Research*, vol. 408, pp. 319–330, 2003.
- [44] A. Gandhi, C. Dumas, J. P. O'Connor, J. R. Parsons, and S. S. Lin, "The effects of local platelet rich plasma delivery on diabetic fracture healing," *Bone*, vol. 38, no. 4, pp. 540–546, 2006.
- [45] H. L. Gooch, J. E. Hale, H. Fujioka, G. Balian, and S. R. Hurwitz, "Alterations of cartilage and collagen expression during fracture healing in experimental diabetes," *Connective Tissue Research*, vol. 41, no. 2, pp. 81–91, 2000.
- [46] C. Wallace, G. E. Reiber, J. LeMaster et al., "Incidence of falls, risk factors for falls, and fall-related fractures in individuals with diabetes and a prior foot ulcer," *Diabetes Care*, vol. 25, no. 11, pp. 1983–1986, 2002.
- [47] S. S. Johnston, C. Conner, M. Aagren, K. Ruiz, and J. Bouchard, "Association between hypoglycaemic events and fall-related fractures in Medicare-covered patients with type 2 diabetes," *Diabetes, Obesity and Metabolism*, vol. 14, no. 7, pp. 634–643, 2012.
- [48] "Lifetime benefits and costs of intensive therapy as practiced in the diabetes control and complications trial," *The Journal of the American Medical Association*, vol. 276, no. 17, pp. 1409–1415, 1996.
- [49] M. M. Campos Pastor, P. J. López-Ibarra, F. Escobar-Jiménez, M. D. Serrano Pardo, and A. García-Cervigón, "Intensive insulin therapy and bone mineral density in type 1 diabetes mellitus: a prospective study," *Osteoporosis International*, vol. 11, no. 5, pp. 455–459, 2000.
- [50] P. R. Cavanagh, J. A. Derr, J. S. Ulbrecht, R. E. Maser, and T. J. Orchard, "Problems with gait and posture in neuropathic patients with insulin-dependent diabetes mellitus," *Diabetic Medicine*, vol. 9, no. 5, pp. 469–474, 1992.
- [51] M. F. Holick, "Vitamin D deficiency," *The New England Journal of Medicine*, vol. 357, no. 3, pp. 266–281, 2007.
- [52] D. Bilik, L. N. McEwen, M. B. Brown et al., "Thiazolidinediones and fractures: evidence from translating research into action for diabetes," *The Journal of Clinical Endocrinology & Metabolism*, vol. 95, no. 10, pp. 4560–4565, 2010.
- [53] P. Vestergaard, L. Rejnmark, and L. Mosekilde, "Are antiresorptive drugs effective against fractures in patients with diabetes?" *Calcified Tissue International*, vol. 88, no. 3, pp. 209–214, 2011.